

# Ultra High Energy Particle Astronomy, Neutrino Masses and Tau Airshowers

**D. Fargion<sup>1,2</sup>, M.Khlopov<sup>1,3</sup>, R.Konoplich<sup>4</sup>, P.G. De Sanctis Lucentini,  
M. De Santis, B. Mele<sup>2</sup>**

<sup>1</sup>Physics Department, Rome University "La Sapienza", Ple.A.Moro 2,00185, Rome, Italy

<sup>2</sup>INFN, Sezione di Roma, Rome, Italy

<sup>3</sup>Center for Cosmo-particle Physics "Cosmion" and M.V.Keldysh Institute of Applied Mathematics RAS, 125047, Moscow, Russia and Moscow Engineering Physics Institute Technical University, Moscow, Russia.

<sup>4</sup>Department of Physics, New York University, N.Y. 10003

**Abstract.** Ultra High Energy (UHE) neutrino Astronomy and relic Neutrino masses may play a key role in solving the Ultra High Energy Cosmic Ray (UHECR) puzzle within the Z-Showering model. Tau air-shower originated by UHE neutrino in matter may probe and amplify this expected UHE neutrino Astronomy. The discover of upcoming and horizontal  $\tau$  air-showers (UPTAUs, HORTAUs), born by UHE,  $\nu_\tau$  interacting inside mount chains or along Earth Crust crown masses at the Horizons edges, will greatly amplify the single UHE  $\nu_\tau$  track. Observing UPTAUs and HORTAUs along their line of showering, from higher balloons or satellites, at Greisen-Zatsepin-Kuzmin (GZK) energies ( $\geq 10^{19}$  eV), may test a calorimeter mass exceeding  $150 \text{ km}^3$  (water equivalent). Observing Horizontal Shower by EUSO will probe even larger ring areas generated in huge terrestrial volumes larger than  $5130 \text{ km}^3$ . These highest GZK energies  $\nu_\tau$  astronomy are well tuned to test the needed abundant  $\nu$  fluence in GZK Z-Showering model where ZeV ( $\geq 10^{21}$  eV) Ultra High Energy neutrinos hit on relic light ( $\sim 0.1 - 3$  eV masses) anti-neutrinos, in hot dark matter halos, creating boosted UHE Z bosons. Their nucleon decay in flight may born secondaries observed on Earth atmosphere as UHECR. The wide EUSO acceptance may test easily Z-showering fluxes as well as GZK neutrinos at their minimal granted fluence. The rare (78) observed upcoming terrestrial gamma flashes observed by BATSE satellite during last decade may be also be traces of such UPTAUs and HORTAUs.

## Contents

<b>1</b>	<b>Introduction: The rise of Ultra High Energy (UHE) Particle astronomy</b>	<b>3</b>
1.1	The Underground $km^3$ detectors for single $\mu$ tracks. . . . .	5
1.2	Ultra Relativistic Neutron Astronomy at EeV and secondary neutrinos . . . . .	5
<b>2</b>	<b>UHE neutrino scattering on relic <math>\nu_r</math> neutrinos in Hot Dark Matter Halos</b>	<b>5</b>
2.1	Solving the GZK puzzle by Z-Burst or ZZ-WW Shower models . . . . .	6
2.2	Relic Neutrino masses, Hot Halos and UHECRs Anisotropy and Clustering . . . . .	7
2.3	UHECR Nucleons from Z showers . . . . .	9
2.4	UHE $\nu - \nu_{relic}$ Cross Sections . . . . .	9
2.5	The UHE neutrino scattering $\nu_e \bar{\nu}_{er}, \nu_\mu \bar{\nu}_{\mu r}, \nu_\tau \bar{\nu}_{\tau r} \rightarrow Z \rightarrow \bar{f} f$ , . . . . .	10
2.6	The $W^+ W^-$ and $ZZ$ Channels . . . . .	11
2.7	The t-channel process $\nu_i \bar{\nu}_{j r} \rightarrow l_i \bar{l}_j$ . . . . .	12
<b>3</b>	<b>Boosted Z-UHECR spectra</b>	<b>12</b>
3.1	TeV tails from UHE electrons in Z-Showers . . . . .	14
<b>4</b>	<b>UHE <math>\nu</math> Astronomy by <math>\tau</math> air-shower: the ideal amplifier</b>	<b>21</b>
4.1	Ultra High Energy $\nu_\tau$ astronomy by Upward and Horizontal $\tau$ , UPTAUs-HORTAUs, detection . . . . .	23
4.2	Tau air showers to discover UHE $\nu$ : UHE $\tau$ decay channels . . . . .	24
<b>5</b>	<b>UPTAUs and HORTAUs connection with Terrestrial Gamma Flash</b>	<b>25</b>
5.1	UPTAUs and HORTAUs toward satellite : TGF events in BATSE data . . . . .	25
<b>6</b>	<b>Skin crown Earth volumes as a function of observation height <math>h</math></b>	<b>28</b>
6.1	Effective Volume in HORTAUs . . . . .	37
6.2	Event rate of upward and horizontal Tau air-showers . . . . .	38
<b>7</b>	<b>UHECR and UHE <math>\nu</math> observed by EUSO</b>	<b>40</b>
7.1	UHE $\nu$ Astronomy by the $\tau$ Showers and UHECRs in EUSO . . . . .	41
7.2	Upward UHE $\nu$ Showering in Air observable by EUSO . . . . .	42
7.3	Downward and Horizontal UHECRs in EUSO . . . . .	43
7.4	Air Induced UHE $\nu$ Shower . . . . .	45
7.5	UHE $\nu_\tau - \tau$ Double Bang Shower . . . . .	45
7.6	UHE $\nu_\tau - \tau$ Air Single Bang Shower . . . . .	45
7.7	HORTAUs in EUSO . . . . .	46
7.8	Visibility and Signatures of UHE neutrino in EUSO . . . . .	47
<b>8</b>	<b>Conclusions</b>	<b>49</b>
<b>9</b>	<b>Appendix A: Influence of Atmosphere depth in HORTAUs</b>	<b>50</b>
<b>10</b>	<b>Appendix B: The UPTAUs area</b>	<b>51</b>

## 1. Introduction: The rise of Ultra High Energy (UHE) Particle astronomy

Astronomy is based on the direct, undeflected radiation from astronomical objects to the observer. The neutral messengers which we did use in last three centuries were mainly photons in the optical range. During last century the whole electromagnetic spectrum opened to Astronomy. Moreover in the last 30 years also neutrino astronomy arose and proved solar and supernova neutrino astronomy. Ultra High Energy Cosmic Ray (UHECR) may offer a New Particle Astronomy because, even charged, they are almost un-bent by galactic and extra-galactic magnetic fields. This UHECR astronomy is bounded (by primordial photon drag, the well known Greisen, Zatsepin, Kuzmin (GZK) cut-off [42],[72]. ) in a very narrow (almost local) Universe (few tens Mpc). However we did't find yet in present UHECR arrival maps any nearby known galactic structures or clear super-galactic imprint. Observed UHECR isotropy call for a cosmic link, well above the narrow GZK radius. Observed UHECR clustering in groups suggest compact sources (as AGN or BL Lacs beaming Jets ) respect to any homogeneous and isotropic halo of primordial topological defects. Recent evidence for a dozen or more BL Lacs sources correlation (some at medium redshift  $z \simeq 0.3 \gg z_{GZK}$ ) with UHECR clustered events are giving support (with the isotropy) to a cosmic origin for UHECR sources [46]. Incidentally UHECR must produce by pion decays GZK neutrino secondaries at a fluence at least comparable with observed UHECR. Therefore there must be a minimal underlying neutrino astronomy at observed GZK cosmic ray level. In order to solve the GZK puzzles it may be necessary to consider the traces of UHE neutrinos either primary (at much higher fluxes) of UHECR by Z-Showering or at least as secondaries. Indeed UHE Relic neutrinos with a light mass may play a role as calorimeter for UHE neutrinos from cosmic distances at ZeV energies. Their scattering may solve the GZK paradox, [18], [20], [71], [68][28], [38]; in this scenario UHE  $\nu$  Astronomy is not just a consequence but itself the cause of UHECR signals.

To test this idea we need to open an independent UHE neutrino Astronomy. Different muon track detectors, cubic  $km^3$  in underground may be reveal them at PeVs energies. Nevertheless UHE neutrino tau may interact on Mountains or better on Earth crust, at a huge concrete calorimeter, leading to Tau Air-Showers, probing easily both (secondary and/or primary) UHE neutrino astronomy at GZK energies. Present article review the problems and the experimental prospects on Mountains, planes detectors quota; we also reconsidered events measured by satellites, like past BATSE, present gamma satellite INTEGRAL, future EUSO experiments. The recent signals in BATSE terrestrial gamma flashes maybe indeed the first evidence for these new UHE neutrino Astronomy upcoming from Earth crust at PeV-EeV energies, leading to UPTAUs and HORTAUs showers. In last figure we summarized the two consequent Flux signal derived by the TGF event rate data in BATSE (1991-2000) experiment, normalized for the estimated BATSE thresholds. These result may be a useful reference estimate for PeV-EeV neutrino fluxes and apparently are well consistent with Z-Showering model for a relic mass within the expected values ( $m \simeq 0.04 - 0.4eV$ ).

Let us remind that the restrictions on any astronomy are related to a the messenger interactions with the surrounding medium on the way to the observer. While Cosmic Rays astronomy is severely blurred by random terrestrial, solar, galactic and extragalactic magnetic lenses, the highest  $\gamma$  ray astronomy (above tens TeV) became more or less blind because of photon-photon opacity (due to electron pair production) at different energy windows. Indeed the Infrared- TeV opacity as well as a more severe Black Body Radiation, BBR,( at  $2.75K$ )-PeV cut-off are bounding the TeV -PeV  $\gamma$  ray astronomy in very nearby cosmic ( or even galactic) volumes. Therefore rarest TeV gamma signals are at present the most extreme trace of High Energy Astronomy. We observe copious cosmic rays at higher ( $\gg 10^{15}eV$ ) energies almost isotropically spread by galactic and cosmic magnetic fields in the sky.

Let us remind, among the  $\gamma$  TeV discoveries, the signals of power-full Jets blazing to us from Galactic (Micro-Quasars) or extragalactic edges (BL Lacs). At PeV energies astrophysical  $\gamma$  cosmic rays should also be presented, but, excluding a very rare and elusive CygX3 event, they have not being up date observed; only upper bounds are known at PeV energies. The missing  $\gamma$  PeV astronomy, as we mentioned, are very probably absorbed because of their own photon interactions (electron pairs creation) at the source environment and/or along the photon propagation into the cosmic Black Body Radiation (BBR) and/or into other diffused background radiation. Unfortunately PeV charged cosmic rays, easily bend and bounded in a random walk by Galactic magnetic fields, loose their original directionality and their astronomical relevance; their tangled trajectory resident time in the Galaxy is much longer ( $\geq 10^3 - 10^5$ ) than any linear neutral trajectory, as in the case of gamma rays, making the charged cosmic rays more probable to be observed by nearly a comparable length ratio. However astrophysical UHE neutrino signals in the wide range  $10^{13}\text{eV}-10^{19}\text{eV}$  (or even higher GZK energies) are unaffected by any radiation cosmic opacity and may easily open a very new exciting window toward Highest Energy sources. Being weakly interacting the neutrinos are an ideal microscope to deeply observe in their accelerator (Jet,SN,GRB, Mini Black Hole) cores they do not experience any strong self opacity as the case of photon. Other astrophysical  $\nu$  sources at lower energies ( $10^8 \text{ eV} - 10^{12} \text{ eV}$ ) should also be present, at least at EGRET fluence level, but their signals are very weak and probably drowned by the dominant diffused atmospheric  $\nu$ , secondaries of muon secondaries, produced as pion decays by the same charged (and smeared) UHE cosmic rays (while hitting terrestrial atmosphere): the so called diffused atmospheric neutrinos. Indeed a modulation of the atmospheric neutrinos signal has inferred the first conclusive evidence for a neutrino mass and for a neutrino flavor mixing. At lowest (MeVs)  $\nu$  energy windows, the abundant and steady solar neutrino flux, (as well as the prompt, but rare, neutrino burst from a nearby Super-Novae (SN 1987A)), has been, in last twenty years, successfully explored, giving support to neutrino flavour mixing and to the neutrino mass reality. More recent additional probes of solar neutrino flavour mixing and reactor neutrino disappearance are giving a robust ground to the neutrino mass existence, at least at minimal  $\sim 0.05 \text{ eV}$  level. Let us mention that Stellar evolution, Supernova explosion but in particular Early Universe had over-produced and kept in thermal equilibrium neutrinos whose relic presence here today pollute the cosmic spaces either smoothly (lightest  $m_\nu \ll 0.001\text{eV}$  relativistic  $\nu$ ) or in denser and even possibly clustered Hot Halos ( $\simeq eVs$  relic  $\nu$  masses). A minimal tiny atmospheric neutrino (above  $0.05 \text{ eV}$ )  $\nu$  mass, beyond the Standard Model, are already making their cosmic energy density component almost two order of magnitude larger than the corresponding  $2.75K$  (Black Body Radiation) BBR radiation density. Here we discuss their role in Z-Shower model and we concentrate on the possibility to detect such a component of the associated UHE neutrino flux astronomy (above PeV-EeV up to GZK energies) by UHE  $\nu_\tau$  interactions in Mountain chains or in Earth Crust leading to Horizontal or Upward Tau air-showers [30], [31],[36] [32], [8]. The article will discuss in next Chapter 2 The Z-Shower scenario and , in next chapter 3 the Z-Shower tail spectra, while in chapter 4 we discuss the idea that UHE  $\tau$  neutrino may amplify its signal by peculiar  $\tau$  air-showers, either upward and horizontal. In next Chapter 5 we discuss the possible connection between observed upward Gamma Flashes and such expected Upward Tau Air-Showers (UPTAUs). In Chapter 6 it has been evaluated the terrestrial skin crown volumes, surrounding each observer at high quota, where UHE neutrino  $\tau$  may hit and give life to Earth-Skimming Tau nearly Horizontal, whose decay in flight may be source of Horizontal Tau air-showers (HORTAUs).In Chapter 7 we consider the HORTAUs signals observable from next generation of UHECR detectors as EUSO and or OWL experiments. In the Conclusion we summarized the tau astronomy and the resulting Terrestrial Gamma Flash interpretation as neutrino UPTAUs and HORTAUs fluxes at ( $\sim 100\text{eV cm}^{-2}\text{s}^{-1}\text{sr}^{-1}$ ) just an

order of magnitude below present neutrino telescope detector and cosmic ray arrays.

### 1.1. The Underground $km^3$ detectors for single $\mu$ tracks.

The UHE  $10^{13}eV - 10^{16}eV$   $\nu$ 's, being weakly interacting and rare, may be detected mainly inside huge volumes, bigger than Super-Kamiokande ones; at present most popular detectors consider underground ones (Cubic Kilometer Size like AMANDA-NESTOR) or (at higher energy  $10^{19}eV - 10^{20}eV$ ) the widest Terrestrial atmospheric sheet volumes (Auger Array Telescope or EUSO atmospheric Detectors). Underground  $km^3$  detection is based mainly on  $\nu_\mu$  tracks above hundred TeV energies, because of their high penetration in matter, leading to  $\mu$  kilometer size lepton tails [54]. Rarest atmospheric horizontal showers are also expected due to  $\nu$  interactions in air (and, as we shall discuss, in the Earth Crust) with more secondary tails. While  $km^3$  detectors are optimal for PeV neutrino muons, the Atmospheric Detectors (AUGER-EUSO like) exhibit a minimal threshold at highest ( $\geq 10^{19}eV$ ) energies. The  $km^3$  sensibility is more tuned to Tens TeV -PeV astronomy while AUGER has wider acceptance above GZK energies. As we shall discuss  $\tau$  air-shower detectors exhibit also huge acceptance at both energy windows being competitive both at PeV as well as at EeV energy range as well as GZK ones; we shall not discuss here the  $Km^3$  detector as the ICECUBE project.

### 1.2. Ultra Relativistic Neutron Astronomy at EeV and secondary neutrinos

Incidentally just around EeV ( $10^{18}eV$ ) energies an associated Galactic Ultra High Energy Neutron Astronomy might be already observed in anisotropic clustering of UHECR data because of the relativistic neutrons boosted lifetime. Therefore UHE neutrons at EeV may be a source candidate of the observed tiny EeV anisotropy in UHECR data. Indeed a 4% galactic anisotropy and clustering in EeV cosmic rays has been recently emerged by AGASA[43] along our nearby galactic spiral arm. These data have been confirmed by a South (Australia) detector(SUGAR) [4]. Therefore AGASA might have already experienced a first UHECR-Neutron astronomy (UHENA) at a very relevant energy flux ( $\sim 10eVcm^{-2}s^{-1}$ ). These EeV-UHENA signals must also be a source of at least comparable parasite ( $10^{17} - 10^{16} eV$ ) secondary tails of UHE neutrino  $\bar{\nu}_e$  from the same neutron beta decay in flight. After and even more abundant UHE  $\tau$  fluxes may be also produced by a larger pion pair production near the same accelerating source of UHE EeV neutrons. Their flavor oscillations and mixing in galactic or extragalactic flights (analogous to atmospheric and solar ones) must guarantee the presence of all lepton flavors fluxes  $\phi$  nearly at equal foot:  $\phi_{\bar{\nu}_e}, \phi_{\bar{\nu}_\mu}, \phi_{\bar{\nu}_\tau} = 1 : 1 : 1$ [30]. The latter UHE  $\bar{\nu}_\tau$  imprint (added to other local astrophysical UHE  $\nu$  production) could be already recorded [30] as Upward and Horizontal Tau air-showers Terrestrial Gamma Flash (considered as secondaries  $\gamma$  of Upward Tau air-showers and Horizontal Tau air-showers): UPTAUs and HORTAUs.

## 2. UHE neutrino scattering on relic $\nu_r$ neutrinos in Hot Dark Matter Halos

At highest energy edges ( $\geq 10^{19} - 10^{20}eV$ ), a somehow correlated new UHE Astronomy is also expected for charged Cosmic Rays; indeed these UHECR have such a large rigidity to avoid any bending by random galactic or extragalactic magnetic fields; being nearly non deflected UHECR should point toward the original sources showing in the sky a new astronomical map. Moreover such UHECR astronomy is bounded by the ubiquitous cosmic  $2.75K^o$  BBR screening (the well known Greisen, Zat'sepin, Kuzmin GZK cut-off) limiting its origination inside a very local ( $\leq 20Mpc$ ) cosmic volume. Surprisingly, these UHECR above GZK (already up to day above 60 events) are not pointing toward any known nearby

candidate source. Moreover their nearly isotropic arrival distributions underlines and testify a very possible cosmic origination, in disagreement with any local (Galactic plane or Halo, Local Group) expected footprint by GZK cut-off. A very weak Super-Galactic imprint seems to be present but at low level and already above GZK volume. This opened a very hot debate in modern astrophysics known as the GZK paradox. Possible solutions has been found recently beyond the Standard Model assuming a non-vanishing neutrino mass. Indeed at such Ultra-High energies, neutrino at ZeV energies ( $\geq 10^{21} eVs$ ) hitting onto relic cosmological light ( $0.1 - 4eV$  masses) neutrinos [12] nearly at rest in Hot Dark Matter (HDM) Halos (galactic or in Local Group) has the unique possibility to produce UHE resonant Z bosons (the so called Z-burst or better Z-Showering scenario). The gauge  $Z, W^+, W^-$ , boson decay may shower the same nucleon secondaries responsible for observed UHECR the different channel cross-sections in Z-WW-ZZ-Shower by scattering on relic neutrinos are shown in Fig.1 while the boosted Z-Shower secondary chains are in Fig.2, Fig.3, Fig.4, Fig.5, Fig.6: [18], [20], [68], [71]; for a more updated scenario see [28], [38].

### 2.1. Solving the GZK puzzle by Z-Burst or ZZ-WW Shower models

If relic neutrinos have a mass (as they should by recent neutrino mass splitting evidences [5]) larger than their maximal thermal energy (which is  $\sim 5 \cdot 10^{-4} eV$  for the temperature  $1.9K^o$ , predicted in Big Bang universe for primordial thermal gas of massless two component neutrinos) they may cluster in Local Group or galactic halos; near eVs masses the clustering seems very plausible and it may play a role in HDM cosmology [17] [13]. Their scattering with incoming extra-galactic UHE neutrinos determine high energy particle cascades which could contribute or dominate the observed UHECR flux at *GZK* edges. The competitive UHE  $\nu$  scattering on terrestrial atmosphere is much less ( $\ll 10^{-3}$ ) effective and it has an angular spread (mostly horizontal) not in agreement with the observed UHECRs. Indeed the possibility that neutrino share a little mass has been reinforced by Super-Kamiokande evidence for atmospheric neutrino anomaly via  $\nu_\mu \leftrightarrow \nu_\tau$  oscillation. An additional evidence of neutral lepton flavor mixing has been very recently reported also by Solar neutrino experiments (SNO, Gallex), accelerator experiment K2k and reactor experiment KamLAND. Consequently there are at least two main extreme scenario for hot dark halos: either  $\nu_\mu, \nu_\tau$  are both extremely light ( $m_{\nu_\mu} \sim m_{\nu_\tau} \sim \sqrt{(\Delta m)^2} \sim 0.05 eV$ ) and therefore hot dark neutrino halo is very wide and spread out to local group clustering sizes (increasing the radius but loosing in the neutrino density clustering contrast), or  $\nu_\mu, \nu_\tau$  may share degenerated (around  $eV$  masses) split by a very tiny different values. In the latter fine-tuned neutrino mass case ( $m_\nu \sim 0.4eV - 1.2eV$ ) (see Fig.2 and Fig.2) the Z peak  $\nu\bar{\nu}_r$  interaction will be the favorite one; in the second case (for heavier non constrained neutrino mass ( $m_\nu \gtrsim 1.5 eV$ )) only a  $\nu\bar{\nu}_r \rightarrow W^+W^-$  and the additional  $\nu\bar{\nu}_r \rightarrow ZZ$  interactions, (see the cross-section in Fig.1)[20] considered here will be the only ones able to solve the GZK puzzle. Indeed the relic neutrino mass within HDM models in galactic halo near  $m_\nu \sim 4eV$ , corresponds to a lower Z resonant incoming energy

$$E_\nu = \left( \frac{4eV}{\sqrt{m_\nu^2 + p_\nu^2}} \right) \cdot 10^{21} eV. \quad (1)$$

This resonant incoming neutrino energy is unable to overcome GZK energies while it is showering mainly a small energy fraction into nucleons ( $p, \bar{p}, n, \bar{n}$ ), at energies  $E_p$  quite below

(See Tab.1).

$$E_p = 2.2 \left( \frac{4eV}{\sqrt{m_\nu^2 + p_\nu^2}} \right) \cdot 10^{19} eV. \quad (2)$$

Therefore too heavy ( $> 1.5eV$ ) neutrino mass are not fit to solve GZK by Z-resonance while WW,ZZ showering as well as t-channel showering may naturally keep open the solution. In particular the overlapping of both the Z and the WW, ZZ channels described in Fig.1, for  $m_\nu \simeq 2.3eV$  while solving the UHECR above GZK they must pile up (by Z-resonance peak activity) events at  $5 \cdot 10^{19}eV$ , leading to a correlation with the observed bump in AGASA data at this energy. There is indeed a first marginal evidence of such a UHECR bump in AGASA and Yakutsk data that may stand for this interpretation. More detailed data are needed to verify such conclusive possibility.

Most of us consider cosmological light relic neutrinos in Standard Model at non relativistic regime neglecting any relic neutrino momentum  $p_\nu$  term. However, at lightest mass values the momentum may be comparable to the relic mass; the spectra may reflect additional relic neutrino-energy injection which are feeding standard cosmic relic neutrino at energies much above the same neutrino mass. It can be easily estimated that neutrino background due to stellar, Super Nova, GRBs, AGN past activities,, presently red-shifted into a KeV-eV  $\nu$  spectra while piling into a relic neutrino grey-body spectra, cannot exceed 0.01% of the thermal cosmological neutrinos. However in cosmological models of unstable neutrinos and primordial Black Hole neutrino evaporation such background may appear quite naturally in  $\simeq eVs$  ranges with or without leading to a present radiation dominated Universe. Therefore it is worth-full to keep the most general mass and momentum term in the target relic neutrino spectra. In this windy ultra-relativistic neutrino cosmology, there is no clustering halos and the unique size to be considered is nearly coincident with the GZK one, defined by the energy loss length for UHECR nucleons ( $\sim 20Mpc$ ). Therefore the isotropic UHECR behavior is guaranteed. The puzzle related to uniform source distribution spectra seems to persist. Nevertheless the UHE neutrino- relic neutrino scattering *do not* follow a flat spectrum (as well as any hypothetical  $\nu$  grey body spectra). This leaves open the opportunity to have a relic relativistic neutrino component at eVs energies as well as the observed non uniform UHECR spectra. This case is similar to the case of a very light neutrino mass much below 0.1 eV.

## 2.2. Relic Neutrino masses, Hot Halos and UHECRs Anisotropy and Clustering

In the simplest case of neutrino dominated cosmology the neutrino mass plays a role in defining its HDM Halos size and the consequent enhancement of UHECR arrival directions due to our peculiar position in the HDM halo. Indeed for a heavy mass case  $\geq 2eV$  HDM neutrino halo are mainly galactic and/or local, reflecting an isotropic or a diffused amplification toward nearby  $M31$  HDM halo. In the lighter case the HDM might include the Local Cluster up to Virgo. To each size corresponds also a different role of UHECR arrival time. The larger the HDM size the longer the UHECR random-walk travel time (in extra-galactic random magnetic fields) and the wider the arrival rate lag between doublets or triplets. The smaller is the neutrino halo the earlier the UHE neutron secondaries by Z shower will play a role: indeed at  $E_n = 10^{20}eV$  UHE neutron are flying a Mpc and their directional arrival (or their late decayed proton arrival) are more on-line toward the source. This may explain the high self collimation and auto-correlation of UHECR discovered very recently [66]. The UHE neutrons Z-Showering fits with the harder spectra observed in clustered events in AGASA [64]. The same UHECR alignment may explain the quite short (2-3 years)[63]

lapse of time observed in AGASA doublets. Indeed the most conservative scenario where UHECR are just primary proton from nearby sources at GZK distances (tens of Mpcs) is no longer acceptable either because the absence of such nearby sources and because of the observed stringent UHECR clustering ( $2^\circ - 2.5^\circ$ ) [64] in arrival direction, as well as because of the short ( $\sim 3$  years) characteristic time lag between clustered events. Finally the same growth with energy of UHECR neutron (and anti-neutron) life-lengths (while being marginal or meaning-less in tens Mpcs GZK flight distances) may naturally explain, within a Mpc Z Showering Neutrino Halo, the arising harder spectra revealed in doublets-triplet spectra [2]. Nevertheless in the modern multi-component Cold Dark Matter (CDM) dominated cosmology the size and density of neutrino halo may loose a direct relationship with neutrino mass and the final scenario should be much more complicated, taken into account the evidences of different types of CDM particles.

For instance, EGRET data on diffuse galactic gamma ray background above 1 GeV together with the results of DAMA direct experimental searches for cosmic WIMPs might be considered [21] [23],[19] as the evidence for the existence of massive stable neutrino of 4th generation with the mass about 50 GeV. This hypothesis can provide explanation for anomalies in cosmic positron spectrum, claimed by HEAT, and is accessible for testing in the special analysis of underground neutrino data [11] and in precise measurements of gamma ray background and cosmic ray fluxes.

UHE neutron secondaries from the same Z showering in HDM halo may also solve an emerging puzzle: the correlations of arrival directions of UHECRs found recently [55] in Yakutsk data at energy  $E = 8 \cdot 10^{18} eV$  toward the Super Galactic Plane are to be compared with the compelling evidence of UHECR events ( $E = 3 \cdot 10^{19} eV$  above GZK) clustering toward well defined BL Lacs at cosmic distances (redshift  $z > 0.1 - 0.2$ ) [66, 67]. Where is the real UHECR sources location? At Super-galactic disk (50 Mpcs wide, within GZK range) or at cosmic ( $\geq 300 Mpcs$ ) edges? It should be noted that even for the Super Galactic hypothesis [55] the common protons are unable to justify the high collimation of the UHECR events. Of course both results (or just one of them) maybe a statistical fluctuation. But both studies seem statistically significant (4.6-5 sigma) and they seem in obvious disagreement. There may be still open the possibility of *two* new categories of UHECR sources both of them located at different distances above GZK ones (the harder the most distant BL Lac sources). But it seems quite unnatural the UHECR propagation by direct nucleons where the most distant are the harder. However our Z-Showering scenario offers different solutions: (1) The Relic Neutrino Masses define different Hierarchical Dark Halos and privileged arrival direction correlated to Hot Relic Neutrino Halos. The real sources are at (isotropic) cosmic edges [66], [67], but their crossing along a longer anisotropic relic neutrino cloud enhances the interaction probability in the Super Galactic Plane. (2) The nearest SG sources are weaker while the collimated BL Lacs are harder: both sources need a Neutrino Halo to induce the Z-Showering UHECR. More data will clarify better the real scenario.

As we noticed above, relic neutrino masses above a few eVs in HDM halo *are not* consistent with naive Z peak; higher energies interactions ruled by WW, ZZ cross-sections may nevertheless solve the GZK cut-off. In this regime there will be also possible to produce t-channel *UHE* lepton pairs by  $\nu_i \bar{\nu}_j \rightarrow l_i \bar{l}_j$  through a virtual W exchange, leading to an additional electro-magnetic showers injection. As we shall see this important and underestimated signal will produce UHE electrons whose final traces are TeV synchrotron photons. The hadronic tail of the Z or  $W^+W^-$  cascade may be the source of final nucleons  $p, \bar{p}, n, \bar{n}$  able to explain UHECR events observed by Fly's Eye and AGASA and other detectors. The same  $\nu \bar{\nu}_r$  interactions are a source of Z and W that decay in a rich shower ramification.

### 2.3. UHECR Nucleons from Z showers

Although protons (or anti-protons) are the most favorite candidates to explain the highest energy air shower observed, one doesn't have to neglect the signature of final neutrons and anti-neutrons as well as electrons and photons. Indeed the UHECR neutrons are produced in Z-WW showering at nearly same rate as the charged nucleons. Above GZK cut-off energies UHE  $n, \bar{n}$ , share a life length comparable with the Hot Galactic Dark Neutrino Halo. Therefore they may be an important component in UHECRs. Moreover prompt UHE electron (positron) interactions with the galactic or extra-galactic magnetic fields or soft radiative backgrounds may lead to gamma cascades from PeV to TeV energies.

Gamma photons at energies  $E_\gamma \simeq 10^{19} - 10^{20} eV$  may freely propagate through galactic or local halo distances (hundreds of kpc to few Mpc) and could also contribute to the extreme edges of cosmic ray spectrum and clustering (see also [68][25]).

The ratio of the final energy flux of nucleons near the Z peak resonance,  $\Phi_p$  over the corresponding electro-magnetic energy flux  $\Phi_{em}$  ratio is, as in Tab.1  $e^+e^-, \gamma$  entry, nearly  $\sim \frac{1}{8}$ . Moreover if one considers at higher  $E_\nu$  energies, the opening of WW, ZZ channels and the six pairs  $\nu_e\bar{\nu}_\mu, \nu_\mu\bar{\nu}_\tau, \nu_e\bar{\nu}_\tau$  (and their anti-particle pairs) t-channel interactions leading to highest energy leptons with no nucleonic relics (as  $p, \bar{p}$ ), this additional injection contributes a factor  $\sim 1.6$  leading to  $\frac{\Phi_p}{\Phi_{em}} \sim \frac{1}{13}$ . This ratio is valid at energies corresponding to the WW, ZZ masses. Since the overall cross section is energy dependent at the center of mass energies above these values, the  $\frac{\Phi_p}{\Phi_{em}}$  decreases more because of the dominant role of t-channel (Fig.1). We focus here on Z, and WW, ZZ channels showering in hadrons for GZK events. The important role of UHE electron showering into TeV radiation is discussed below.

### 2.4. UHE $\nu - \nu_{relic}$ Cross Sections

Extragalactic neutrino cosmic rays are free to move on cosmic distances up our galactic halo without constraint on their mean free path, because the interaction length with cosmic background neutrinos is greater than the actual Hubble distance. A Hot Dark Matter galactic or local group halo model with relic light neutrinos (primarily the heaviest  $\nu_\tau$  or  $\nu_\mu$ ), acts as a target for the high- energy neutrino beams. The relic number density and the halo size are large enough to allow the  $\nu\nu_{relic}$  interaction. As a consequence high energy particle showers are produced in the galactic or local group halo, overcoming the GZK cut-off. There is an upper bound density clustering for very light Dirac fermions due to the maximal Fermi degeneracy whose number density contrast is  $\delta n \propto m_\nu^3$ , while one finds that the neutrino free-streaming halo grows only as  $\propto m_\nu^{-1}$ . Therefore the overall interaction probability grows  $\propto m_\nu^2$ , favoring heavier non relativistic (eVs) neutrino masses. In this frame above few eV neutrino masses only WW-ZZ channel are operative. Nevertheless the same lightest relic neutrinos may share higher Local Group velocities (thousands  $\frac{Km}{s}$ ) or even nearly relativistic speeds and it may therefore compensate the common density bound:

$$n_{\nu_i} \leq 1.9 \cdot 10^3 \left( \frac{m_i}{0.1eV} \right)^3 \left( \frac{v_{\nu_i}}{2 \cdot 10^3 \frac{Km}{s}} \right)^3 \quad (3)$$

From the cross section side there are three main interaction processes that have to be considered leading to nucleons in the UHE neutrino scattering with relic neutrinos .

**channel 1.** The UHE neutrino anti-neutrino (and charge conjugation) relic scattering  $\nu_e\bar{\nu}_{er}, \nu_\mu\bar{\nu}_{\mu r}, \nu_\tau\bar{\nu}_{\tau r} \rightarrow Z \rightarrow \bar{f}f$ , fermion pair decay at the Z resonance.

**channel 2.** The UHE neutrino anti-neutrino (and charge conjugation) relic scattering  $\nu_e \bar{\nu}_{er}, \nu_\mu \bar{\nu}_{\mu r}, \nu_\tau \bar{\nu}_{\tau r} \rightarrow W^+ W^-$  or  $\rightarrow Z Z$  leading to hadrons, electrons, photons, through W and Z decay.

**channel 3.** The  $\nu_e - \bar{\nu}_\mu, \nu_e - \bar{\nu}_\tau, \nu_\mu - \bar{\nu}_\tau$  and antiparticle conjugate interactions of different flavor neutrinos mediated in the  $t$ -channel by the W exchange (i.e.  $\nu_\mu \bar{\nu}_{\tau r} \rightarrow \mu^- \tau^+$ ). These reactions are sources of prompt UHE electrons pairs as well as secondary electron pairs ( by muon or tau pair decays) as well as photons resulting by hadronic ( $\pi^0$ )  $\tau$  decay secondaries. Most of these UHE electron energies are soon converted in electromagnetic radiation (photons) by inverse Compton scattering on BBR or synchrotron radiation (by galactic or extragalactic magnetic fields).

## 2.5. The UHE neutrino scattering $\nu_e \bar{\nu}_{er}, \nu_\mu \bar{\nu}_{\mu r}, \nu_\tau \bar{\nu}_{\tau r} \rightarrow Z \rightarrow \bar{f} f$ ,

The interaction of neutrinos of the same flavor can occur via a Z exchange in the  $s$ -channel ( $\nu_i \bar{\nu}_{ir}$  and charge conjugated). The cross section for hadron production in  $\nu_i \bar{\nu}_{ir} \rightarrow Z^* \rightarrow \text{hadrons}$  is

$$\sigma_Z(s) = \frac{8\pi s \Gamma(Z^0 \rightarrow \text{invis.}) \Gamma(Z^0 \rightarrow \text{hadr.})}{M_Z^2 (s - M_Z^2)^2 + M_Z^2 \Gamma_Z^2} \quad (4)$$

where  $\Gamma(Z^0 \rightarrow \text{invis.}) \simeq 0.5 \text{ GeV}$ ,  $\Gamma(Z^0 \rightarrow \text{hadr.}) \simeq 1.74 \text{ GeV}$  and  $\Gamma_Z \simeq 2.49 \text{ GeV}$  are respectively the experimental Z width into invisible products, the Z width into hadrons and the Z full width [57].

A  $\nu \nu_r$  interaction mediated in the  $s$ -channel by the Z exchange, shows a peculiar peak in the cross section due to the resonant Z production at  $s = M_Z^2$ . However, this occurs for a very narrow and fine-tuned windows of arrival neutrino energies  $\nu_i$  (for fixed target neutrino masses and momentum  $\bar{\nu}_{ir}$ ):

$$E_{\nu_i} = \left( \frac{4eV}{\sqrt{m_{\nu_i}^2 + p_{\nu_i}^2}} \right) \cdot 10^{21} \text{ eV}. \quad (5)$$

The effective peak cross section reaches the value ( $\langle \sigma_Z \rangle = 4.2 \cdot 10^{-32} \text{ cm}^2$ ). We assumed here for a more general case (non relativistic and nearly relativistic relic neutrinos) that the averaged cross section has to be extended over an energy window comparable to a half of the center of mass energy. The consequent effective averaged cross-section is described in Fig.1 as a lower truncated hill curve.

So in this mechanism the energy of the UHE neutrino cosmic ray is related to the mass of the relic neutrinos, and for an initial neutrino energy fixed at  $E_\nu \simeq 10^{22} \text{ eV}$ , the Z resonance requires a mass for the heavier neutral lepton around  $m_\nu \simeq 0.4 \text{ eV}$ . Apart from this narrow resonance peak at  $\sqrt{s} = M_Z$ , the asymptotic behavior of the cross section is proportional to  $1/s$  for  $s \gg M_Z^2$ .

The  $\nu \bar{\nu} \rightarrow Z \rightarrow \text{hadrons}$  reactions have been proposed by [18][20] [68] [71] with a neutrino clustering on Supercluster, cluster, Local Group, and galactic halo scale within the few tens of Mpc limit fixed by the GZK cut-off. Due to the enhanced annihilation cross-section in the Z pole, the probability of a neutrino collision is reasonable even for a neutrino density contrast as modest as  $\delta n_\nu / n_\nu \geq 10^2$ . The potential wells of such structures might enhance the neutrino local group density with an efficiency at comparable with observed baryonic clustering discussed above. In this range the presence of extended local group halo should be reflected into anisotropy (higher abundance) toward Andromeda, while a much

lighter neutrino mass may correspond to a huge halo containing even Virgo maybe Coma and the Super Galactic Plane.

## 2.6. The $W^+W^-$ and $ZZ$ Channels

The reactions  $\nu_\tau\bar{\nu}_\tau \rightarrow W^+W^-$ ,  $\nu_\mu\bar{\nu}_\mu \rightarrow W^+W^-$ ,  $\nu_e\bar{\nu}_e \rightarrow W^+W^-$ , [16], have been previously introduced in order to explain UHECR as the Fly's Eye event at ( $3 \cdot 10^{20} eV$ ) detected in 1991 and last AGASA data for neutrino mass a few eVs clustered in galactic or local hot dark halos[20]. The cross section is then given by

$$\sigma_{WW}(s) = \sigma_{asym} \frac{\beta_W}{2s} \frac{1}{(s - M_Z^2)} \{4L(s) \cdot C(s) + D(s)\}.$$

where  $\beta_W = (1 - 4M_W^2/s)^{1/2}$ ,  $\sigma_{asym} = \frac{\pi\alpha^2}{2\sin^4\theta_W M_W^2} \simeq 108.5 pb$ , and the functions  $L(s)$ ,  $C(s)$ ,  $D(s)$  are defined as

$$L(s) = \frac{M_W^2}{2\beta_W s} \ln\left(\frac{s + \beta_W s - 2M_W^2}{s - \beta_W s - 2M_W^2}\right)$$

$$C(s) = s^2 + s(2M_W^2 - M_Z^2) + 2M_W^2(M_Z^2 + M_W^2) \quad (6)$$

$$D(s) = \frac{[s^2(M_Z^4 - 60M_W^4 - 4M_Z^2M_W^2) + 20M_Z^2M_W^2s(M_Z^2 + 2M_W^2) - 48M_Z^2M_W^4(M_Z^2 + M_W^2)]}{12M_W^2(s - M_Z^2)}$$

This result should be extended with the additional new  $ZZ$  interaction channel considered in [25]:

$$\sigma_{ZZ} = \frac{G^2 M_Z^2}{4\pi} y \frac{(1 + \frac{y^2}{4})}{(1 - \frac{y}{2})} \left\{ \ln \left[ \frac{2}{y} \left( 1 - \frac{y}{2} + \sqrt{1 - y} \right) \right] - \sqrt{1 - y} \right\}$$

where  $y = \frac{4M_Z^2}{s}$  and  $\frac{G^2 M_Z^2}{4\pi} = 35.2 pb$ .

These cross-section values are plotted in Fig.1. The asymptotic behavior of this function is proportional to  $\sim (\frac{M_W^2}{s}) \ln(\frac{s}{M_W^2})$  for  $s \gg M_Z^2$ .

A nucleon arising from WW and ZZ hadronic decay could provide a reasonable solution to the UHECR events above GZK. We assume that the fraction of pions and nucleons related to the total number of particles from the W boson decay is almost the same as in the Z decay boson. So each W hadronic decay (Probability  $P \sim 0.68$ ) leads on average to about 37 particles, where  $\langle n_{\pi^0} \rangle \sim 9.19$ ,  $\langle n_{\pi^\pm} \rangle \sim 17$ , and  $\langle n_{p,\bar{p},n,\bar{n}} \rangle \sim 2.7$ . In addition we have to expect by the subsequent decays of  $\pi$ 's (charged and neutral), kaons and resonances ( $\rho, \omega, \eta$ ) produced, a flux of secondary UHE photons and electrons. On average it results [57] that the energy in the bosons decay is not uniformly distributed among the particles. Each charged pion will give an electron (or positron) and three neutrinos, that will have less than one per cent of the initial W boson energy, while each  $\pi^0$  decays in two photons, each with 1 per cent of the initial W energy. In the Tab.1 we show all the channel reactions leading from single Z in nuclear and electro-magnetic components up to the observed UHECR; in the same Tab.2 we follow the chain reaction and the probability for the scattering event assuming a low relic neutrino mass  $m_\nu \simeq 0.154 eV$  and a neutrino number density contrast in local group halo  $\delta n_\nu/n_\nu \simeq 40$ .

### 2.7. The t-channel process $\nu_i \bar{\nu}_{jr} \rightarrow l_i \bar{l}_j$

Processes  $\nu_i \bar{\nu}_{jr} \rightarrow l_i \bar{l}_j$  ( $i \neq j$ ) (like  $\nu_\mu \bar{\nu}_\tau \rightarrow \mu \bar{\tau}$  for example) occur through the W boson exchange in the t-channel. The cross-section has been derived in [20], while the energy threshold depends on the mass of the heavier lepton produced,

$E_{\nu_{th}} = 3.95 \cdot 10^{18} eV (m_\nu / 0.4 eV)^{-1} (m_{\tau,\mu,e} / m_\tau)^2$ , with the term  $(m_\tau / m_{\tau,\mu,e})$  including the different thresholds in all the possible interactions:  $\nu_\tau \bar{\nu}_\mu$  (or  $\nu_\tau \bar{\nu}_e$ ),  $\nu_\mu \bar{\nu}_e$ , and  $\nu_e \bar{\nu}_e$ .

We could consider the reactions  $\nu_i \bar{\nu}_j \rightarrow l_i \bar{l}_j$  ( $i = j$ ), keeping both s channel and t channel, while in reactions  $\nu_i \bar{\nu}_j \rightarrow l_i \bar{l}_j$  ( $i \neq j$ ) do occur only via t channel.

In the ultra-relativistic limit ( $s \simeq 2E_\nu m_{\nu_r} \gg M_W^2$  where  $\nu_r$  refers to relic clustered neutrinos) the cross-section tends to the asymptotic value  $\sigma_{\nu \bar{\nu}_r} \simeq 108.5 pb$ .

$$\sigma_W(s) = \sigma_{asym} \frac{A(s)}{s} \left\{ 1 + \frac{M_W^2}{s} \cdot \left[ 2 - \frac{s + B(s)}{A(s)} \ln \left( \frac{B(s) + A(s)}{B(s) - A(s)} \right) \right] \right\}$$

where  $\sigma_{asym}$  is the asymptotic behaviour of the cross section in the ultra-relativistic limit and where  $\sqrt{s}$  is the center of mass energy, the functions A(s), B(s) are defined as

$$A(s) = \sqrt{[s - (m_\tau + m_\mu)^2][s - (m_\tau - m_\mu)^2]}$$

$$B(s) = s + 2M_W^2 - m_\tau^2 - m_\mu^2$$

and

$$s \simeq 2E_\nu m_\nu = 2 \cdot 10^{23} \frac{E_\nu}{10^{22} eV} \frac{m_\nu}{10 eV} eV^2 \gg M_W^2. \quad (7)$$

These t-channel interactions lead to electro-magnetic showers and do not offer any nuclear secondary able to explain UHECR events.

### 3. Boosted Z-UHECR spectra

Let us examine the destiny of UHE primary particles (nucleons, electrons and photons) ( $E_e \lesssim 10^{21} eV$ ) produced after hadronic or leptonic W decay. As we have already noticed in the introduction, we'll assume that the nucleons, electrons and photons spectra (coming from W or Z decay) after  $\nu\nu$  scattering in the halo, follow a power law that in the center of mass system is  $\frac{dN^*}{dE^* dt^*} \simeq E^{*- \alpha}$  where  $\alpha \sim 1.5$ . This assumption is based on detailed Monte Carlo simulation of a heavy fourth generation neutrino annihilations [50] [19] [23] and with the model of quark - hadron fragmentation spectrum suggested by Hill [52].

In order to determine the shape of the particle spectrum in the laboratory frame, we have to introduce the Lorentz relativistic transformations from the center of mass system to the laboratory system. The number of particles is clearly a relativistic invariant  $dN_{lab} = dN^*$ , while the relation between the two time intervals is  $dt_{lab} = \gamma dt^*$ , the energy changes like  $\epsilon_{lab} = \gamma \epsilon^* (1 + \beta \cos \theta^*) = \epsilon^* \gamma^{-1} (1 - \beta \cos \theta)^{-1}$ , and finally the solid angle in the laboratory frame of reference becomes  $d\Omega_{lab} = \gamma^2 d\Omega^* (1 - \beta \cos \theta)^2$ . Substituting these relations one obtains

$$\left( \frac{dN}{d\epsilon dt d\Omega} \right)_{lab} = \frac{dN^*}{d\epsilon^* dt^* d\Omega^*} \gamma^{-2} (1 - \beta \cos \theta)^{-1} = \frac{\epsilon_*^{-\alpha} \gamma^{-2}}{4\pi} \cdot (1 - \beta \cos \theta)^{-1} = \frac{\epsilon^{-\alpha} \gamma^{-\alpha-2}}{4\pi} (1 - \beta \cos \theta)^{-\alpha-1}$$

and integrating over  $\theta$  (omitting the lab notation) one loses the spectrum dependence on the angle.

The consequent fluence derived by the solid angle integral is:

$$\frac{dN}{d\epsilon dt} \epsilon^2 = \frac{\epsilon^{-\alpha+2} \gamma^{\alpha-2}}{2\beta\alpha} [(1+\beta)^\alpha - (1-\beta)^\alpha] \simeq \frac{2^{\alpha-1} \epsilon^{-\alpha+2} \gamma^{\alpha-2}}{\alpha}$$

There are two extreme cases to be considered: the case where the interaction occurs at Z peak resonance and therefore the center of mass Lorentz factor  $\gamma$  is frozen at a given value (eq.1) and the case (WW,ZZ pair channel) where all energies are allowable and  $\gamma$  is proportional to  $\epsilon^{1/2}$ . Here we focus only on Z peak resonance. The consequent fluence spectrum  $\frac{dN}{d\epsilon dt} \epsilon^2$ , as above, is proportional to  $\epsilon^{-\alpha+2}$ . Because  $\alpha$  is nearly 1.5 all the consequent secondary particles will also show a spectra proportional to  $\epsilon^{1/2}$  following normalized energies in Tab.1 as shown in Fig.(2-6). In the latter case (WW,ZZ pair channel), the relativistic boost reflects on the spectrum of the secondary particles, and the spectra power law becomes  $\propto \epsilon^{\alpha/2+1} = \epsilon^{0.25}$ . These channels will be studied in details elsewhere. In Fig.(2 -6) we show the spectra of protons, photons and electrons coming from Z hadronic and leptonic decay assuming a nominal primary CR energy flux  $\sim 20 \text{ eV s}^{-1} \text{ sr}^{-1} \text{ cm}^{-2}$ , due to the total  $\nu\bar{\nu}$  scattering at GZK energies as shown in Fig.(2-6). We assume an interaction probability  $P \equiv \sigma_{\nu-\nu} n_\nu l_{halo}$ , for a relic halo neutrino density contrast  $n_\nu/n_{\nu-cosmic} \sim 40$ , and integral distance  $l_{halo} \sim 3 \text{ Mpc}$  whose peak value is  $P \sim 8 \cdot 10^{-3}$  and a corresponding UHE incoming neutrino energy flux  $\sim 2200 \text{ eV s}^{-1} \text{ sr}^{-1} \text{ cm}^{-2}$  near but below present UHE neutrino flux bound from AMANDA,MACRO, Baikal as well as Goldstone data. The same probability result  $P \sim 8 \cdot 10^{-3}$  may be obtained assuming a lower neutrino number contrast but a longer (up to factor ten) integral halo distance:  $n_\nu/n_{\nu-cosmic} \sim 4$ ,  $l_{halo} \sim 30 \text{ Mpc}$ , just within the GZK cut-off maximal distance. The product of such primary UHE neutrino fluxes with the above probability leads to the primary Z-Showering peak at energies  $\sim 20 \text{ eV cm}^{-2} \text{ s}^{-1} \text{ sr}^{-1} \text{ cm}^{-2}$  at  $\sim 10^{22} \text{ eV}$  observed in UHECR nucleon flux peak  $\sim 1.2 \text{ eV cm}^{-2} \text{ s}^{-1} \text{ sr}^{-1} \text{ cm}^{-2}$  at  $\sim 10^{20} \text{ eV}$  in AGASA data. On the contrary for the much lower and last HIRES reports the observed flux of UHECR are an order of magnitude below  $\sim 0.1 - 0.2 \text{ eV cm}^{-2} \text{ s}^{-1} \text{ sr}^{-1} \text{ cm}^{-2}$ , and they may simply require either a lower relic neutrino density contrast (within 0.4eV neutrino mass model) or (within the same density contrast), or (and) a lower incoming neutrino flux, and/or just a larger ( $m_\nu \sim 1.2 \text{ eV}$ ) relic neutrino mass (see Fig.3).

UHE electrons and photons are mostly produced by charged and neutral pions. From Tab.2, one can see that, on average, the ratio  $E_e^{\pi^\pm}/E_\gamma^{\pi^0} \sim 2$ . While the  $dN/dE \times E^2$  for photons (by W (or Z) decay) is almost one order of magnitude greater than the corresponding nucleon spectra.

The gamma (MeV - TeV) galactic background could present a component due to UHE electron interactions in our galactic halo. The initial energy of the ultra-relativistic particle is gradually converted in gamma photons through different steps involving radiative processes as synchrotron radiation and electron pair production (see Fig.7-Fig.8).

An electron lifetime in the Galaxy is approximately given by

$$\tau_e \simeq \frac{2.8 \cdot 10^{12}}{\gamma} \text{ yr}$$

that means for electron energy  $E_e \sim 10^{16} \text{ eV}$  a characteristic time scale:  $\tau \sim 10^{-4} \text{ yr}$ .

We considered as final electron production channel the reaction  $\nu_e \nu_\tau$  (Tab.1) through W exchange whose probability is one order of magnitude higher than channel  $\nu_\mu \nu_\mu \rightarrow W^+ W^-$  introduced as the mechanism able to produce Fly's Eye event at  $3.2 \cdot 10^{20} \text{ eV}$ . In Tab.2 we

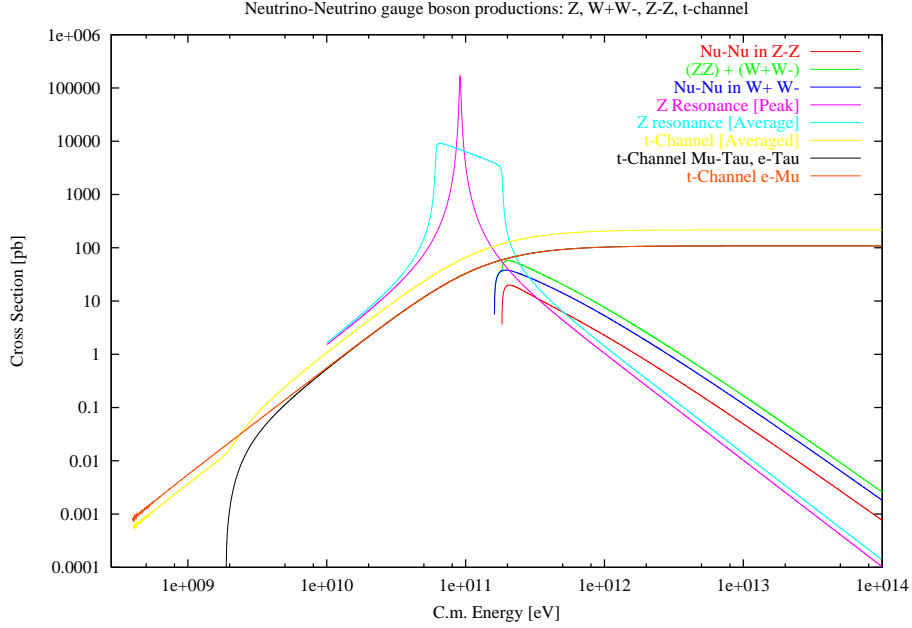


**Figure 1.** The neutrino-relic neutrino cross-sections at center of mass energy. The Z-peak energy will be smoothed into the inclined-tower curve, while the WW and ZZ channel will guarantee a Showering also above a  $2eV$  neutrino masses. The presence of t-channel plays a role in electromagnetic showering at all energies above the Z-peak.

Secondaries by $\nu\nu \rightarrow Z$ Interactions: $E_\nu = 10^{22}eV$ , Fluence $F_\nu = 2000eVcm^{-2}s^{-1}$ , ( $m_\nu = 0.4 eV$ )					
	Multiplicity	Energy (%)	$\sum E_{CM}(GeV)$	Peak Energy (EeV)	$\frac{dN}{dE} E^2$ (eV)
$p$	2.7	6 %	5.4	$2.2 \cdot 10^2$	1.2
$\pi_0$	13	21.4 %	19.25	$1.9 \cdot 10^2$	4.25
$\gamma_{\pi^0}$	26	21.4 %	19.25	95	4.25
$\pi^\pm$	26	42.8 %	38.5	$1.9 \cdot 10^2$	4.25
$(e^+e^-)_\pi$	26	12 %	11	50	2.3
$(e^+e^-)_{prompt}$	2	3.3 %	2.7	$5 \cdot 10^3$	1.32
$(e^+e^-)_\mu$	2	1.1 %	0.9	$1.6 \cdot 10^3$	0.45
$(e^+e^-)_\tau$	2	1.5 %	1.3	$1.2 \cdot 10^3$	0.6

**Table 1.** The total detailed energy percentage distribution into neutrinos, protons, neutral and charged pions and consequent gamma, electron pair particles both from hadronic and leptonic channels. We used LEP data for Z decay. We assumed that on average number of 37 particles produced during a Z (W) hadronic decay. The number of prompt pions both charged (18) and neutral (9), in the hadronic decay is increased by 8 and 4 respectively due to decays of  $K^0$ ,  $K^\pm$ ,  $\rho$ ,  $\omega$ , and  $\eta$ . We assumed that the most energetic neutrinos produced in the hadronic decay mainly come from charged pion decay. So their number is roughly three times the number of  $\pi^0$ 's. UHE photons are mainly relics of neutral pions.

indicate the chain leading to electrons through W W decay. This channel leads to electrons with energies  $E_e \sim 10^{19} \div 10^{20} eV$

### 3.1. TeV tails from UHE electrons in Z-Showers

As it is shown in Tab.2 and Fig.7-8, each electron (positron) energy due to  $\pi^\pm$  decays are around  $E_e \sim 2 \cdot 10^{19} eV$  for an initial  $E_Z \sim 10^{22} eV$  ( and incoming UHE neutrino energy  $E_\nu \sim 10^{22} eV$ ) assuming a nominal target neutrino mass  $m_\nu \simeq 0.4eV$ . Such electron pairs

---

MAIN Z CHANNEL REACTIONS CHAINS FOR FINAL PROTON PRODUCTION

---

Reaction	Probability	Multiplicity	Secondary energy
1d) $p + \gamma \rightarrow (p, n) + 9\pi$	$P_{1d} \simeq 1$	$M_{1d} = 6$	$E_\pi \sim \frac{E_p}{10}$
2d) $\pi^+ \rightarrow \mu^+ + \nu_\mu$ $\pi^- \rightarrow \mu^- + \bar{\nu}_\mu$	$P_{2d} \simeq 1$	$M_{2d} = 1$	$E_\nu \sim 0.21E_\pi = 2.1 \cdot 10^{-2} E_p$
2d') $\mu^+ \rightarrow e^+ + \nu_e + \bar{\nu}_\mu$ $\mu^- \rightarrow e^- + \bar{\nu}_e + \nu_\mu$	$P_{2d'} \simeq 1$	$M_{2d'} = 1$	$E_\nu \sim 0.26E_\pi = 2.6 \cdot 10^{-2} E_p$
3d) $\nu_\mu + \bar{\nu}_{\mu_r} \rightarrow Z^* \rightarrow 2p + X$ $\bar{\nu}_\mu + \nu_{\mu_r} \rightarrow Z^* \rightarrow 2p + X$	$P_{\nu\nu} = \sigma_{\nu_\mu \bar{\nu}_\mu} n_{\nu_r} l_g \sim 10^{-3}$	$M_{3d} = 2$	$E_p \sim \frac{E_{\nu\mu}}{80} \sim 2.6 \cdot 10^{-4} E_p$
3d') $\nu_\mu + \bar{\nu}_{\mu_r} \rightarrow Z^* \rightarrow 2p + X$ $\bar{\nu}_\mu + \nu_{\mu_r} \rightarrow Z^* \rightarrow 2p + X$	$P_{\nu\nu} = \sigma_{\nu_\mu \bar{\nu}_\mu} n_{\nu_r} l_g \sim 8 \cdot 10^{-4}$	$M_{3d'} = 2$	$E_p \sim \frac{E_{\nu\mu}}{83} \sim 3.15 \cdot 10^{-4} E_p$
finally: eq.(1d)	$\boxed{d P_{tot}^Z = \Pi_i M_i P_i \sim 4 \cdot 10^{-3}}$		$\boxed{E_p^Z \sim 10^{24} eV}$
	$\boxed{d' P_{tot}^Z = \Pi_i M_i P_i \sim 8 \cdot 10^{-3}}$		

Additional reactions not included in the present analysis:

Z channels if there is neutrino flavor mixing  $\nu_\mu \leftrightarrow \nu_\tau$

3'd)  
 $\bar{\nu}_\tau + \nu_{\tau_r} \rightarrow Z^* \rightarrow 2p + X$   
 $\nu_\tau + \bar{\nu}_{\tau_r} \rightarrow Z^* \rightarrow 2p + X$

Z channel whose efficiency is however suppressed by lower  $\nu_e, \bar{\nu}_e$  energies and  $n_{\nu_e}, n_{\bar{\nu}_e}$  densities

3''d)  
 $\bar{\nu}_e + \nu_{e_r} \rightarrow Z^* \rightarrow 2p + X$

---

<sup>a</sup> This multiplicity refers only to charged pions

<sup>b</sup> In calculating the probability for the  $\nu\nu$  interaction we assumed here:  $m_{\nu_r} = 0.154eV$ , (nearly twice the observed atmospheric neutrino mass splitting)  $n_{\nu_r} = 2 \cdot 10^3 cm^{-3}$  (a number density contrast above cosmic background  $\simeq 40$ ), the distance integral inside the halo volume  $l_g \sim 10^{25} cm$ .

The  $\sigma_{\nu_\mu \bar{\nu}_\mu}$  value has been obtained from the corresponding cross section and center of mass energy

**Table 2.** Energy peak and energy fluence for different decay channels as described in the text; the energy of the proton and of the pion are respectively the averaged ones observed in LEP data for Z decay .

while not radiating efficiently in extra-galactic magnetic fields will be interacting with the

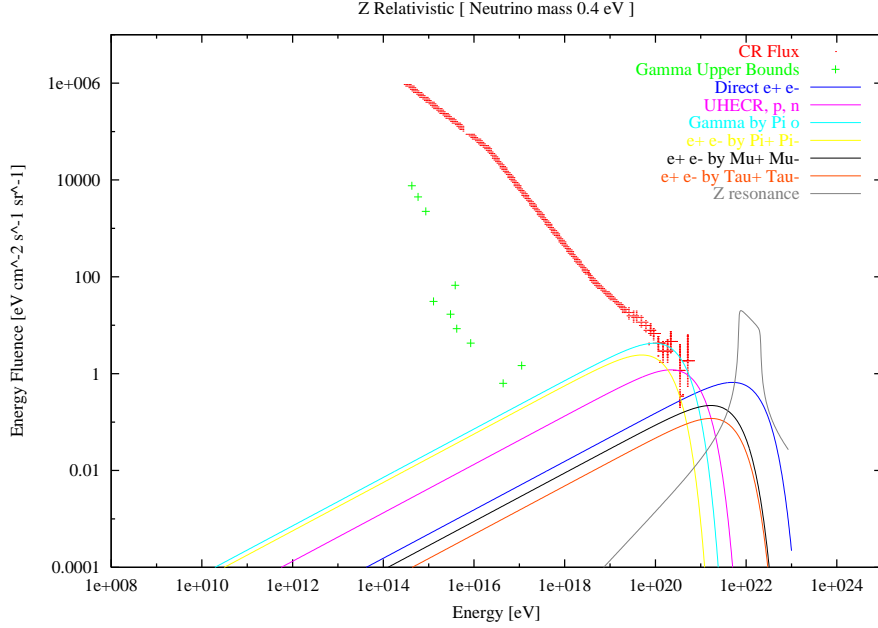


**Figure 2.** Z-Showering Energy Flux distribution for different channels assuming a light (fine tuned) relic neutrino mass  $m_\nu = 0.4eV$  [24], [28],[38]. The total detailed energy percentage distribution into neutrino, protons, neutral and charged pions and consequent gamma, electron pair particles both from hadronic and leptonic Z,  $WW$ ,  $ZZ$  channels. We also calculated the electro-magnetic contribution due to the t-channel  $\nu_i\nu_j$  interactions as described in previous Fig.2. Most of the  $\gamma$  radiation will be degraded around PeV energies by  $\gamma\gamma$  pair production with cosmic 2.75 K BBR, or with cosmic radio background. The electron pairs instead, are mainly relics of charged pions and will rapidly lose energies into synchrotron radiation. Note that the nucleon injection energy fits the present AGASA data as well as the most recent evidence of a corresponding tiny Majorana neutrino mass  $m_\nu \simeq 0.4eV$  [49]. Lighter neutrino masses are able to modulate UHECR at higher energies [28].

galactic magnetic field ( $B_G \simeq 10^{-6} G$ ) leading to direct TeV photons:

$$\begin{aligned}
 E_\gamma^{sync} &\sim \gamma^2 \left( \frac{eB}{2\pi m_e} \right) \sim \\
 &\sim 27.2 \left( \frac{E_e}{2 \cdot 10^{19} eV} \right)^2 \left( \frac{m_\nu}{0.4 eV} \right)^{-2} \left( \frac{B}{\mu G} \right) TeV.
 \end{aligned} \tag{8}$$

The same UHE electrons will radiate less efficiently with extra- galactic magnetic field ( $B_G \simeq 10^{-9} G$ ) leading also to 27.2 GeV photons direct peak. The spectrum of these photons is characterized by a law  $dN/dEdt \sim E^{-(\alpha+1)/2} \sim E^{-1.25}$  where  $\alpha$  is the power law of the electron spectrum, and it is showed in Fig.2-6 above. As regards the prompt electrons at higher energy ( $E_e \simeq 10^{21} eV$ ), in particular in the t-channels, their interactions with the extra-galactic field first and galactic magnetic fields later are sources of another kind of synchrotron emission around energies  $E_\gamma^{sync}$  of tens PeV:

$$\sim 6.8 \cdot 10^{13} \left( \frac{E_e}{10^{21} eV} \right)^2 \left( \frac{m_\nu}{0.4 eV} \right)^{-2} \left( \frac{B}{nG} \right) eV \tag{9}$$

$$\sim 6.8 \cdot 10^{16} \left( \frac{E_e}{10^{21} eV} \right)^2 \left( \frac{m_\nu}{0.4 eV} \right)^{-2} \left( \frac{B}{\mu G} \right) eV \tag{10}$$

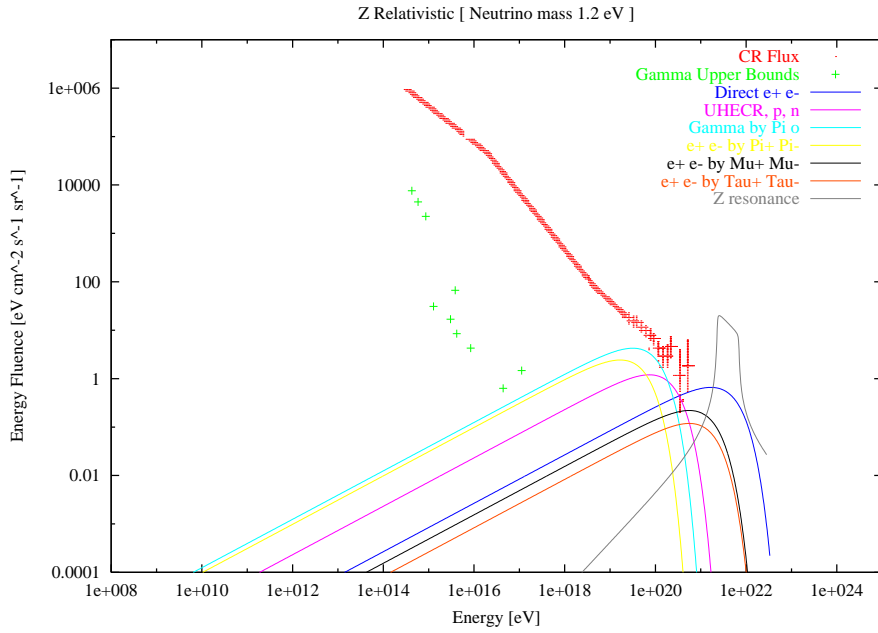


**Figure 3.** Z-Showering Energy Flux distribution for different channels assuming a light (fine tuned) relic neutrino mass  $m_\nu = 1.2\text{eV}$  able to partially fill the highest  $10^{20}\text{eV}$  cosmic ray edges. Note that this value leads to a Z-Knee cut-off, above the GZK one, well tuned to present Hires data [28], [46].

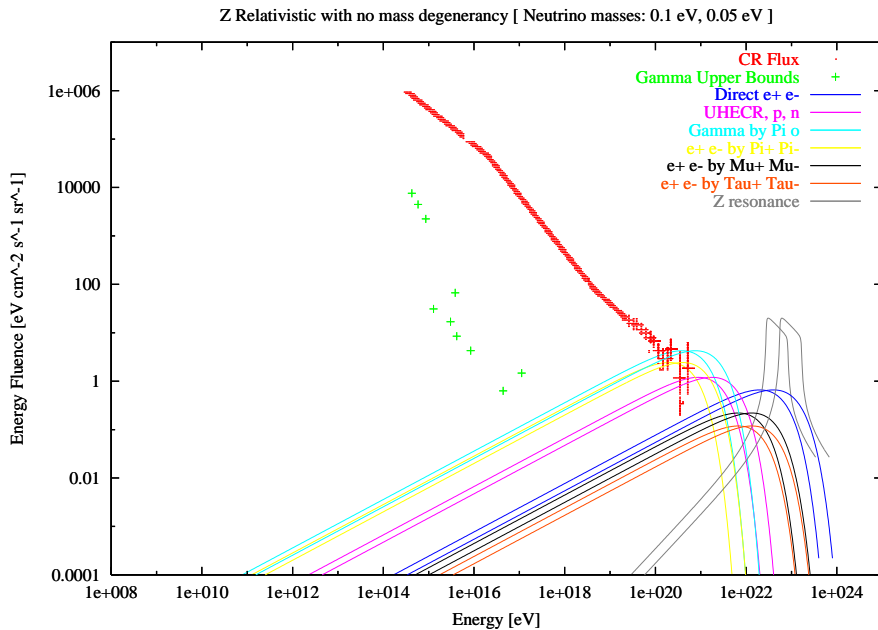


**Figure 4.** Z-Showering Energy Flux distribution for different channels assuming a non degenerated twin light neutrino masses near atmospheric splitting mass values  $m_\nu = 0.1\text{eV}, m_\nu = 0.05\text{eV}$  able to partially fill the highest  $10^{20}\text{eV}$  cosmic ray edges. [28], [46].

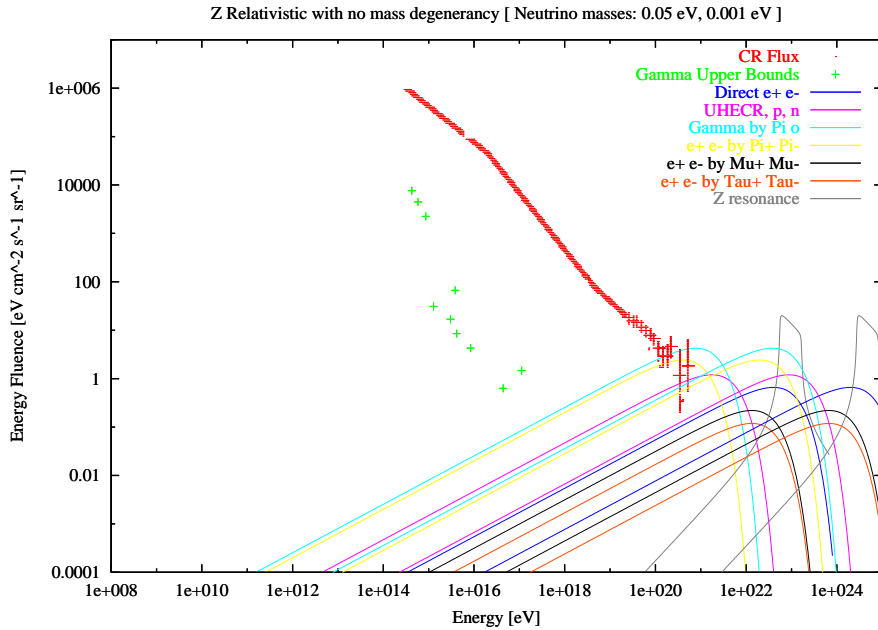


**Figure 5.** Z-Showering Energy Flux distribution for different channels assuming a lightest relic neutrino mass  $m_\nu = 0.05eV$  (atmospheric neutrino mass),  $m_\nu = 0.001eV$ , just a small fraction (a seventh part) of the minimal solar neutrino mass split, able to partially fill the highest  $10^{20}eV$  cosmic ray edges; [40],[39],[61] and most recent claims by KamLAND [47]. Note that no suppression for neutrino density has been assumed here.[28], [46].

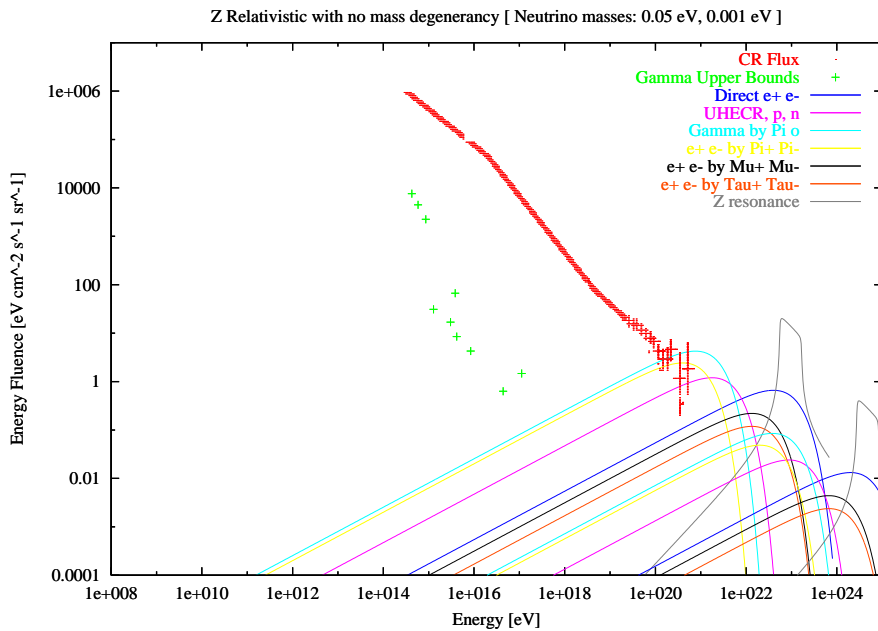


**Figure 6.** Z-Showering Energy Flux distribution for different channels assuming a lightest relic neutrino mass  $m_\nu = 0.05eV$  (atmospheric neutrino mass),  $m_\nu = 0.001eV$  ( just a small fraction (a seventh part) of the minimal solar neutrino mass split) able to partially fill the highest  $10^{20}eV$  cosmic ray edges. Note that here a realistic suppression for lightest neutrino density has been assumed. [28], [46].

The corresponding rate of energy loss is [45]

$$\left(\frac{1}{E} \frac{dE}{dt}\right)^{-1} = 3.8 \times \left(\frac{E}{10^{21}}\right)^{-1} \left(\frac{B}{10^{-9}G}\right)^{-2} \text{ kpc.} \quad (11)$$

For the first case the interaction length is few Kpcs while in the second one in few days light flight (see Fig7-Fig.8). Again one has the same power law characteristic of a synchrotron spectrum with index  $E^{-(\alpha+1/2)} \sim E^{-1.25}$ . Photons at  $10^{16} \div 10^{17}$  eV scatter onto low-energy photons from isotropic cosmic background ( $\gamma + BBR \rightarrow e^+e^-$ ) converting their energy in electron pairs. The expression for the pair production cross-section is:

$$\sigma(s) = \frac{1}{2} \pi r_0^2 (1 - v^2) \left[ (3 - v^4) \ln \frac{1 + v}{1 - v} - 2v(2 - v^2) \right] \quad (12)$$

where  $v = (1 - 4m_e^2/s)^{1/2}$ ,  $s = 2E_\gamma \epsilon (1 - \cos \theta)$  is the square energy in the center of mass frame,  $\epsilon$  is the target photon energy,  $r_0$  is the classic electron radius, with a peak cross section value at

$$\frac{4}{137} \times \frac{3}{8\pi} \sigma_T \ln 183 = 1.2 \times 10^{-26} \text{ cm}^2$$

Because the corresponding attenuation length due to the interactions with the microwave background is around ten kpc, the extension of the halo plays a fundamental role in order to make this mechanism efficient. As it is shown in the contribution to gamma signals of tens PeV by Z (or W) hadronic decay, could be compatible with actual experimental limits fixed by CASA-MIA detector on such a range of energies. Considering a halo extension  $l_{halo} \gtrsim 100 \text{ kpc}$ , the secondary electron pair creation becomes efficient, leading to a suppression of the signal of tens PeV. So electrons at  $E_e \sim 3.5 \cdot 10^{16} \text{ eV}$  loose again energy through additional synchrotron radiation[45], with maximum  $E_\gamma^{sync}$  around

$$\sim 79 \left(\frac{E_e}{10^{21} \text{ eV}}\right)^4 \left(\frac{m_\nu}{0.4 \text{ eV}}\right)^{-4} \left(\frac{B}{\mu G}\right)^3 \text{ MeV.} \quad (13)$$

Since the relevant signal piles up at TeV it is not able to pollute significantly the MeV-GeV region.

Gamma rays with energies up to 20 TeV have been observed by terrestrial detector only from nearby sources like Mrk 501 ( $z = 0.033$ ) or very recently from MrK 421. This is puzzling because the extra-galactic TeV spectrum should be, in principle, significantly suppressed by the  $\gamma$ -rays interactions with the extra-galactic Infrared background, leading to electron pair production and TeV cut-off. The recent calibration and determination of the infrared background by DIRBE and FIRAS on COBE have inferred severe constrains on TeV propagation. Indeed, as noticed by Kifune [48], and Protheroe and Meyer[59] we may face a severe infrared background - TeV gamma ray crisis. This crisis imply a distance cut-off, incidentally, comparable to the GZK one. Let us remind also an additional evidence for IR-TeV cut-off is related to the possible discover of tens of TeV counterparts of BATSE *GRB970417*, observed by Milagrato[1], being most GRBs very possibly at cosmic edges, at distances well above the IR-TeV cut-off ones. In this scenario it is also important to remind the possibilities that the Fly's Eye event has been correlated to TeV pile up events in HEGRA [44]. The very recent report (private communication 2001) of the absence of the signal few years later at HEGRA may be still consistent with a bounded Z-Showering volume and a limited UHE TeV tail activity. To solve the IR-TeV cut-off one may alternatively invoke unbelievable extreme hard intrinsic spectra or exotic explanation as gamma ray superposition of photons or sacrilegious Lorentz invariance violation.

Let us remind that UHE neutrinos are un-effected by magnetic fields and by BBR screening; they may reach us from far cosmic edges without significant absorption. The UHE

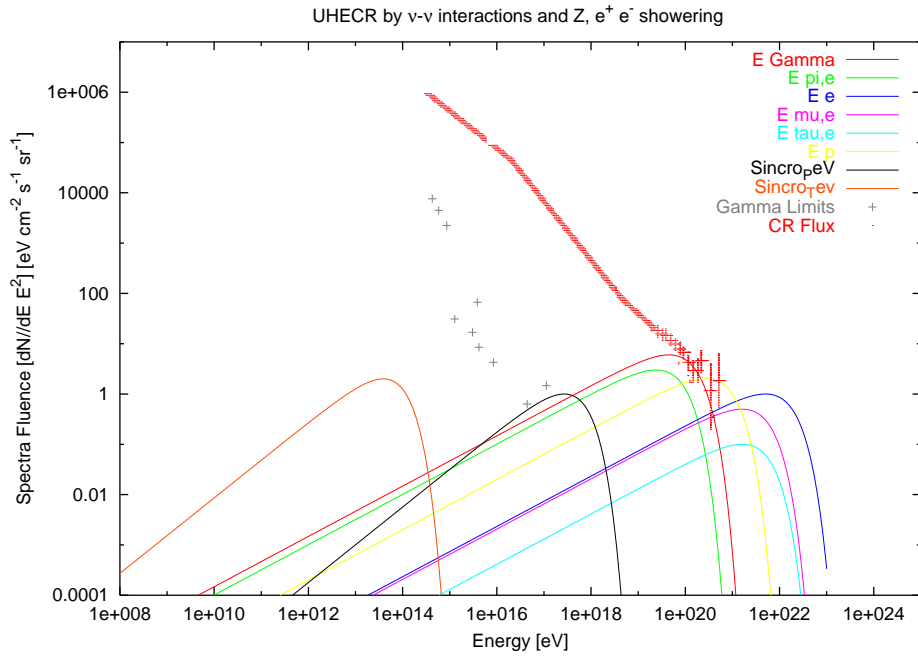


**Figure 7.** Energy fluence by Z showering as in figures above and the consequent  $e^+e^-$  synchrotron radiation

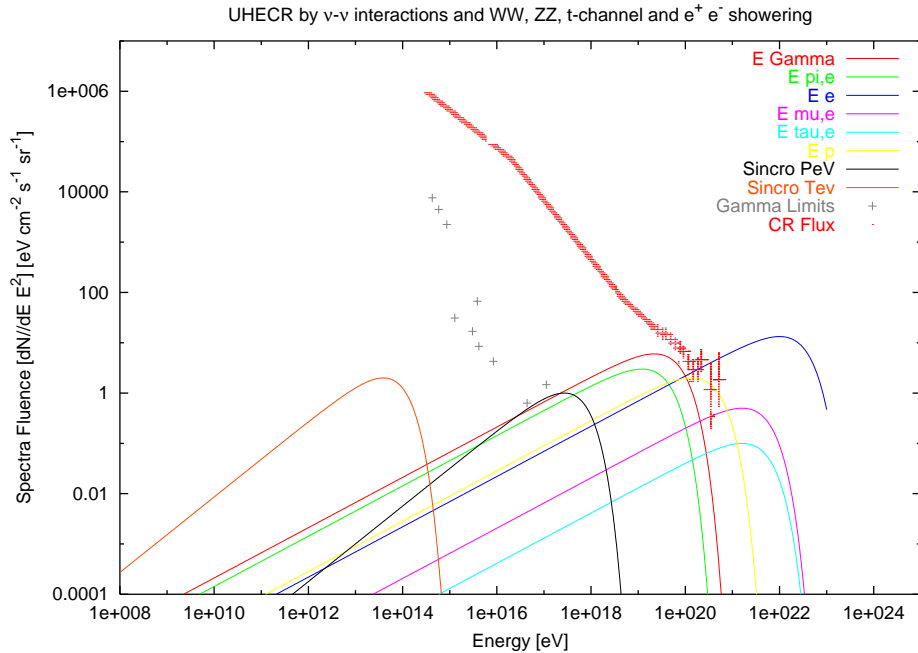


**Figure 8.** Energy fluence by WW, ZZ, t-channel showering and the consequent  $e^+e^-$  synchrotron radiation. The lower energy Z showering is not included to make spectra more understandable.

Z-shower in its ultra-high energy nucleonic secondary component may be just the observed final UHECR event on Earth. This possibility has been reinforced by very recent correlations (doublets and triplets events) between UHECR directions with brightest Blazars sources at

cosmic distances (redshift  $\geq 0.1$ ) quite beyond ( $\geq 300 Mpc$ ) any allowed GZK cut-off [41], [43], [62]. Therefore there might be a role for GZK neutrino fluxes, either at very high fluence as primary in the Z-Showering scenario or, at least, as (but at lower intensities) necessary secondaries of all those UHECR primary absorbed in cosmic BBR radiation fields by GZK cut of. Naturally other solutions as topological defects or primordial relics decay may play a role as a source of UHECR, but the observed clustering [43], [65], [62], seems to favor compact sources possibly overlapping far BL Lac sources [41]. The most recent evidence for self-correlations clustering at  $10^{19}$ ,  $2 \cdot 10^{19}$ ,  $4 \cdot 10^{19}$  eVs energies observed by AGASA (Teshima, ICRR26 Hamburg presentation 2001) maybe a first reflection of UHECR Z-Showering secondaries:  $p, \bar{p}, n, \bar{n}$  [28]. A very recent solution beyond the Standard Model (but within Super-Symmetry) consider Ultra High Energy Gluinos as the neutral particle bearing UHE signals interacting nearly as a hadron in the terrestrial atmosphere [7]; this solution has a narrow window for gluino masses allowable (and serious problems in production bounds), but it is an alternative that deserves attention. To conclude this brief Z-Shower model survey one finally needs to scrutiny the UHE  $\nu$  astronomy and to test the GZK solution within Z-Showering Models by any independent search on Earth for such UHE neutrinos traces above PeV reaching even EeV-ZeV extreme energies.

#### 4. UHE $\nu$ Astronomy by $\tau$ air-shower: the ideal amplifier

Recently [22], [30] a new competitive UHE  $\nu$  detection has been proposed. It is based on ultra high energy  $\nu_\tau$  interaction in matter and its consequent secondary  $\tau$  decay (different  $\tau$  decay channels are given in Tab.3) in flight while escaping from the rock (Mountain Chains, Earth Crust) or water (Sea,Ice) in air leading to UPward or HORizontal TAU air-showers (UPTAU's and HORTAU's), [26], [27]. In a pictorial way one may compare the UPTAU's and HORTAU's as the double bang processes expected in  $km^3$  ice-water volumes [56] : the double bang is due first to the UHE  $\nu_\tau$  interaction in matter and secondly by its consequent  $\tau$  decay in flight. Here we consider a (hidden) UHE  $\nu$ -N Bang *in* (the rock-water within a mountain or the Earth Crust) and a  $\tau$  bang *out* in air, whose shower is better observable at high altitudes. A similar muon double bang amplifier is not really occurring because of the extremely large decay length of ultra-relativistic ( $\gtrsim 10^{13}$  eV) muons. The main power of the UPTAU's and HORTAU's detection is the huge amplification of the UHE neutrino signal, which may deliver almost all its energy in numerous secondaries traces (Cherenkov light, gamma, X photons, electron pairs, collimated muon bundles) in a wider cone volume. Indeed the multiplicity in  $\tau$  air-showers secondary particles,  $N_{opt} \simeq 10^{12}(E_\tau/PeV)$ ,  $N_\gamma(< E_\gamma > \sim 10 MeV) \simeq 10^8(E_\tau/PeV)$ ,  $N_{e^-e^+} \simeq 2 \cdot 10^7(E_\tau/PeV)$ ,  $N_\mu \simeq 3 \cdot 10^5(E_\tau/PeV)^{0.85}$  facilitates the UPTAU's-HORTAU's discovery. These HORTAU's, also named Skimming neutrinos [36], studied also in peculiar approximation in the frame of AUGER experiment, in proximity of Ande Mountain Chains (see Fig.9) [22], [8], may be also originated on front of large volcano [22], [53] either by  $\nu_\tau N$ ,  $\bar{\nu}_\tau N$  interactions as well as by  $\bar{\nu}_e e \rightarrow W^- \rightarrow \bar{\nu}_\tau \tau$ . Also UHE  $\nu_\tau N$ ,  $\bar{\nu}_\tau N$  at EeV may be present in rare AGASA Horizontal Shower (one single definitive event observed was used as an upper bound on EeV neutrino flux [69]) facing Mountain Chain around the Akeno Array (see Fig.9). This new UHE  $\nu_\tau$  detection is mainly based on the oscillated UHE neutrino  $\nu_\tau$  originated by more common astrophysical  $\nu_\mu$ , secondaries of pion-muon decay at PeV-EeV-GZK energies. The existence of these oscillations can be provided by Super Kamiokande evidences for flavor mixing within GeVs atmospheric neutrino data [39] as well as by recent evidences of complete solar neutrino mixing observed by SNO detector [4] and by most recent claims on the disappearance of neutrino fluence from nearby nuclear reactors [47]. Let us remind that HORTAU's (see Fig.9) from mountain chains must nevertheless occur, even for no flavor mixing, as being inevitable  $\bar{\nu}_e$  secondaries of common

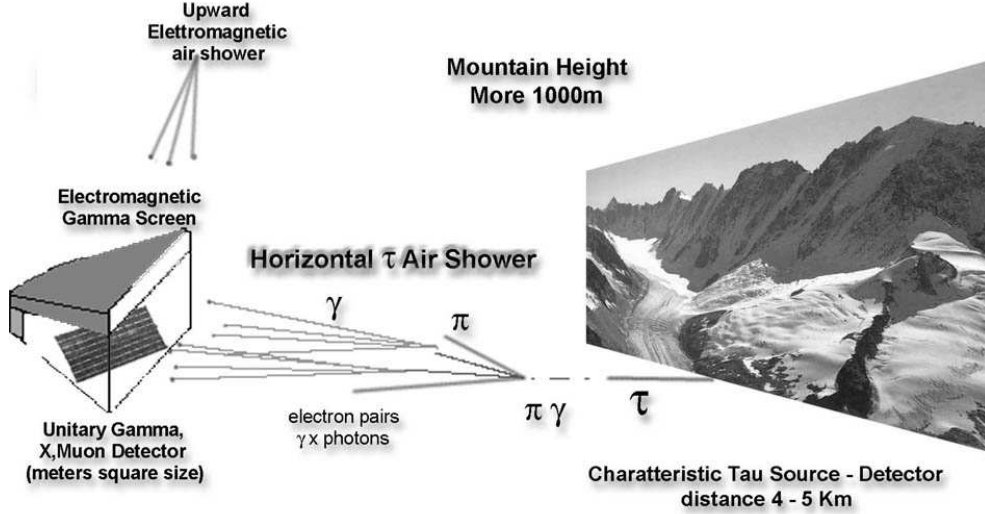


**Figure 9.** The Horizontal Tau on front of a Mountain Chain; different interaction lengths will reflect in different events rate [22], [30].

pion-muon decay chains ( $\pi^- \rightarrow \mu^- + \bar{\nu}_\mu \rightarrow e^- + \bar{\nu}_e$ ) near the astrophysical sources at PeV energies. These PeV  $\bar{\nu}_e$  are mostly absorbed by the Earth and are only rarely arising as UPTAUs (see Fig.10-11 and cross-section in Fig.12). Their Glashow resonant interaction allow them to be observed as HORTAUs only within very narrow and nearby crown edges at horizons (not to be discussed here).

At wider energies windows ( $10^{14}eV - 10^{20}eV$ ) only neutrino  $\nu_\tau, \bar{\nu}_\tau$  play a key role in UPTAUs and HORTAUs. These Showers might be easily detectable looking downward the Earth's surface from mountains, planes, balloons or satellites observer. Here the Earth itself acts as a "big mountain" or a wide beam dump target (see Fig.10-11). The present upward  $\tau$  at horizons should not be confused with an independent and well known, complementary (but rarer) Horizontal Tau air-shower originated inside the same terrestrial atmosphere: we may refer to it as to the Atmospheric Horizontal Tau air-shower. These rare events are responsible for very rare double bang in air. Their probability to occur, as derived in detail in next paragraph (summarized in the last column of Tab.5 below, labeled as R, being the ratio between the events caused by HORTAUs in the ground and such events occurring in the air) is more than two order magnitude below the event rate of HORTAUs. The same UPTAUs (originated in Earth Crust) have a less competitive upward showering due to  $\nu_e \bar{\nu}_e$  interactions within atmosphere, showering in thin upward air layers [6]: this atmospheric Upward Tau presence is a very small additional contribute, because rocks are more than 3000 times denser than the air, see Tab.5. Therefore at different heights we need to estimate (See for detail next paragraph) the UPTAUs and HORTAUs event rate occurring along the thin terrestrial crust below the observer, keeping care of their correlated variables: from a very complex sequence of functions we shall be able to define and evaluate the effective HORTAUs volumes keeping care of the thin shower beaming angle, atmosphere opacity and detector thresholds. At the end of the study, assuming any given neutrino flux, one might be easily able to estimate at each height  $h_1$  the expected event rate and the ideal detector size and sensibility for most detection techniques (Cherenkov, photo-luminescent, gamma rays, X-ray, muon bundles). The Upcoming Tau air-showers and Horizontal ones may be already recorded as Terrestrial Gamma Flashes (see TGF Recorded Data in Tab.4 ) as shown by their partial



**Figure 10.** The Upward Tau air-shower UPTAU and its open fan-like jets due to geo-magnetic bending at high quota. The gamma Shower is pointing to an orbital satellite detector as old GRO-BATSE or very recent Integral [30], [26], [27].

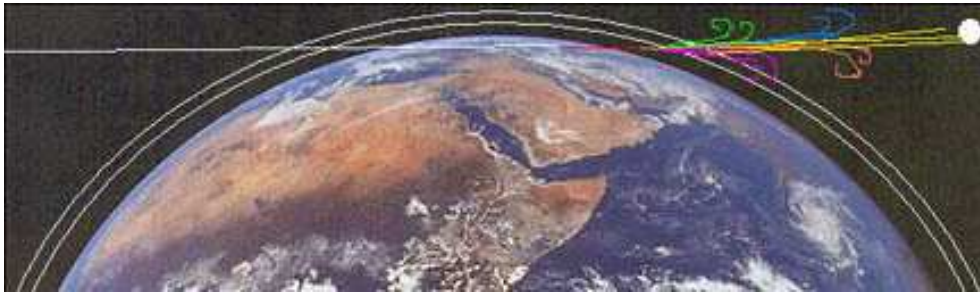


**Figure 11.** The Horizontal-Shower HORTAU and its open fan-like jets due to geo-magnetic bending at high quota. The gamma Shower is pointing to an orbital satellite detector as old GRO-BATSE or very recent Integral just at the horizons [30], [26], [27].

Galactic signature shown in Fig.14 (over EGRET celestial background) and in Fig.15(over EeV anisotropy found by AGASA).

#### 4.1. Ultra High Energy $\nu_\tau$ astronomy by Upward and Horizontal $\tau$ , UPTAU $s$ -HORTAU $s$ , detection

The  $\tau$  airshowers are observable at different height  $h_1$  leading to different underneath observable terrestrial areas and crust volumes. HORTAU $s$  in deep valley are also related to the peculiar geographical morphology and composition [30]. We remind in this case the very important role of UHE  $\bar{\nu}_e e \rightarrow W^- \rightarrow \bar{\nu}_\tau \tau^-$  channels which may be well observable even in absence of any  $\nu_\tau$ ,  $\bar{\nu}_\tau$  UHE sources or any neutrino flavor mixing: its Glashow peak resonance makes these neutrinos unable to cross all the Earth across but it may be observable beyond mountain chain [30]; while testing  $\tau$  air-showers beyond a mountain chain one must consider the possible amplification of the signal because of possible New TeV Physics (see cross-section in Fig.12)[30]. In the following we shall consider in general the main  $\nu_\tau N$ ,  $\bar{\nu}_\tau N$  nuclear interactions on the Earth crust. It should be kept in mind also that UPTAU $s$  and in particular HORTAU $s$  are showering at very low densities and their geometrical escaping opening angle from Earth (here assumed at far distances  $\theta \sim 1^\circ$  for rock and  $\theta \sim 3^\circ$  for water) is not in general conical (like common down-ward showers) but their ending tails are more shaped in thin fan-like twin Jets . These showers will be opened in a characteristic twin fan-jet ovals looking like the 8-shape, bent and split in two thin elliptical beams by the

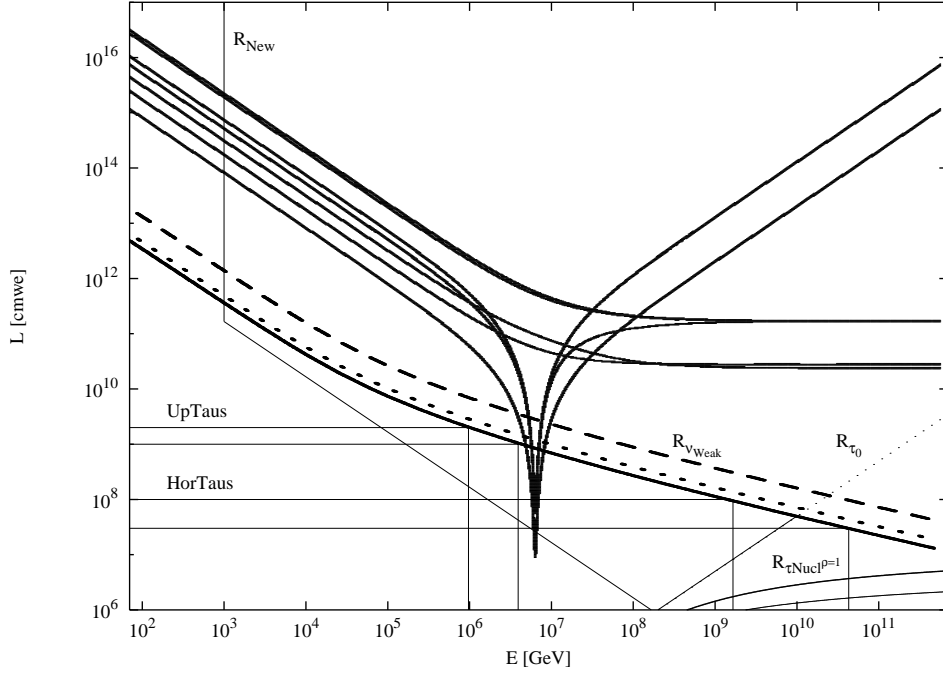


**Figure 12.** Different interaction lengths for Ultra High Energy Neutrinos, reflecting in differences of event rates either for Horizontal Shower from Mountain Chains as well as from Upward and Horizontal ones from Earth Crust. A severe decrease of the neutrino interaction length,  $R_{New}$ , is due to a New TeV gravity interaction. This interaction increases by 2 – 3 order of magnitude the neutrino birth probability (in respect to known interactions), leading to expected tens of thousand events a year (in respect to a hundred a year). Here it has been considered a ten-km length Array detector on front of a Mountain Chain, see Fig.9, assuming a cosmic neutrino fluence of  $10^3 eV cm^{-2} s^{-1}$  [30], [69].

geo-magnetic fields. These fan shapes are not widely open by the Terrestrial Magnetic Fields while along the North-South magnetic field lines. These UPTAUs-HORTAUs duration times are also much longer than common down-ward showers because their showering occurs at much lower air density and they are more extended: from microsecond in the case of UPTAUs reaching from mountains to millisecond in the case of UPTAUs and HORTAUs originated on Earth and observed from satellites. Indeed the GRO observed upcoming Terrestrial Gamma Flashes which are possibly correlated with the UPTAUs [30]; these events show the expected millisecond duration times. In order to estimate the rate and the fluence of UPTAUs and HORTAUs one has to estimate the observable crown terrestrial crust mass, facing a complex chain of questions, leading for each height  $h_1$ , to an effective observable surface and volume from where UPTAUs and HORTAUs might be originated. From this effective volume it is easy to estimate the observable rates, assuming a given incoming UHE  $\nu$  flux model for galactic or extragalactic sources. Here we shall only refer (see Appendices A-B) to the Masses estimate unrelated to any UHE  $\nu$  flux models.

#### 4.2. Tau air showers to discover UHE $\nu$ : UHE $\tau$ decay channels

The  $\tau$  air-shower morphology would reflect the rich and structured behaviors of  $\tau$  decay modes. Indeed let us label the main "eight finger" UHE decay channels (hadronic or electromagnetic) and the consequent air-shower imprint, with corresponding probability ratio as shown in the Tab.3.

This complex air-shower modes would exhibit different interaction lengths in air at 1

atmosphere ( $\sim 300$  meters for electromagnetic interaction length, 500 meters for hadronic interaction length or, more precisely 800 meters for  $\tau$  pions secondaries). The consequent air-shower statistics will reflect these imprint multi-channel modes also in its energy and structured time arrival to detectors beyond mountains, on planes, balloons or satellites. Possibly these channels may also be reflected in observed terrestrial Gamma Flashes.

Decay	Secondaries	Probability	Air-shower
$\tau \rightarrow \mu^- \bar{\nu}_\mu \nu_\tau$	$\mu^-$	$\sim 17.4\%$	Unobservable
$\tau \rightarrow e^- \bar{\nu}_e \nu_\tau$	$e^-$	$\sim 17.8\%$	1 Electromagnetic
$\tau \rightarrow \pi^- \nu_\tau$	$\pi^-$	$\sim 11.8\%$	1 Hadronic
$\tau \rightarrow \pi^- \pi^0 \nu_\tau$	$\pi^-, \pi^0 \rightarrow 2\gamma$	$\sim 25.8\%$	1 Hadronic, 2 Electromagnetic
$\tau \rightarrow \pi^- 2\pi^0 \nu_\tau$	$\pi^-, 2\pi^0 \rightarrow 4\gamma$	$\sim 10.79\%$	1 Hadronic, 4 Electromagnetic
$\tau \rightarrow \pi^- 3\pi^0 \nu_\tau$	$\pi^-, 3\pi^0 \rightarrow 6\gamma$	$\sim 1.23\%$	1 Hadronic, 6 Electromagnetic
$\tau \rightarrow \pi^- \pi^+ \pi^- \nu_\tau$	$2\pi^-, \pi^+$	$\sim 10\%$	3 Hadronic
$\tau \rightarrow \pi^- \pi^+ \pi^- \pi^0 \nu_\tau$	$2\pi^-, \pi^+, \pi^0 \rightarrow 2\gamma$	$\sim 5.18\%$	3 Hadronic, 2 Electromagnetic

**Table 3.** Tau decay channels, their Shower tail nature in each case and their corresponding probabilities to occur. The probabilities for pion secondaries take into account the contribution of  $K$  mesons originated from  $\tau$  decay. [30]

## 5. UPTAUs and HORTAUs connection with Terrestrial Gamma Flash

The steps linking simple terrestrial spherical geometry and its different geological composition and high energy neutrino physics and UHE  $\tau$  interactions leading to Tau air-showers are not straightforward. The same UHE  $\tau$  decay in flight and its air-showering physics at various quota (and air density) behave differently. Detector physics threshold and background noises, signal rates should also be kept in mind [30]. Let us remind that a few Tau decay modes in muon channel do not lead to any observable air-shower.

### 5.1. UPTAUs and HORTAUs toward satellite : TGF events in BATSE data

Let us estimate the UPTAUs (and HORTAUs) possible role to trigger a Terrestrial Gamma Flash (TGF). These short (millisecond)  $\gamma$  ray burst, upcoming from the Earth, have been rarely (78 events in 10 year of records) been observed by the most sensible  $\gamma$  experiment: BATSE in GRO satellite (1991 – 2000). Their interpretation have been first related to upward lightening. The present rate of observed TGF at best (low threshold and hard channel trigger set up) is much lower ( $\sim$  factor ten) then predicted one [30] for an incoming neutrino flux  $\simeq 10^3 eV cm^{-2} s^{-1} sr^{-1}$ : it may be well possible that the usual BATSE threshold trigger is suppressing and hiding this rate; otherwise tens of PeV UHE  $\nu_\tau$  are the TGF events source at BATSE sensibility edges. The other possibility is that the real neutrino fluence is only  $\simeq 2 \cdot 10^2 eV cm^{-2} s^{-1} sr^{-1}$ . Nevertheless a small (factor 3  $\div$  5) suppression, may reduce the  $N_{ev}$  to the observed TGF rate on an expected higher  $\simeq 10^3 eV cm^{-2} s^{-1} sr^{-1}$  fluence.

Moreover HORTAUs at tens EeV [30] may also lead to rare upward events at a rate comparable to TGF events. The last secondaries from a  $\tau$  air shower from  $3PeV$  neutrinos

BATSE TERRESTRIAL GAMMA FLASH APRIL-1991-MAY-2000								
N	N° trigger	Date	Time	R.A.	Dec.	$\Delta\theta$	$\Delta\theta$ geo	
1	106	910422	2531,1	99,74	-11,31	4,42000	18.298	
2	868	911005	Unpublished					
3	1300	920115	47202,7	217,85	-32,34	16,71000	50.007	
4	1334	920201	72420,0	Unpublished				
5	1433	920224	36547,3	Unpublished				
6	1457	920301	81250,8	Unpublished				
7	1470	920309	47072,1	330,568	-7,418	3,14600	27.240	
8	1787	920810	61515,2	305,76	-47,18	4,26000	20.965	
9	1915	920909	28074,5	89,59	-34,33	5,28000	39.621	
10	2144	930124	54533,6	205,66	-25,83	5,59000	47.205	
11	2185	930211	53095,8	8,4	26,64	0,23000	67.271	
12	2221	930305	55291,0	10,84	64,61	4,73000	131.747	
13	2223	930306	52583,1	319,652	-51,879	0,24893	51.343	
14	2248	930315	60330,1	59,71	13,27	0,25000	151.511	
15	2348	930520	7337,7	281,52	-16,86	6,15000	59.370	
16	2370	930603	14440,5	252,45	-42,27	6,21000	24.210	
17	2444	930712	50022,5	127,12	44,73	7,83000	35.895	
18	2457	930723	18386,9	312,52	-51,84	117,33000	23.727	
19	2465	930726	16888,2	284,41	-61,57	6,40000	38.168	
20	2516	930905	79941,0	244,25	-27,38	7,19000	32.963	
21	2573	931009	38648,6	205,96	11,98	36,38000	35.732	
22	2692	931212	48679,7	208,722	16,279	5,97512	17.985	
23	2754	940112	49046,2	180,72	-5,97	8,90000	55.155	
24	2808	940209	22876,9	215,02	55,15	0,14000	44.431	
25	2835	940219	58464,9	323,46	-13,5	5,49000	35.827	
26	2955	940501	35887,9	215,49	41,74	83,37000	46.590	
27	3148	940831	Unpublished					
28	3192	940925	Unpublished					
29	3233	941010	Unpublished					
30	3244	941016	Unpublished					
31	3258	941026	Unpublished					
32	3264	941030	Unpublished					
33	3274	941105	Unpublished					
34	3277	941109	Unpublished					
35	3285	941116	Unpublished					
36	3302	941127	Unpublished					
37	3309	941203	Unpublished					
38	3310	941203	Unpublished					
39	3313	941207	Unpublished					
40	3314	941208	Unpublished					
41	3315	941209	Unpublished					
42	3331	941228	Unpublished					
43	3377	950129	23619,5	132,94	7,82	11,79000	33.696	
44	3382	950130	Unpublished					
45	3446	950228	Unpublished					
46	3457	950305	Unpublished					
47	3470	950316	Unpublished					
48	3474	950318	Unpublished					
49	3478	950321	Unpublished					
50	3500	950410	Unpublished					
51	3501	950410	Unpublished					
52	3813	950922	4147,7	177,363	-12,77	8,38576	51.854	
53	3925	951128	25539,1	306,176	43,554	9,31987	52.484	
54	3931	951204	55267,1	189,102	-0,774	10,23038	135.400	
55	4355	960113	81867,3	186,553	29,061	13,82847		
56	5006	960224	67333,9	278,398	-8,922	8,50541	21.476	
57	5317	960323	55341,3	66,203	26,187	8,12474	21.036	
58	5520	960625	85244,2	61,958	-31,575	11,75859	46.283	
59	5577	960817	13701,4	88,000	19,354	11,00976	32.489	
60	5578	960817	46631,7	75,155	-10,188	13,80963	17.464	
61	5579	960817	47563,0	155,715	7,750	13,28786	37.480	
62	5582	960820	39893,0	91,151	29,822	8,91121	29.862	
63	5583	960820	83982,2	250,510	-56,233	469,78418	116.460	
64	5587	960827	74000,9	245,215	-48,473	11,66136	54.871	
65	5588	960829	35537,6	249,631	-30,47	7,50174	29.902	
66	5598	960909	42071,1	336,451	-27,808	6,35217	43.103	
67	5665	961111	6460,7	38,713	69,385	17,44419	73.637	
68	6185	970416	71107,7	226,787	12,669	6,25850	16.835	
69	6773	980522	76751,8	63,817	44,243	10,37695	61.128	
70	6777	980523	46630,2	334,484	-2,996	6,34613	31.810	
71	7168	981021	57752,1	146,259	-34,542	12,68023	51.353	
72	7208	981111	44176,3	198,714	-29,859	5,58169	27.523	
73	7229	981125	44884,9	303,202	4,903	2,16981	54.592	
74	7325	990114	53731,0	120,195	-16,118	12,77933	13.653	
75	7844	991108	17993,6	48,525	19,338	2,09525	23.785	
76	8006	000301	66475,5	32,827	15,393	13,72290	8.099	
77	8083	000421	19655,1	269,193	24,965	11,22290	64.423	
78	8108	000516	8015,6	205,982	-22,922	10,48456	23.684	

**Table 4.** All BATSE terrestrial gamma burst data 1991 – 2000. The colored TGF events associate common arrival directions (as Galactic Center, A.G.Center) associated also in time clustering; the date,time, celestial coordinate, error bar, and TGF-Earth Center angle are listed below; Hard Trigger set up Trigger periods (channel 3+4) have a colored orange side label. They mark a higher rate TGF activity visibly correlated (with two different plateau in corresponding to higher TGF acceptance).

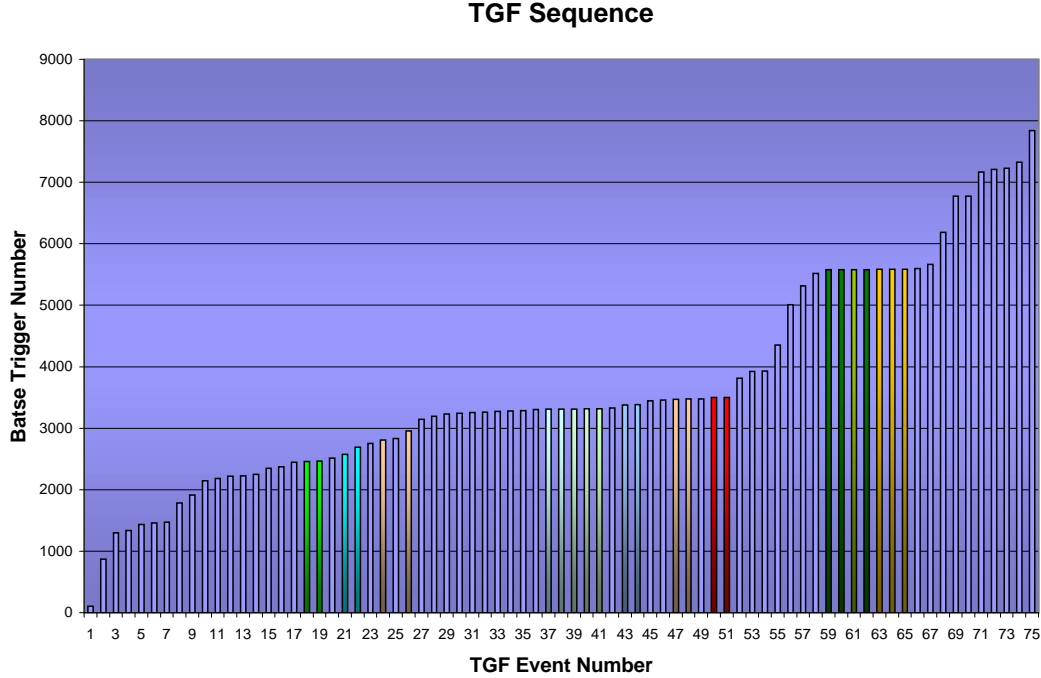


**Figure 13.** All BATSE terrestrial gamma burst data 1991 – 1999. The colored TGF events associate both common arrival directions (as Galactic Center, A.G.Center) as well as their time clustering; the date,time, celestial coordinate, error bar, and TGF-Earth Center angle are listed in Table above; Trigger periods (channel 3+4) have a higher and more prolific TGF activity. They mark two different plateau in corresponding to higher TGF acceptance. Last Trigger 8006,8083,8108 on last year 2000, not included in the present table, confirmed and didn't change the general result above.

are mainly hard ( $10^5 eV$  or above) bremsstrahlung gamma photons produced by electron pairs whose approximated number flux is comparable to

$$N_\gamma \simeq \frac{E}{\langle E_\gamma \rangle} \sim 3 \cdot 10^{10} \left( \frac{E}{3 PeV} \right) \quad (14)$$

The atmosphere opacity may reduce the final value at least by 1/3:  $N_\gamma \sim 10^{10}$ . The expected  $X - \gamma$  flux at large 500 Km distances, is diluted even within a beamed angle  $\Delta\Omega \simeq 2 \cdot 10^{-5}$ , leading to nearly  $\Phi_\gamma \sim 10^{-2} \text{ph/cm}^2$ . The characteristic  $\gamma$  burst duration is roughly defined by  $L/c \sim$  few milliseconds in agreement with the observed TGF events (See Appendix A). The consequent TGF  $\gamma$  burst number flux on BATSE is estimated to be  $\Phi_\gamma S \sim 10^2$  events, what is just comparable with observed TGFs fluence,(see Appendix B). The HORTAUs while being more energetic ( $\sim 10^3$  factor for same  $\nu$  energy fluence) are rarer by the same factor (for equal  $\nu$  energy fluence) and by smaller arrival angle (two order of magnitude) as well as diluted by the longer tangential distances ( factor  $\sim 25$ ); however most of these suppressions are well recovered by much higher and efficient  $\nu$  cross-sections at GZK energies, longer  $\tau$  tracks, possible rich primary spectra and higher HORTAUs  $\Phi_\gamma$  fluence, making them complementary

or even comparable to UPTAUs signals. The bremsstrahlung spectra are hard, as the observed TGF ones. The possible air shower time structure may reflect the different eight  $\tau$  decay channels (mainly involving hadronic and/or electromagnetic decay products). The complex interplay between UHE  $\nu$  interaction with nuclear matter overimposed on  $\bar{\nu}_e e$  interactions is shown in (Fig.12). The extremely narrow energy window where  $\bar{\nu}_e e$  rate is comparable to  $\nu_\tau N$  while being transparent to Earth makes UPTAUs-HORTAUs-TGF connection unrelated to  $\bar{\nu}_e e$  resonant  $W^-$  events possible only in HORTAUs beyond a mountain. The characteristic interaction regions responsible for UPTAUs and HORTAUs are within a narrow energy band shown in (Fig.12). Peculiar  $\nu_\tau N$  interaction (Fig.12) departing from parton model, would lead to a less restrictive UHE  $\nu_\tau$  - Earth opacity, and a more abundant vertical UPTAUs-TGF event rate at higher energies; the TGF data do not support such a large flux variability and therefore it might moderately favor the narrow energy window (PeV - few tens PeV) constrained by parton model or the EeV energy window for HORTAUs. Indeed the TGF data, collected by NASA BATSE archive and described in Tab.3 are located in celestial map with their corresponding error boxes. They are better readable, after few error bar calibration, in a galactic map over the diffused GeV - EGRET gamma background signal. One notes the surprising clustering of TGF sources in the galactic plane center at maximal EGRET fluence; their correlations with important known TeV are displayed. Let us remark that the last discovered TeV source, 1ES1426+428, associated with BL Lac object at redshift  $z = 0.129$ , do find also a correlated event in the TGF BATSE Trigger, 2955, source, making more plausible the TGF astrophysical nature than any random terrestrial lightning origin (Fig.15). One should foresee that UPTAUs must be correlated to geological sites of higher terrestrial densities, (rock over sea). The HORTAUs location birth is correlated with higher terrestrial crust elevation, (Mountain chains and Earth Crust discontinuity) because target matter has a more deep penetrating probability. All these air-showers may be better opened (and observed) at the places with highest terrestrial magnetic field. Additional remarkable correlations occur with AGASA UHECR non-homogeneities at EeV energy band as shown in Fig.15, as well as with most COMPTEL  $\gamma$  sources toward the  $l = 18^\circ$  in galactic plane. Some important locations of known galactic and extra-galactic source (as nearby QSRs 3C273 and 3C279) are displayed in Fig.15 over the EeV AGASA map. Very recent and rarest UHECR AGASA triplet clustering, near or above GZK energies, pointing toward BL Lac 1ES0806 + 524, finds, surprisingly, a corresponding TGF event, within its error box: BATSE (Trigger 2444). Also two (among four) additional UHECR AGASA doublets (2EG J0432+2910 and TEX 1428+370) are well correlated to TGF events (Trigger 5317,2955). The present TGF- $\tau$  air-shower identification could not be produced by UHE  $\bar{\nu}_e$  charged current at ( $E_{\bar{\nu}_e} = M_W^2/2m_e = 6.3 \cdot 10^{15}$  eV); therefore it stands for the UHE  $\nu_\tau \bar{\nu}_\tau$  presence. Consequently it could be the result of flavor mixing  $\nu_\mu \leftrightarrow \nu_\tau$  from far PSRs or AGNs sources toward the Earth. The TGF- $\tau$  air-shower connection may be soon verified and reinforced (or partially mystified) by the BATSE-GRO publishing of 28 missing TGFs data (as well as future GLAST data): we foresee that BATSE-TGF hide additional directional imprint of UHE  $\nu_\tau$  sources, (maybe the missing Mrk 421 and Mrk 501 extragalactic sources).

## 6. Skin crown Earth volumes as a function of observation height $h$

Below we define, list and estimate the sequence of the key variables whose dependence (shown below or derived in Appendices) leads to the desired HORTAUs volumes (useful to estimate the UHE  $\nu$  prediction rates) summarized in Tab.5 and in Conclusions. These Masses estimates are somehow only lower bounds that ignore an additional contribution by more penetrating or regenerated  $\tau$  [51]. Let us show the main functions whose interdependence with the observer altitude leads to an estimate of UPTAUs and HORTAUs equivalent detection

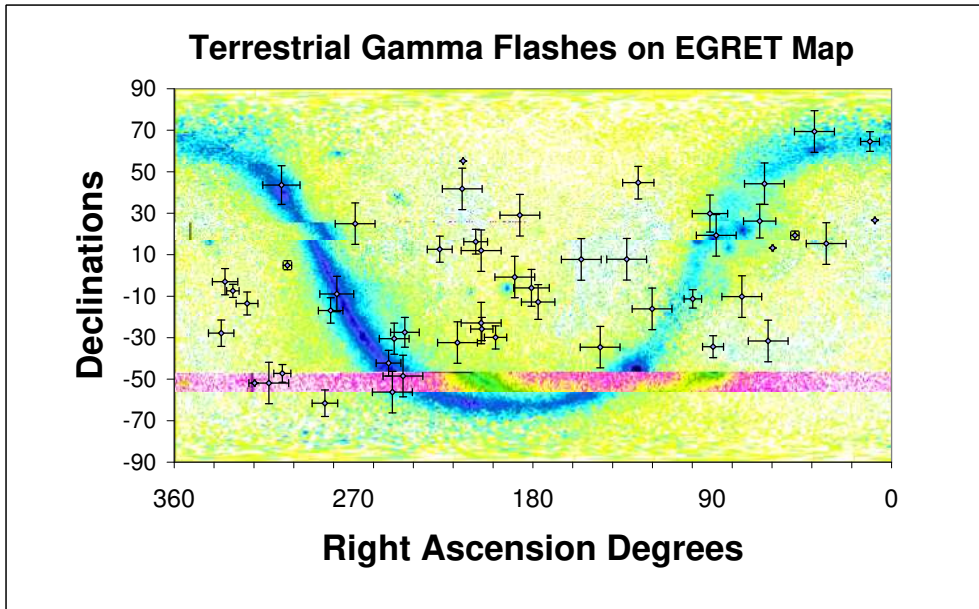


**Figure 14.** The Terrestrial Gamma Flash arrival map over the EGRET (hundred MeV-GeV) data in celestial coordinates. It manifests the partial galactic signature and the clustering of repeater events toward the Galactic Center. Also some relevant repeater events are observed toward anti-galactic direction and to well known extragalactic sources (see next map and [30]).

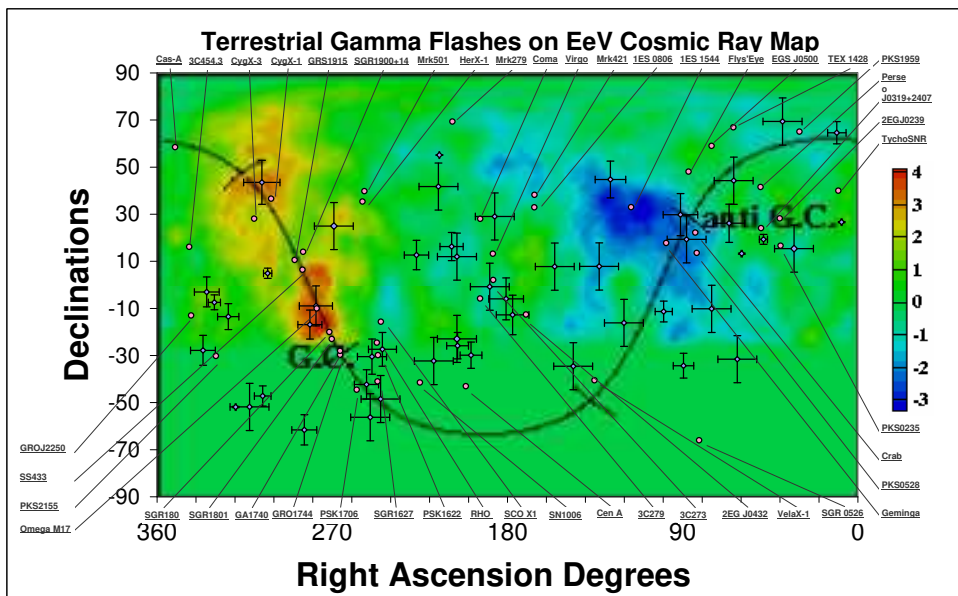


**Figure 15.** The Terrestrial Gamma Flash arrival map over the EeV anisotropic map ( $10^{18} eV$ ) data in celestial coordinates. Some relevant X- $\gamma$ -TeV sources are also shown in the same region; see [30].

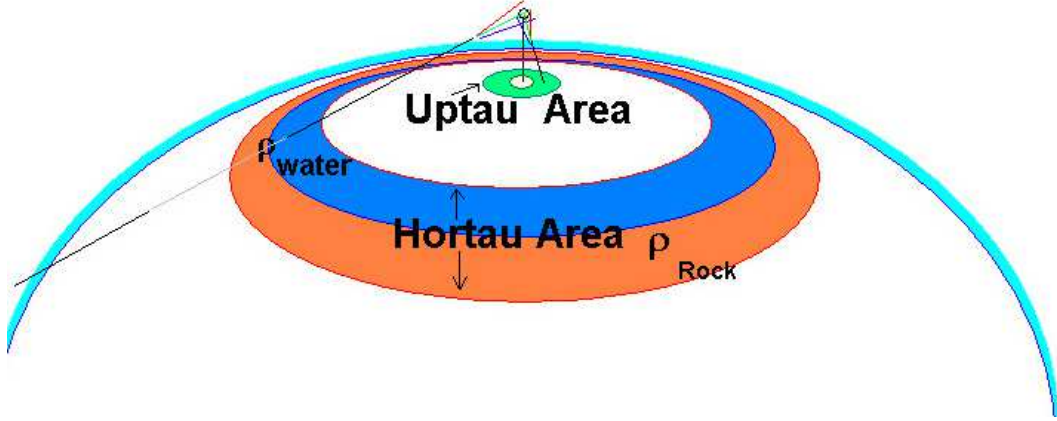


**Figure 16.** The Upward Tau air-shower Ring or Crown Areas, labelled UPTAUs and the Horizontal Tau air-shower Ring Area, labelled by HORTAU, where the  $\tau$  is showering and flashing toward an observer at height  $h_1$ . The HORTAU Ring Areas are described both for water and rock matter density.

Surfaces, (See Fig.16-17), Volumes and Masses (see Tab.5).

- (i) The horizontal distance  $d_h$  at given height  $h_1$  toward the horizons (see Fig.17):

$$d_h = \sqrt{(R_{\oplus} + h_1)^2 - (R_{\oplus})^2} = 113 \sqrt{\frac{h_1}{km}} \cdot km \sqrt{1 + \frac{h_1}{2R_{\oplus}}} \quad (15)$$

The corresponding horizontal edge angle  $\theta_h$  below the horizons ( $\pi/2$ ) is (see Fig.17):

$$\theta_h = \arccos \frac{R_{\oplus}}{(R_{\oplus} + h_1)} \simeq 1^\circ \sqrt{\frac{h_1}{km}} \quad (16)$$

(All the approximations here and below hold for height  $h_1 \ll R_{\oplus}$  )

- (ii) The consequent characteristic energy  $E_{\tau_h}$   $\tau$  lepton decaying in flight from  $d_h$  distance just nearby the source:

$$E_{\tau_h} = \left( \frac{d_h}{c\tau_0} \right) m_{\tau} c^2 \simeq 2.2 \cdot 10^{18} eV \sqrt{\frac{h_1}{km}}$$

For each low quota ( $h_1 \leq$  a few kms) there exists a characteristic air depth, which is necessary for Tau decay to develop a detectable shower. The corresponding distance is  $d_{Sh} \sim 6kms \ll d_h$ . More precisely at low quota ( $h_1 \ll h_o$ , where  $h_o$  is the air density decay height= 8.55 km.) one finds:

$$d_{Sh} \simeq 5.96km \left[ 1 + \ln \frac{E_{\tau}}{10^{18}eV} \right] \cdot e^{\frac{h_1}{h_o}} \quad (17)$$

Because these distances are usually much shorter than the far horizons distances, we may neglect them. However at high altitude ( $h_1 \geq h_o$ ) this is no longer the case (see Appendix A). Therefore we shall introduce from here and in next steps a small, but important modification, whose physical motivation is just to include the air dilution role at highest quota:  $h_1 \rightarrow \frac{h_1}{1+h_1/H_o}$ , where, as in Appendix A,  $H_o = 23$  km. Then previous definition (at height  $h_1 < R_{\oplus}$ ) becomes:

$$E_{\tau_h} \simeq 2.2 \cdot 10^{18} eV \sqrt{\frac{h_1}{1 + h_1/H_o}} \quad (18)$$

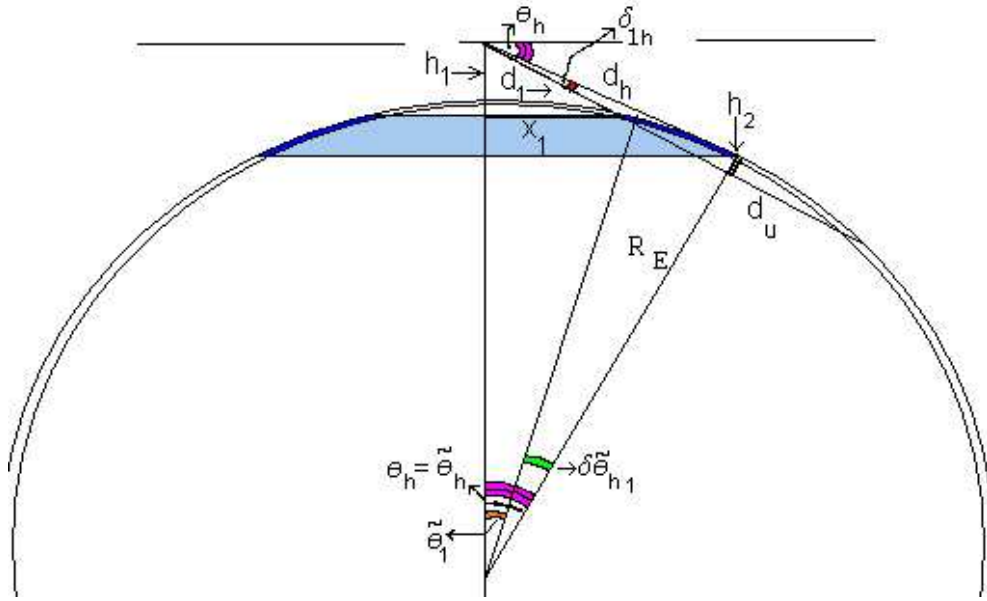


**Figure 17.** The geometrical disposal defining the UPTAUs and HORTAUs Ring (Crown or Coronas) Areas as in the text; the distances are exaggerated for simplicity.

**Table 5.** The Table of the main parameters leading to the effective HORTAUs Mass from the observer height  $h_1$ , the corresponding  $\tau$  energy  $E_\tau$  able to let the  $\tau$  reach him from the horizons. The observed total Area  $A_{TOT}$  underneath the observer is shown as well as the corresponding  $\tau$  propagation length in matter  $l_\tau$ . The opening angle seen by the observer toward the terrestrial Crown crust  $\delta\tilde{\theta}_{h_1}$  and  $l_\tau$  has to be projected orthogonally in the Earth Crust,  $l_{\tau\perp} = l_\tau \cdot \sin \delta\tilde{\theta}_{h_1}$ , are also evaluated. The final Ring Areas for both (water,rock) densities  $A_R$  at each characteristic high altitudes  $h_1$  are shown with the consequent observable Volume  $\Delta V$ , (made by  $\Delta V = A_R \cdot l_{\tau\perp} = A_R \cdot l_\tau \cdot \sin \delta\tilde{\theta}_{h_1}$ ). Finally the consequent effective Volume and Mass  $\Delta V_{eff.} = \Delta V \frac{\Delta\Omega}{4\pi}$ ,  $\Delta M_{eff.} = \Delta V_{eff.} \cdot \rho$ , (within the very narrow  $\tau$  airshower solid angle  $\frac{\Delta\Omega}{4\pi} \simeq 2.5 \cdot 10^{-5}$ ) as a function of density  $\rho$  and height  $h_1$ . In the last Row the Ratio  $R = \Delta M_{eff.} / \Delta M_{Atm}$  defines the ratio of HORTAUs produced within the Earth Crown Skin over the atmospheric ones: this ratio nearly reflects the matter density over the air one and it reaches nearly two order of magnitude and describes the larger probability to observe a HORTAU over the probability to observe a double bang in the air at EUSO or OWL detectors.

$\rho$	$h_1$ (km)	$E_{th}$ (eV)	$A_{TOT}$ (km <sup>2</sup> )	$l_\tau$ (km)	$\delta\tilde{\theta}_{h_1}$	$l_{\tau\perp}$ (km)	$A_R$ (km <sup>2</sup> )	$\Delta V$ (km <sup>3</sup> )	$\Delta V_{eff}$ (km <sup>3</sup> )	$\Delta M_{eff.}$ ( $\frac{km^3}{\rho}$ )	$R$
1	2	$3.12 \cdot 10^{18}$	$8 \cdot 10^4$	21.7	$1.31^\circ$	0.496	$7.9 \cdot 10^4$	$3.95 \cdot 10^4$	0.987	0.987	49.6
2.65	2	$3.12 \cdot 10^{18}$	$8 \cdot 10^4$	11	$0.97^\circ$	0.186	$7.2 \cdot 10^4$	$1.34 \cdot 10^4$	0.335	0.89	49.2
1	5	$4.67 \cdot 10^{18}$	$2 \cdot 10^5$	24.3	$1.79^\circ$	0.76	$1.9 \cdot 10^5$	$1.45 \cdot 10^5$	3.64	3.64	75
2.65	5	$4.67 \cdot 10^{18}$	$2 \cdot 10^5$	12.1	$1.07^\circ$	0.225	$1.45 \cdot 10^5$	$3.2 \cdot 10^4$	0.82	2.17	59.6
1	25	$8 \cdot 10^{18}$	$10^6$	27.5	$2.36^\circ$	1.13	$7.16 \cdot 10^5$	$8.12 \cdot 10^5$	20.3	20.3	113
2.65	25	$8 \cdot 10^{18}$	$10^6$	13.1	$1.08^\circ$	0.247	$3.83 \cdot 10^5$	$9.5 \cdot 10^4$	2.4	6.3	65.45
1	500	$1.08 \cdot 10^{19}$	$1.8 \cdot 10^7$	29.4	$2.72^\circ$	1.399	$4.3 \cdot 10^6$	$6 \cdot 10^6$	150.6	150.6	140
2.65	500	$1.08 \cdot 10^{19}$	$1.8 \cdot 10^7$	13.8	$1.07^\circ$	0.257	$1.75 \cdot 10^6$	$4.5 \cdot 10^5$	11.3	30	68

This procedure, applied tacitly everywhere, guarantees that there we may extend our results to those HORTAUs at altitudes where the residual air density must exhibit a sufficient slant depth. For instance, highest  $\gg 10^{19}eV$  HORTAUs will not be easily observable because their  $\tau$  life distance exceeds (usually) the horizons air depth length. The parental UHE  $\nu_\tau, \bar{\nu}_\tau$  or  $\bar{\nu}_e$  of energies  $E_{\nu_\tau}$  able to produce such UHE  $E_\tau$  in matter are:

$$E_{\nu_\tau} \simeq 1.2E_{\tau_h} \simeq 2.64 \cdot 10^{18}eV \cdot \sqrt{\frac{h_1}{km}} \quad (19)$$

(iii) The neutrino (underground) interaction lengths at the corresponding energies is  $L_{\nu_\tau}$ :

$$\begin{aligned} L_{\nu_\tau} &= \frac{1}{\sigma_{E\nu_\tau} \cdot N_A \cdot \rho_r} = 2.6 \cdot 10^3 km \cdot \rho_r^{-1} \left( \frac{E_{\nu_h}}{10^8 \cdot GeV} \right)^{-0.363} \\ &\simeq 304 km \cdot \left( \frac{\rho_{rock}}{\rho_r} \right) \cdot \left( \frac{h_1}{km} \right)^{-0.1815} \end{aligned} \quad (20)$$

For more details see [54], [30]. It should be remind that here we ignore the  $\tau$  multi-bangs [51] that reduce the primary  $\nu_\tau$  energy and pile up the lower energies HORTAUs (PeV-EeV).

The maximal neutrino depth  $h_2(h_1)$ , see Fig.17 -Fig.19 above, under the chord along the UHE neutrino-tau trajectory of length  $L_\nu(h_1)$  has been found:

$$h_2(h_1) = \frac{L_{\nu_h}^2}{2^2 \cdot 2(R - h_2)} \simeq \frac{L_{\nu_h}^2}{8R_\oplus} \simeq 1.81 \cdot km \cdot \left( \frac{h_1}{km} \right)^{-0.363} \cdot \left( \frac{\rho_{rock}}{\rho_r} \right)^2$$

See Fig.17, for more details. Because the above  $h_2$  depths are in general not too deep respect to the Ocean depths, we shall consider respectively either sea (water) or rock (ground) materials as Crown matter density.

(iv) The corresponding opening angle observed from height  $h_1$ ,  $\delta_{1h}$  encompassing the underground height  $h_2$  at horizons edge (see Fig.17) and the nearest UHE  $\nu$  arrival directions  $\delta_1$  is:

$$\begin{aligned} \delta_{1h}(h_2) &= 2 \arctan \frac{h_2}{2d_h} = 2 \arctan \left[ \frac{8 \cdot 10^{-3} \cdot \left( \frac{h_1}{km} \right)^{-0.863} \left( \frac{\rho_{rock}}{\rho_r} \right)^2}{\sqrt{1 + \frac{h_1}{2R_\oplus}}} \right] \\ &\simeq 0.91^\circ \left( \frac{\rho_{rock}}{\rho_r} \right)^2 \cdot \left( \frac{h_1}{km} \right)^{-0.863} \end{aligned} \quad (21)$$

(v) The underground chord  $d_{u_1}$  (see Fig.17-19) where UHE  $\nu_\tau$  propagates and the nearest distance  $d_1$  for  $\tau$  flight (from the observer toward Earth) along the same  $d_{u_1}$  direction, within the angle  $\delta_{1h}$  defined above, angle below the horizons (within the upward UHE neutrino and HORTAUs propagation line) is:

$$d_{u_1} = 2 \cdot \sqrt{\sin^2(\theta_h + \delta_{1h})(R_\oplus + h_1)^2 - d_h^2} \quad (22)$$

Note that by definition and by construction  $L_\nu \equiv d_{u_1}$ . The nearest HORTAUs distance corresponding to this horizontal edges still transparent to UHE  $\tau$  is:

$$d_1(h_1) = (R_\oplus + h_1) \sin(\theta_h + \delta_{1h}) - \frac{1}{2}d_{u_1} \quad (23)$$

Note also that for the height  $h_1 \geq km$  :

$$\frac{d_{u_1}}{2} \simeq (R_\oplus + h_1) \sqrt{\delta_{1h} \sin 2\theta_h} \simeq 158 \sqrt{\frac{\delta_{1h}}{1^\circ}} \sqrt{\frac{h_1}{km}} km.$$

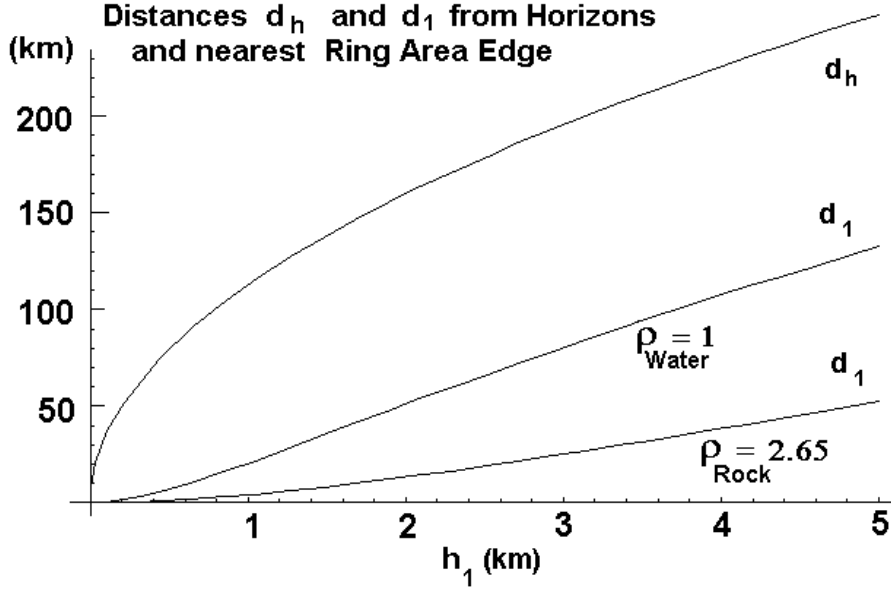


**Figure 18.** Distances from the observer to the Earth ( $d_1$ ) for different matter densities and to the Horizons ( $d_h$ ) for low altitudes.

- (vi) The same distance projected cord  $x_1(h_1)$  along the horizontal line (see Fig.17) is:

$$x_1(h_1) = d_1(h_1) \cos(\theta_h + \delta_{1h}) \quad (24)$$

The total terrestrial Area  $A_T$ , underneath any observer at height  $h_1$ , is (see Fig.16-17-20):

$$A_T = 2\pi R_{\oplus}^2 (1 - \cos \tilde{\theta}_h) = 2\pi R_{\oplus} h_1 \left( \frac{1}{1 + \frac{h_1}{R_{\oplus}}} \right) A_T = 4 \cdot 10^4 km^2 \left( \frac{h_1}{km} \right) \left( \frac{1}{1 + \frac{h_1}{R_{\oplus}}} \right),$$

where  $\tilde{\theta}_h$  is the opening angle from the Earth center (see Fig.17). At first sight one may be tempted to consider all the Area  $A_T$  for UPTAUs and HORTAUs, but because of the shower air opacity (HORTAUs) or for its small slant depth (UPTAUs) this is incorrect. While for HORTAUs there is a more complex Area estimated above and in the following, for UPTAUs the Area Ring (or Disk) is quite simpler to derive very similar geometrical variables summarized in Appendix B.

- (vii) The Earth Ring Crown crust area  $A_R(h_1)$  delimited by the horizons distance  $d_h$  and the nearest distance  $d_1$  is still transparent to UHE  $\nu_{\tau}$  (see Fig.16-19). The ring area  $A_R(h_1)$  is computed from the internal angles  $\delta\tilde{\theta}_h$  and  $\delta\tilde{\theta}_1$  defined at the Earth center (Fig.17)(note that  $\delta\tilde{\theta}_h = \delta\theta_h$  but in general  $\delta\tilde{\theta}_1 \neq \delta\theta_1$ ).

$$A_R(h_1) = 2\pi R_{\oplus}^2 (\cos \tilde{\theta}_1 - \cos \tilde{\theta}_h) = 2\pi R_{\oplus}^2 \left( \sqrt{1 - \left( \frac{x_1(h_1)}{R_{\oplus}} \right)^2} - \frac{R_{\oplus}}{R_{\oplus} + h_1} \right) \quad (25)$$

Here  $x_1(h_1)$  is the cord defined above.

- (viii) The characteristic interaction tau lepton length  $l_{\tau}$  is defined at the average  $E_{\tau_1}$ , from interaction in matter (rock or water). These lengths have been derived by analytical equations keeping care of the Tau lifetime, the photo-nuclear losses, the electro-weak

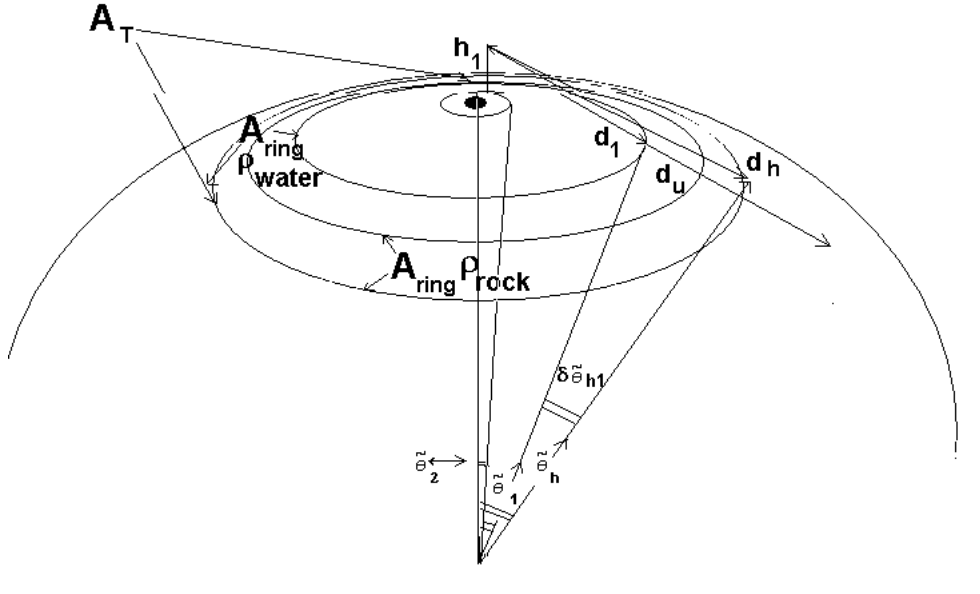


**Figure 19.** Total and Ring (Crown) Areas and Angles for UPTAUs-HORTAUS observed at different heights.

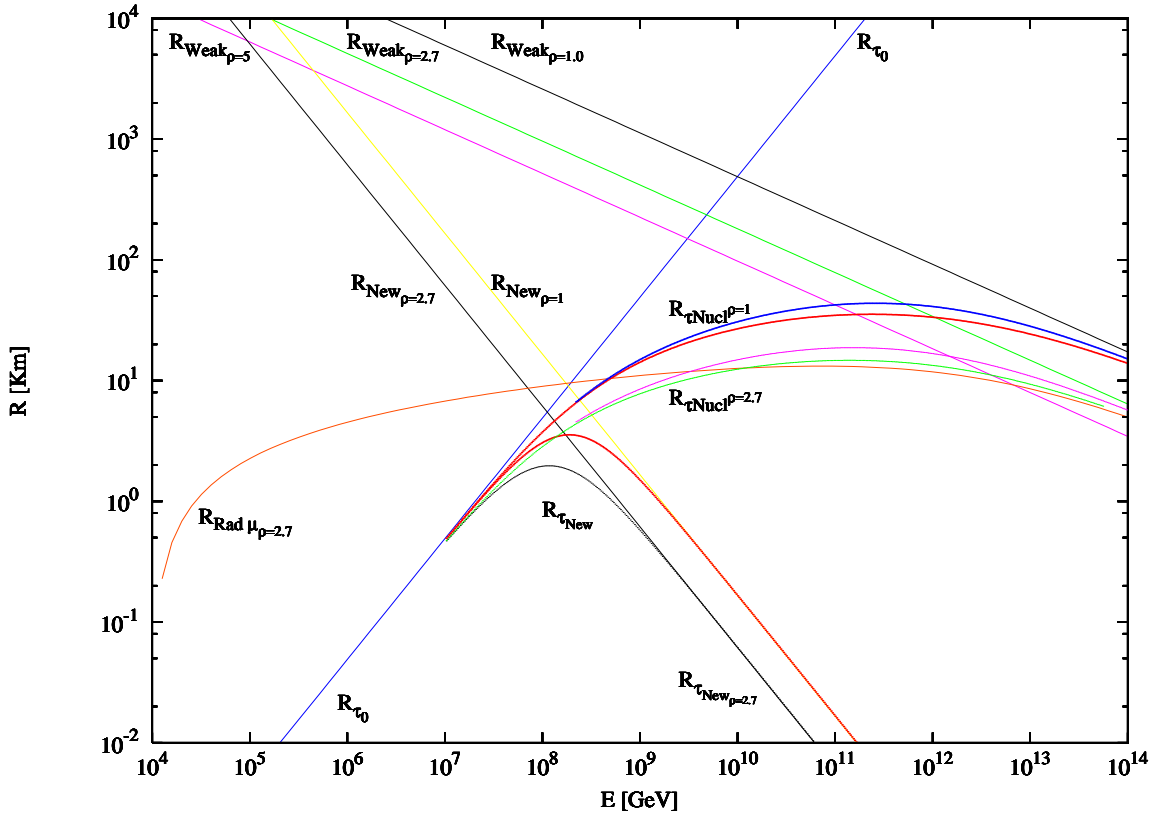


**Figure 20.** Lepton  $\tau$  (and  $\mu$ ) Interaction Lengths for different matter densities:  $R_{\tau_0}$  is the free  $\tau$  length,  $R_{\tau_{New}}$  is the New Physics TeV Gravity interaction range at corresponding densities,  $R_{\tau_{Nucl}\cdot\rho}$ , [30], see also [3], [14], is the combined  $\tau$  Ranges keeping care of all known interactions and lifetime and mainly the photo-nuclear interaction. There are two slightly different split curves (for each density) by two comparable approximations in the interaction laws.  $R_{Weak\rho}$  is the electro-weak Range at corresponding densities (see also [54]), [30].

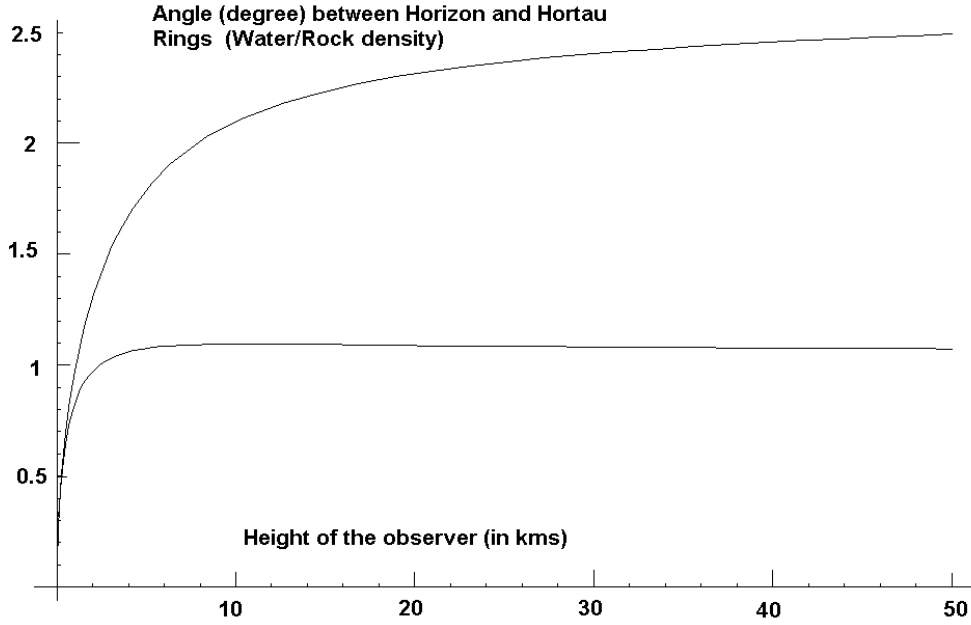


**Figure 21.** Opening angle  $\delta\tilde{\theta}_{h_1}$  toward Ring Earth Skin for density  $\rho_{water}$  and  $\rho_{rock}$ .(see Fig.17)

losses [30]. See Fig.20 below. The tau length along the Earth Skimming distance  $l_{\tau_2}$  should be vertically projected ( multiplied by  $\sin(\delta\tilde{\theta}_{h_1})$ ) in order to find the observable skin volume; the angle  $\delta\tilde{\theta}_{h_1}$  is given by:

$$\delta\tilde{\theta}_{h_1} \equiv \tilde{\theta}_h - \arcsin\left(\frac{x_1}{R_{\oplus}}\right) \quad (26)$$

The same quantity  $\tilde{\theta}_{h_1}$ , See Fig.21,in a more direct approximation:

$$\sin \delta\tilde{\theta}_{h_1} \simeq \frac{L_{\nu}}{2R_{\oplus}} = \frac{304km}{2R_{\oplus}} \left(\frac{\rho_{rock}}{\rho}\right) \frac{h_1}{km}^{-0.1815}$$

For highest ( $h \gg H_o=23km$ ) altitude the exact approximation reduces to:

$$\delta\tilde{\theta}_{h_1} \simeq 1^{\circ} \left(\frac{\rho_{rock}}{\rho}\right) \left(\frac{h_1}{500 \cdot km}\right)^{-0.1815}$$

Therefore the penetrating  $\tau$  skin depth  $l_{\tau\downarrow}$  is

$$l_{\tau\downarrow} = l_{\tau} \cdot \sin \delta\tilde{\theta}_{h_1} \simeq 0.0462 \cdot l_{\tau} \left(\frac{\rho_{water}}{\rho}\right) \frac{h_1}{km}^{-0.1815} \quad (27)$$

where the  $\tau$  ranges in matter,  $l_{\tau}$  have been calculated and shown in Fig.20. The consequent Observable Ring Areas at two different ranges of quota are displayed in Fig.22-Fig.23.

- (ix) The final analytical expression for the Earth Crust Skin Volumes and Masses under the Earth Skin inspected by HORTAUs are derived combining the above functions on HORTAUs Areas with the previous lepton Tau  $l_{\tau\downarrow}$  vertical depth:

$$V_{h_1} = A_R(h_1) \cdot l_{\tau\downarrow}; \quad (28)$$

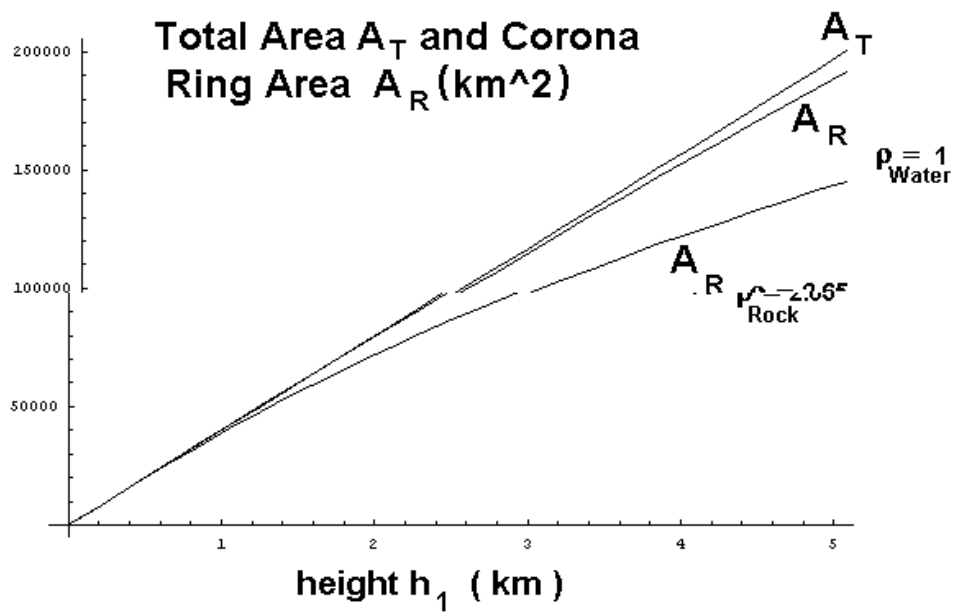


**Figure 22.** Total Area  $A_T$  and Ring (Crown or Coronas) Areas for two densities  $A_R$  at low altitudes.

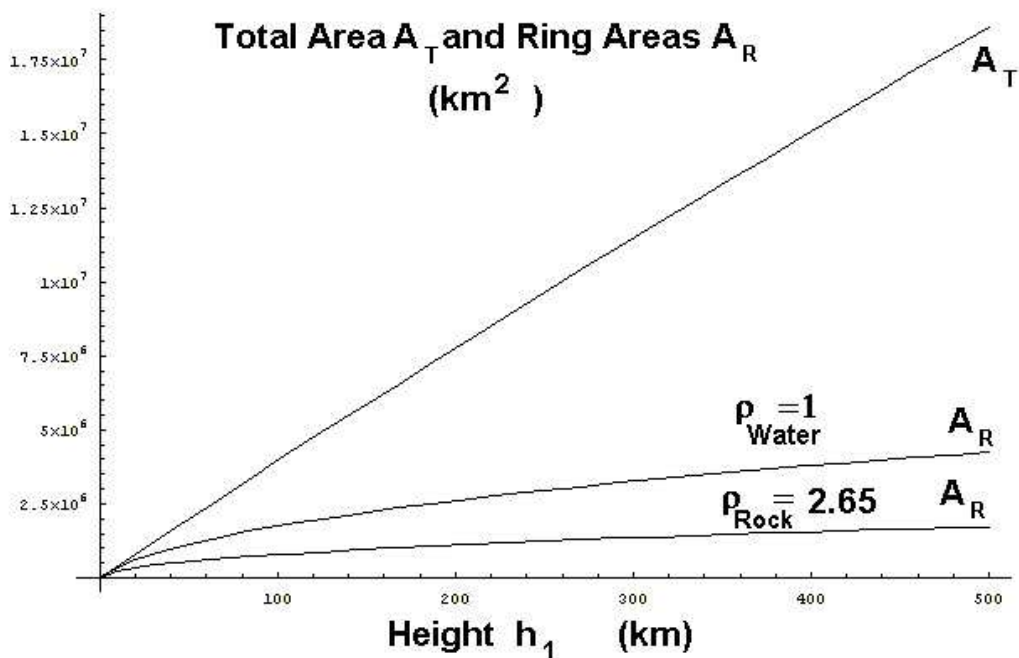


**Figure 23.** Total Area  $A_T$  and Ring (Crown) Areas for two densities  $A_R$  at high altitudes.

The detecting mass is directly proportional to this volume:

$$M_{h_1} = V_{h_1} \cdot \rho \quad (29)$$

- (x) A more approximated but easy to handle expression for Ring area for high altitudes ( $h_1 \gg 2km$   $h_1 \ll R_{\oplus}$ ) may be summarized as:

$$\begin{aligned} A_R(h_1) &\simeq 2\pi R_{\oplus}^2 \sin \theta_h \delta \tilde{\theta}_{h_1} \propto \rho^{-1} \\ &\simeq 2\pi R_{\oplus}^2 \sqrt{\frac{2h_1}{R_{\oplus}}} \left( \frac{\sqrt{1 + \frac{h_1}{2R_{\oplus}}}}{1 + \frac{h_1}{R_{\oplus}}} \right) \left( \frac{L_{\nu}}{2R_{\oplus}} \right) \end{aligned} \quad (30)$$

At high altitudes the above approximation, corrected accordingly to the exact one, shown in Fig.23, becomes:

$$A_R(h_1) \simeq 2\pi R_{\oplus} d_{h_1} \delta \tilde{\theta}_{h_1} \simeq 4.65 \cdot 10^6 \sqrt{\frac{h_1}{500km}} \left( \frac{\rho_{water}}{\rho} \right) km^2 \quad (31)$$

Within the above approximation the final searched Volume  $V_{h_1}$  and Mass  $M_{h_1}$  from where HORTAUs may be generated is:

$$V_{h_1} = \frac{\pi}{2} \sqrt{\frac{2h_1}{R_{\oplus}}} \left( \frac{\sqrt{1 + \frac{h_1}{2R_{\oplus}}}}{1 + \frac{h_1}{R_{\oplus}}} \right) L_{\nu}^2 l_{\tau} \propto \rho^{-3} \quad (32)$$

$$M_{h_1} = \frac{\pi}{2} \sqrt{\frac{2h_1}{R_{\oplus}}} \left( \frac{\sqrt{1 + \frac{h_1}{2R_{\oplus}}}}{1 + \frac{h_1}{R_{\oplus}}} \right) L_{\nu}^2 l_{\tau} \rho \propto \rho^{-2} \quad (33)$$

- (xi) The effective observable Skin Tau Mass  $M_{eff.}(h_1)$  within the thin HORTAU or UPTAUs Shower angle beam  $\simeq 1^\circ$  is suppressed by the solid angle of view  $\frac{\delta\Omega}{\Omega} \simeq 2.5 \cdot 10^{-5}$ .

$$\Delta M_{eff.}(h_1) = V_{h_1} \cdot \rho \frac{\delta\Omega}{\Omega} \quad (34)$$

The lower bound Masses  $M_{eff.}(h_1)$  (summarized in the Tab.5 and in Fig.24) are exactly estimated for different realistic high quota experiments.

### 6.1. Effective Volume in HORTAUs

The discovery of the expected UHE neutrino astronomy is urgent and just behind the corner. If the Terrestrial Gamma Flashes are indeed the traces of such PeV-EeV UHE neutrino tau, then the neutrino flux is just at the level of  $\simeq 2 \cdot 10^2 eV cm^{-2} s^{-1} sr^{-1}$  and might be accessible by AMANDA in a near future. To make further progress in studies of UHE neutrino astronomy huge volumes are necessary. Beyond underground  $km^3$  detectors a new generation of UHE neutrino calorimeters lays on front of mountain chains and just underneath our feet: The Earth itself offers huge Crown Volumes as Beam Dump calorimeters observable via upward Tau Air Showers, UPTAUs and HORTAUs. Their effective Volumes as a function of the quota  $h_1$  have been derived by an analytical function variables in equations above and Appendix B. These Volumes and Masses are discussed below and summarized in the last column of Tab.5. At a few tens meter altitude the UPTAUs and HORTAUs Ring are almost overlapping. At low altitude  $h_1 \leq 2 Km$  the HORTAUs are nearly independent on the matter density  $\rho$ :  $\Delta M_{eff.}(h_1 = 2Km)(\rho_{Water}) = 0.987 km^3$   $\Delta M_{eff.}(h_1 = 2km)(\rho_{Rock}) = 0.89 km^3$  These volumes are the effective Masses expressed in Water equivalent volumes. On the

contrary at higher quotas, like highest Mountain observations sites, Airplanes, Balloons and Satellites, the matter density of the HORTAUs Ring (Crown) Areas plays more and more dominant role asymptotically *proportional* to  $\rho^{-2}$ :  $\Delta M_{eff.}(h_1 = 5km)(\rho_{Water}) = 3.64km^3$ ;  $\Delta M_{eff.}(h_1 = 5km)(\rho_{Rock}) = 2.17km^3$ . From Air-planes or balloons the effective volumes  $M_{eff.}$  increase and the density  $\rho$  plays a relevant role.  $\Delta M_{eff.}(h_1 = 25km)(\rho_{Water}) = 20.3km^3$ ;  $\Delta M_{eff.}(h_1 = 25km)(\rho_{Rock}) = 6.3km^3$ . Finally from satellite altitudes the same effective volumes  $M_{eff.}$  are reaching extreme values:

$$\Delta M_{eff.}(h_1 = 500 km)(\rho_{Water}) = 150.6 km^3$$

$$\Delta M_{eff.}(h_1 = 500 km)(\rho_{Rock}) = 30 km^3$$

These masses must be compared with other proposed  $km^3$  detectors, keeping in mind that these HORTAUs signals conserve the original UHE  $\nu$  direction information within a degree. One has to discriminate HORTAUS (only while observing from satellites) from Horizontal High Altitude Showers (HIAS) [27], due to rare UHECR showering on high atmosphere. While wide (RICE) one might also remind the UPTAUs (at PeV energies) volumes as derived in Appendix B and in [30] whose values (assuming an arrival angle  $\simeq 45^\circ - 60^\circ$  below the horizons) are nearly *proportional* to the density  $\rho$ :

$$\Delta M_{eff.}(h_1 = 500 km)(\rho_{Water}) = 5.9 km^3$$

$$\Delta M_{eff.}(h_1 = 500 km)(\rho_{Rock}) = 15.6 km^3$$

These widest masses values, here estimated analytically for main quota, are offering an optimal opportunity to reveal UHE  $\nu$  at PeV and EeV-GZK energies by crown array detectors (scintillation, Cherenkov, photo-luminescent) facing vertically the Horizontal edges, located at high mountain peaks or at air-plane low sides and finally on balloons and satellites. As it can be seen in the last columns of Tab.5, the ratio  $R$  between HORTAUs events and Showers over atmospheric UHE  $\nu$  interaction is a greater and greater number with growing height, implying a dominant role (above two orders of magnitude) of HORTAUs grown in Earth Skin Crown over Atmospheric HORTAUs. These huge acceptance may be estimated by comparison with other detector thresholds (see Fig.24 adapted to present Z-Shower GZK- $\nu$  models).

## 6.2. Event rate of upward and horizontal Tau air-showers

The event rates for HORTAUs are given at first approximation by the following expression normalized to any given neutrino flux  $\Phi_\nu$ :

$$\dot{N}_{year} = \Delta M_{eff.} \cdot \frac{\Phi_\nu}{\Phi_{\nu_o}} \cdot \dot{N}_o \cdot \frac{\sigma_{E_\nu}}{\sigma_{E_{\nu_o}}} \quad (35)$$

where the  $\dot{N}_o$  is UHE neutrino rate estimated for the water mass within the  $km^3$  volume, at any given (unitary) energy  $E_{\nu_o}$ , in absence of any Earth shadowing. In our case we shall normalize our estimate at  $E_{\nu_o} = 3$  PeV energy for standard electro-weak charged current in a standard parton model [54] and we shall assume a model-independent neutrino maximal flux  $\Phi_\nu$  at a flat fluence value of nearly  $\Phi_{\nu_o} \simeq 3 \cdot 10^3 eV cm^{-2} \cdot s^{-1} \cdot sec^{-1} \cdot sr^{-1}$  corresponding to a characteristic Fermi power law in UHE  $\nu$  primary production rate decreasing as  $\frac{dN_\nu}{dE_\nu} \simeq E_\nu^{-2}$  just below present AMANDA bounds. The consequent rate becomes:

$$\dot{N}_{year} = 29 \frac{\Delta M_{eff.}}{\rho \cdot km^3} \cdot \frac{\Phi_\nu}{\Phi_{\nu_o}} \cdot \frac{\sigma_{E_\nu}}{\sigma_{E_{\nu_o}}}$$

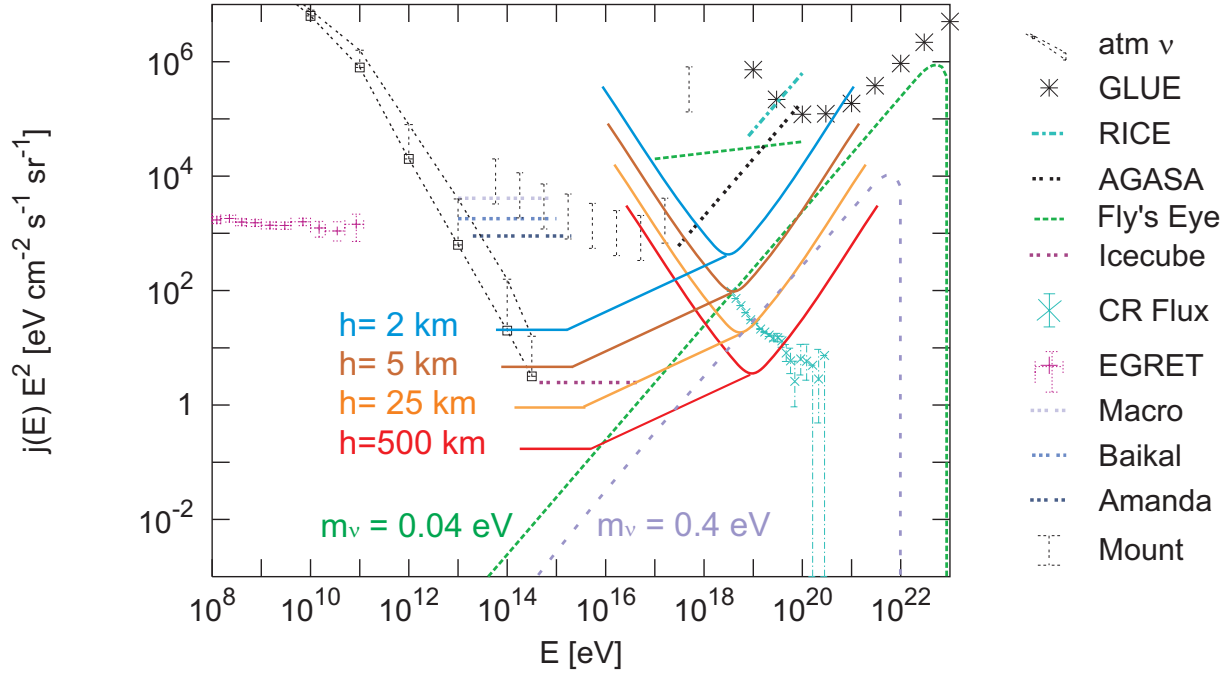


**Figure 24.** UPTAUs (lower bound on the center) and HORTAUs (right parabolic curves) sensibility at different observer heights  $h$  (2, 5, 25, 500km) assuming a  $km^3$  scale volume (see Table above) adapted over a present neutrino flux estimate in Z-Shower model scenario [46], [20] for light (0.4 – 0.04 eV) neutrino masses  $m_\nu$ ; two corresponding density contrast has been assumed [28]; the lower parabolic bound thresholds are at different operation height, in Horizontal (Crown) Detector facing toward most distant horizons edge; these limits are fine tuned (as discussed in the text); we are assuming a duration of data records of a decade comparable to the BATSE record data (a decade). The parabolic bounds on the EeV energy range in the right sides are nearly un-screened by the Earth opacity while the corresponding UPTAUs bounds in the center below suffer both of Earth opacity as well as of a consequent shorter Tau interaction length in Earth Crust, that has been taken into account. [30], [31], [32].

$$= 29 \cdot \left( \frac{E_\nu}{3 \cdot 10^6 \cdot GeV} \right)^{-0.637} \frac{\Delta M_{eff.}}{\rho \cdot km^3} \cdot \frac{\Phi_\nu}{\Phi_{\nu o}} \quad (36)$$

For highest satellites and for a characteristic UHE GZK energy fluence  $\Phi_{\nu o} \simeq 3 \cdot 10^3 eV cm^{-2} \cdot s^{-1} \cdot sr^{-1}$  (as the needed Z-Showering one), the consequent event rate observable  $\dot{N}_{year}$  above the Sea is :

$$= 24.76 \cdot \left( \frac{E_\nu}{10^{10} \cdot GeV} \right)^{-0.637} \frac{h}{500km} \cdot \frac{\Phi_\nu}{\Phi_{\nu o}} \quad (37)$$

This event rate is comparable to UPTAUs one (for comparable fluence) and it may be an additional source of Terrestrial Gamma Flashes already observed by GRO in last decade [30]. These event rates are considered as the detector thresholds for UPTAUs and HORTAUs and they are summarized in Tab.5 and in Fig.24 with other present and future experimental thresholds.

## 7. UHECR and UHE $\nu$ observed by EUSO

EUSO experiment, while monitoring the downward Earth atmosphere layers, may observe among common Ultra High Energy Cosmic Rays, UHECR, also High Energy Neutrino-Induced Showers either blazing upward to the detectors at high ( $\sim$  PeV) energies or at much higher GZK,  $\sim E_\nu \geq 10^{19}$  eV energies, showering horizontally in air or vertically downward. A small fraction of these upward, horizontal and vertical Shower maybe originated by a direct astrophysical UHE neutrino interacting on terrestrial air layers itself; however the dominant UHE neutrino signals are Upward and Horizontal Tau air-showers, UPTAUSs and HORTAUs (or Earth skimming  $\nu$ ), born within widest Earth Crust Crown (Sea or Rock) Areas, by UHE  $\nu_\tau + Nuclei \rightarrow \tau$  interactions, respectively at PeV and GZK energies: their rate and signatures are shown in a neutrino fluence map for EUSO thresholds versus other UHE air interacting neutrino signals and backgrounds. The effective target masses originating HORTAUs, to be observable by EUSO, may exceed (on sea) a wide and huge ring volume  $\simeq 5130 km^3$ . The consequent HORTAUS event rate (even at 10% EUSO duty cycle lifetime) may deeply test the expected Z-Burst models by at least a hundred of yearly events. Even rarest but inescapable GZK neutrinos (secondary of photopion production of observed cosmic UHECR) might be discovered in a few (or a tens) horizontal shower events; in this view an extension of EUSO detectability up to  $\sim E_\nu \geq 10^{19}$  eV threshold is to be preferred. A wider collecting EUSO telescope (3m diameter) might be considered.

The very possible discover of the UHECR astronomy, the solution of the GZK paradox, the very urgent rise of an UHE neutrino astronomy are among the main goals of EUSO project. This advanced experiment in a very near future will encompass AGASA-HIRES and AUGER and observe for highest cosmic ray showers on Earth Atmosphere recording their tracks from International Space Station by Telescope facing dawn-ward the Earth. The recent doublets and triplets clustering found by AGASA seem to favor compact object (as AGN) over more exotic topological relic models, mostly fine tuned in mass (GUT, Planck one) and time decay rate to fit all the observed spectra. However the missing AGN within a GZK volume is wondering. A possible remarkable correlation recently shows that most of the UHECR event cluster point toward BL Lac sources [41]. This correlation favors a cosmic origination for UHECRs, well above the near GZK volume. In this frame a relic neutrino mass [12],  $m_\nu \simeq 0.4$  eV or ( $m_\nu \simeq 0.1 \div 5$  eV) may solve the GZK paradox [18], [20],[71],[68],[28],[38] overcoming the proton opacity being ZeV UHE neutrinos transparent (even from cosmic edges to cosmic photon Black Body drag) while interacting in resonance with relic neutrinos masses in dark halos (Z-burst or Z-WW showering models). These light neutrino masses do not solve the galactic or cosmic dark matter problem but it is well consistent with old and recent solar neutrino oscillation evidences [40],[39],[61] and most recent claims by KamLAND [47] of anti-neutrino disappearance (all in agreement within a Large Mixing Angle neutrino model and  $\Delta m_\nu^2 \sim 6.9 \cdot 10^{-5} eV^2$ ) as well as these light masses are in agreement with atmospheric neutrino mass splitting ( $\Delta m_\nu \simeq 0.07$  eV) and in possible fine tune with more recent neutrino double beta decay experiment mass claim  $m_\nu \simeq 0.4$  eV [49]. In this Z-WW Showering for light neutrino mass models large fluxes of UHE  $\nu$  are necessary,[20],[68][28], [38],[46] or higher than usual gray-body spectra of target relic neutrino or better clustering are needed [28][60]: indeed a heaviest neutrino mass  $m_\nu \simeq 1.2 - 2.2$  eV while still being compatible with known bounds, might better gravitationally cluster leading to denser dark local-galactic halos and lower neutrino fluxes[28][60]. It should remarked that in this frame the main processes leading to UHECR above GZK are mainly the WW-ZZ and the t-channel interactions [20],[28].

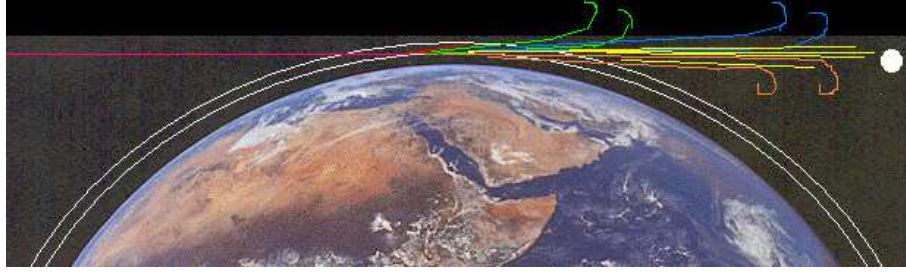


**Figure 25.** A very schematic Horizontal High Altitude Shower (HIAS); its fan-like imprint is due to geo-magnetic bending of charged particles at high quota ( $\sim 44km$ ). It is similar to HORTAUs event due to Earth Skimming neutrinos. The Shower may point to a satellite as old gamma GRO-BATSE detectors or very recent Beppo-Sax, Integral, HETE, Chandra or future Agile and Swift ones. [30],[26],[27]. The HIAS Showers are open and forked in five (either three or at least two main component): ( $e^+$ ,  $e^-$ ,  $\mu^+$ ,  $\mu^-$ ,  $\gamma$ , or just positive-negative); these multi-finger tails may be seen as split tails by EUSO.

These expected UHE neutrino fluxes might and must be experienced in complementary and independent tests.

### 7.1. UHE $\nu$ Astronomy by the $\tau$ Showers and UHECRs in EUSO

While longest  $\mu$  tracks in  $km^3$  underground detector have been, in last three decades, the main searched UHE neutrino signal, Tau Air-showers by UHE neutrinos generated in Mountain Chains or within Earth skin crust at PeV up to GZK ( $> 10^{19}$  eV) energies have been recently proved to be a new powerful amplifier in Neutrino Astronomy [22], [30],[8],[53],[36]. This new Neutrino  $\tau$  detector will be (at least) complementary to present and future, lower energy,  $\nu$  underground  $km^3$  telescope projects (from AMANDA, Baikal, ANTARES, NESTOR, NEMO, IceCube). In particular Horizontal Tau Air shower may be naturally originated by UHE  $\nu_\tau$  at GZK energies crossing the thin Earth Crust at the Horizon showering far and high in the atmosphere [30],[26],[27],[8],[36]. UHE  $\nu_\tau$  are abundantly produced by flavor oscillation and mixing from muon (or electron) neutrinos, because of the large galactic and cosmic distances respect to the neutrino oscillation ones (for already known neutrino mass splitting). Therefore EUSO may observe many of the above behaviors and it may constrains among models and fluxes and it may also answer open standing questions. I will briefly enlist, in this first preliminary presentation, the main different signatures and rates of UHECR versus UHE  $\nu$  shower observable by EUSO at 10% duty cycle time within a 3 year record period, offering a first estimate of their signals. Part of the results on UHECR are probably well known, nevertheless they are here re-estimated. Part of the results, regarding the UPTAUs and HORTAUs, are new and they rule the UHE  $\nu$  Astronomy in EUSO.

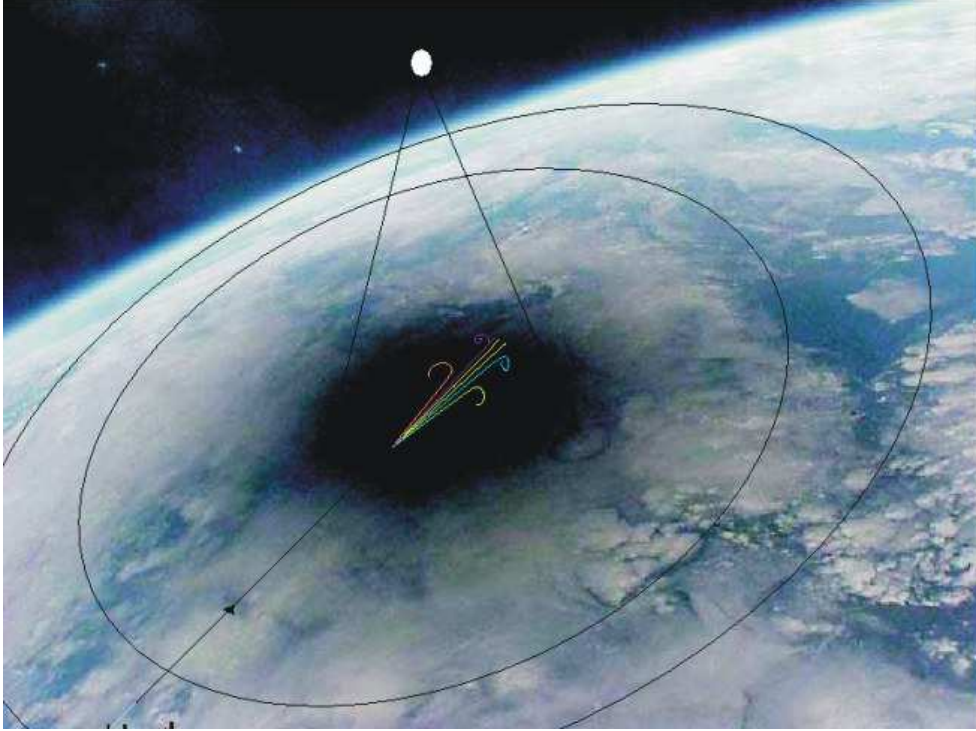


**Figure 26.** A Horizontal High Altitude Shower or similar Horizontal Tau air-shower (HORTAU) and its open fan-like jets due to geo-magnetic bending seen from a high quota by EUSO satellite. The forked Shower is a multi-finger containing a inner  $\gamma$  core and external fork spirals due to  $e^+e^-$  pairs (first opening) and  $\mu^+\mu^-$  pairs [30], [26], [27].

### 7.2. Upward UHE $\nu$ Showering in Air observable by EUSO

Let us first consider the last kind of Upward  $\tau$  signals due to their interaction in Air or in Earth Crust. The Earth opacity will filter mainly  $10^{14} - 10^{15}$  eV upward events [54],[51],[3],[14],[30]; therefore only the direct upward  $\nu$  shower in air or the UPTAUs around PeV will be able to flash toward EUSO telescope facing downward the Earth. The showers eject in a narrow beam ( $2.5 \cdot 10^{-5}$  solid angle) jet an apparent total energy corresponding to  $10^{19} - 10^{20}$  eV isotropically emitted energy. The shower will be opened in a fan like shape and it will emerge from the Earth atmosphere spread as a triplet or multi-dot signal aligned orthogonal to a local terrestrial magnetic field lines. This signature will be easily revealed. However the effective observed air mass by EUSO is not 10% (because of duty cycle) of the inspected air volume  $\sim 150 km^3$ , but because of the narrow blazing shower cone it corresponds only to  $3.72 \cdot 10^{-3} km^3$ . The target volume increases for upward neutrino Tau interacting vertically in Earth Crust in last matter layer (either rock or water), making upward relativistic  $\simeq PeV \tau$  whose decay in the air born finally UPTAUs; in this case the effective target mass is (for water or rock) respectively  $5.5 \cdot 10^{-2} km^3$  or  $1.5 \cdot 10^{-1} km^3$ . These volume are not extreme. The consequent foreseen thresholds are summarized for 3 EUSO years of data recording in Fig.24. The UPTAUs signal is nearly 15 times larger than the Air-Induced  $\nu$  Shower. A more detailed analysis may show an additional factor three (due to the neutrino flavors) in favor of Air-Induced Showers, but the more transparent role of PeV multi-generating upward  $\nu_\tau$  while crossing the Earth, makes the results summarized in figure. The much wider acceptance of BATSE in respect to EUSO and the consequent better threshold (in BATSE) is due to the wider angle view of the gamma detector, the absence of any

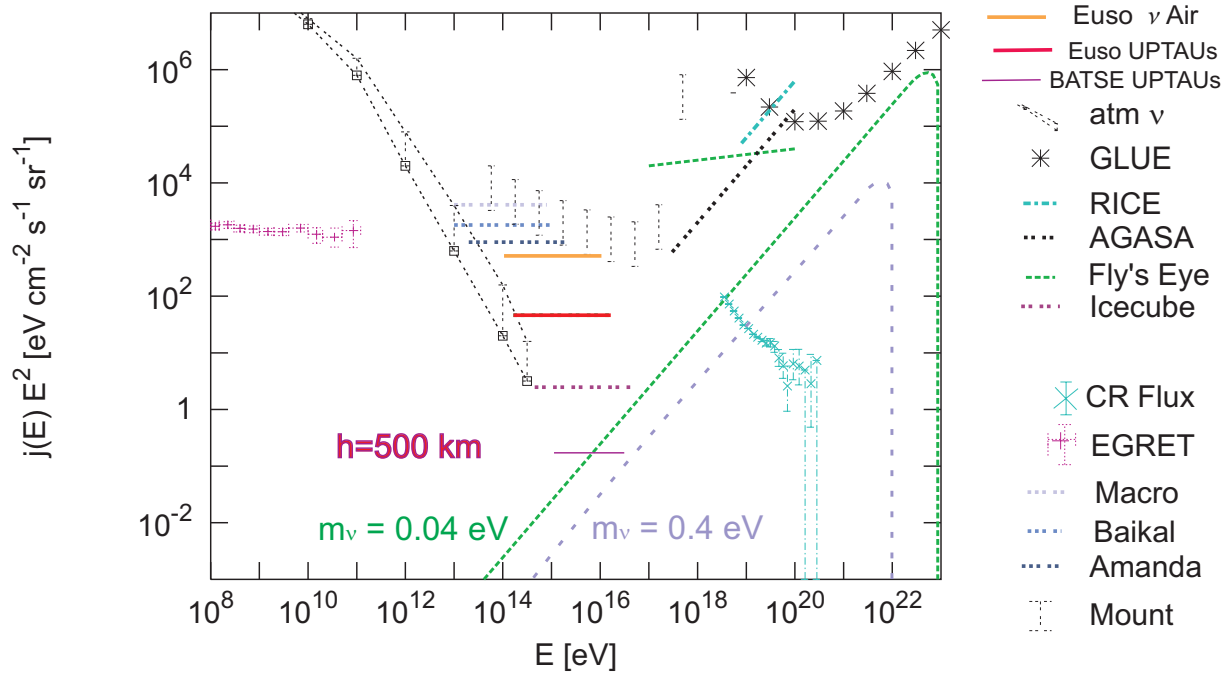


**Figure 27.** Upward Neutrino air-shower and Upward Tau Air-shower, UPTAUs, Gamma and Cosmic Rays Fluence Thresholds and bounds in different energy windows for different past and future detectors. The UPTAUs threshold for EUSO has been estimated for a three year experiment lifetime. BATSE recording limit is also shown from height  $h = 500 \text{ km}$  and for ten year record. Competitive experiments are also shown as well as the Z-Shower expected spectra in light neutrino mass values  $m_\nu = 0.4, 0.04 \text{ eV}$ . [30], [26],[46], [28],[33].

suppression factor as in EUSO duty cycle, as well as the 10 (for BATSE) over 3 (for EUSO) years assumed of record life-time. Any minimal neutrino fluence  $\Phi_{\nu_\tau}$  of PeV neutrino

$$\Phi_{\nu_\tau} \geq 10^2 \text{ eV cm}^{-2} \text{ s}^{-1}$$

might be detectable by EUSO.

### 7.3. Downward and Horizontal UHECRs in EUSO

Reconsider briefly the nature of common Ultra High Cosmic Rays (UHECR) showers. Their rate will offer a useful test for any additional UHE neutrino signals. Assume for a sake of simplicity a characteristic opening angle of EUSO telescope of  $30^\circ$  and a nominal satellite height of 400 km, leading to an approximate atmosphere area under inspection of EUSO  $\sim 1.5 \cdot 10^5 \text{ km}^2$ . Let us discuss the UHECR shower. In this case the estimated rate is a  $\sim 2 \cdot 10^3$  event/year above  $3 \cdot 10^{19}$  eV. Among these "GZK" UHECR (either proton, nuclei or  $\gamma$ ) nearly 7.45%  $\approx 150$  event/year will shower in Air Horizontally with no Cherenkov hit on the ground. The critical angle of  $\sim 6.7^\circ$  corresponding to 7.45% of all the events, is derived from first interacting quota (here assumed for Horizontal Hadronic Shower near 44 km following [30],[26],[27]). Indeed the corresponding horizontal edge critical angle  $\theta_h = 6.7^\circ$  below the horizons ( $\pi/2$ ) is given, as in previous eq.

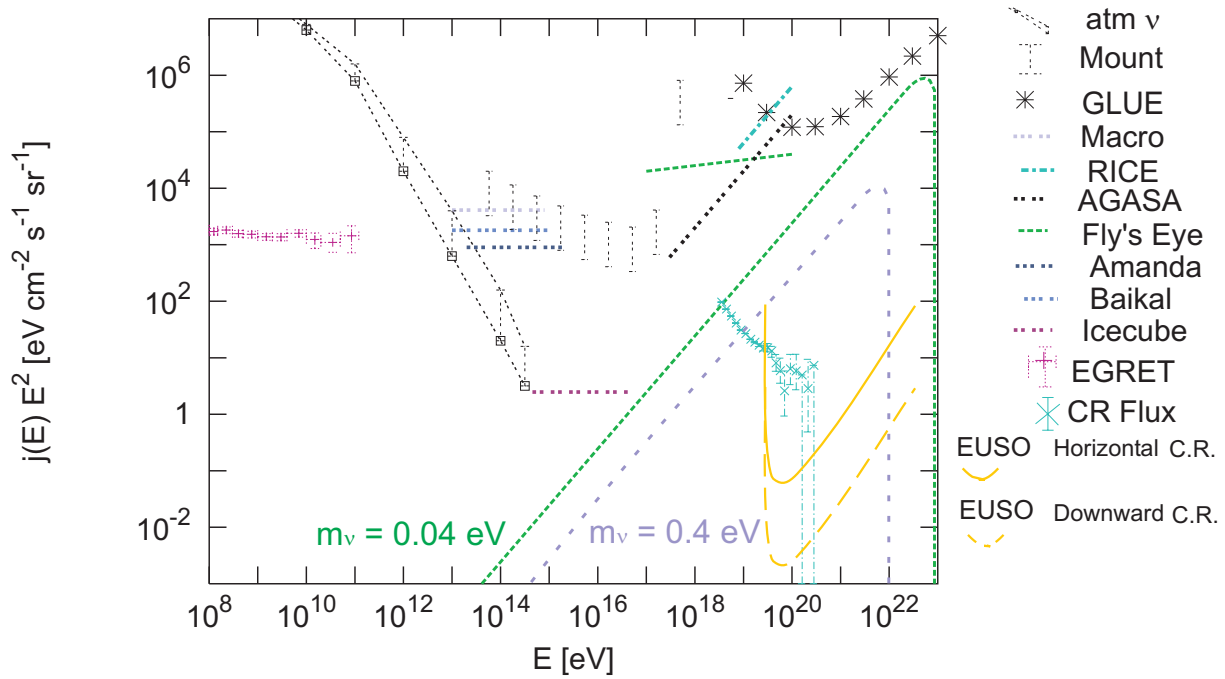


**Figure 28.** Neutrino, Gamma and Cosmic Rays Fluence Thresholds and bounds in different energy windows. The Cosmic Rays Fluence threshold for EUSO has been estimated for a three year experiments lifetime. The parabolic bound shape threshold may differ upon the EUSO optics and acceptance. Competitive experiment are also shown as well as the Z-Shower expected spectra in light mass values. [30], [26],[46], [28],[33].

17, but used at an interacting height  $h$  near 44 km:  $\theta_h = \arccos \frac{R_\oplus}{(R_\oplus + h_1)} \simeq 1^\circ \sqrt{\frac{h_1}{\text{km}}}$ . These Horizontal High Altitude Showers (HIAS)[26],[27], will be able to produce a new peculiar showering, mostly very long (hundred kilometers) and bent and forked (by few or several degrees) by local geo-magnetic fields. The total UHECR above  $3 \cdot 10^{19}$  eV will be  $\sim 6000$  UHECR and  $\sim 450$  Horizontal Showers within 3 years; these latter horizontal signals are relevant because they may mimic Horizontal induced  $\nu$  air-shower, but mainly at high quota ( $\geq 30 - 40\text{km}$ ) and downward see Fig.28. On the contrary UHE neutrino tau showering, HORTAUs, to be discussed later, are also at high quota ( $\geq 23\text{km}$ ), but upward-horizontal. Their outcoming angle will be ( $\geq 0.2^\circ - 3^\circ$ ) upward. Therefore it may be necessary to have a good angular ( $\leq 0.2 - 0.1^\circ$ ) resolution to distinguish between the two signals as a key discriminator between HORTAUs and horizontal UHECR. While Horizontal UHECR are an important piece of evidence in the UHECR calibration and its GZK study, at the same time they are a severe background noise competitive with Horizontal-Vertical GZK Neutrino Showers originated in Air, to be discussed below. However Horizontal-downward UHECR are not confused with upward Horizontal HORTAUs by UHE neutrinos to be summarized in last section. Note that air-induced Horizontal UHE neutrino as well as all down-ward air-induced UHE  $\nu$  will shower mainly at lower altitudes ( $\leq 10\text{km}$ ); however they are respectively only a small ( $\leq 2\%$ ,  $\leq 8\%$ ) fraction than HORTAUs showers to be discussed in the following. An additional factor 3 due to their three flavor over  $\tau$  unique may lead to respectively ( $\leq 6\%$ ,  $\leq 24\%$ ) ratio of air induced  $\nu$  shower in air over all HORTAUs events: a contribute ratio that may be in principle a useful test to study the balanced neutrino flavor mixing.

#### 7.4. Air Induced UHE $\nu$ Shower

UHE  $\nu$  may hit an air nuclei and shower vertically or horizontally or more rarely nearly up-ward: its trace maybe observable by EUSO preferentially in inclined or horizontal case. Indeed vertical down-ward ( $\theta \leq 60^\circ$ ) neutrino induced air showers occur mainly at lowest quota and they will only partially shower their UHE  $\nu$  energy because of the small slant depth ( $\leq 10^3 gcm^{-2}$ ) in most vertical down-ward UHE  $\nu$  shower. The observed EUSO air mass ( $1500 km^3$ , corresponding to a  $\sim 150 km^3$  for 10% EUSO record time) is the UHE neutrino calorimeter only ideally. Indeed only the inclined ( $\sim \theta \geq 60^\circ$ ) and horizontal air-showers ( $\sim \theta \geq 83^\circ$ ) (induced by GZK UHE neutrino) may reach their maximum output and their events maybe well observed; therefore only a small fraction ( $\sim 30\%$  corresponding to  $\sim 50 km^3$  mass-water volume for EUSO observation) of vertical downward UHE neutrino may be seen by EUSO. This signal may be somehow hidden (or masked) by the more common downward UHECR showers. The key reading signature will be the shower height origination: ( $\geq 40 km$ ) for most downward-horizontal UHECR, ( $\leq 10 km$ ) for most inclined-horizontal Air UHE  $\nu$  Induced Shower. A corresponding smaller fraction ( $\sim 7.45\%$ ) of totally Horizontal UHE neutrino Air shower, orphan of their final Cherenkov flash, in competition with the horizontal UHECR, may be also clearly observed: their observable mass is only  $V_{Air-\nu-Hor} \sim 11.1 km^3$  for EUSO observation duty cycle. These masses reflect into a characteristic threshold behavior shown by bounds in Fig.30.

#### 7.5. UHE $\nu_\tau - \tau$ Double Bang Shower

A more rare, but spectacular, double  $\nu_\tau - \tau$  bang in Air (comparable in principle to the PeV expected "double bang" in water [56]) may be exciting, but difficult to be observed; the EUSO effective calorimeter mass for such Horizontal event is only 10% of the UHE  $\nu$  Horizontal ones ( $\sim 1.1 km^3$ ); therefore its event rate is nearly excluded needing too high neutrino fluxes see Fig.29; indeed it should be also noted that the EUSO energy threshold ( $\geq 3 \cdot 10^{19} eV$ ) implies such a very large  $\tau$  Lorentz boost distance; such large  $\tau$  track exceed (by more than a factor three) the EUSO disk Area diameter ( $\sim 450 km$ ); therefore the expected Double Bang Air-Horizontal-Induced  $\nu$  Shower thresholds are suppressed by a corresponding factor as shown in Fig.29. More abundant single event Air-Induced  $\nu$  Shower (Vertical or Horizontal) thresholds are facing different Air volumes and quite different visibility as shown and summarized in Fig.6. It must be taken into account an additional factor three (because of three light neutrino states) in the Air-Induced  $\nu$  Shower arrival flux respect to incoming  $\nu_\tau$  (and  $\bar{\nu}_\tau$ ), making the Air target not totally a negligible calorimeter.

#### 7.6. UHE $\nu_\tau - \tau$ Air Single Bang Shower

There are also a sub-category of  $\nu_\tau - \tau$  "double bang" due to a first horizontal UHE  $\nu_\tau$  charged current interaction in air nuclei (the first bang) that is lost from the EUSO view; their UHE secondary  $\tau$  fly and decay leading to a Second Air-Induced Horizontal Shower, within the EUSO disk area. These horizontal "Double-Single  $\tau$  Air Bang" Showers are produced within a very wide Terrestrial Crown Air Area whose radius is exceeding  $\sim 600 - 800 km$  surrounding the EUSO Area of view. However it is easy to show that they will just double the Air-Induced  $\nu$  Horizontal Shower rate due to one unique flavor. Therefore the total Air-Induced Horizontal Shower (for all 3 flavors and the additional  $\tau$  decay in flight) are summarized and considered in Fig.30 including also

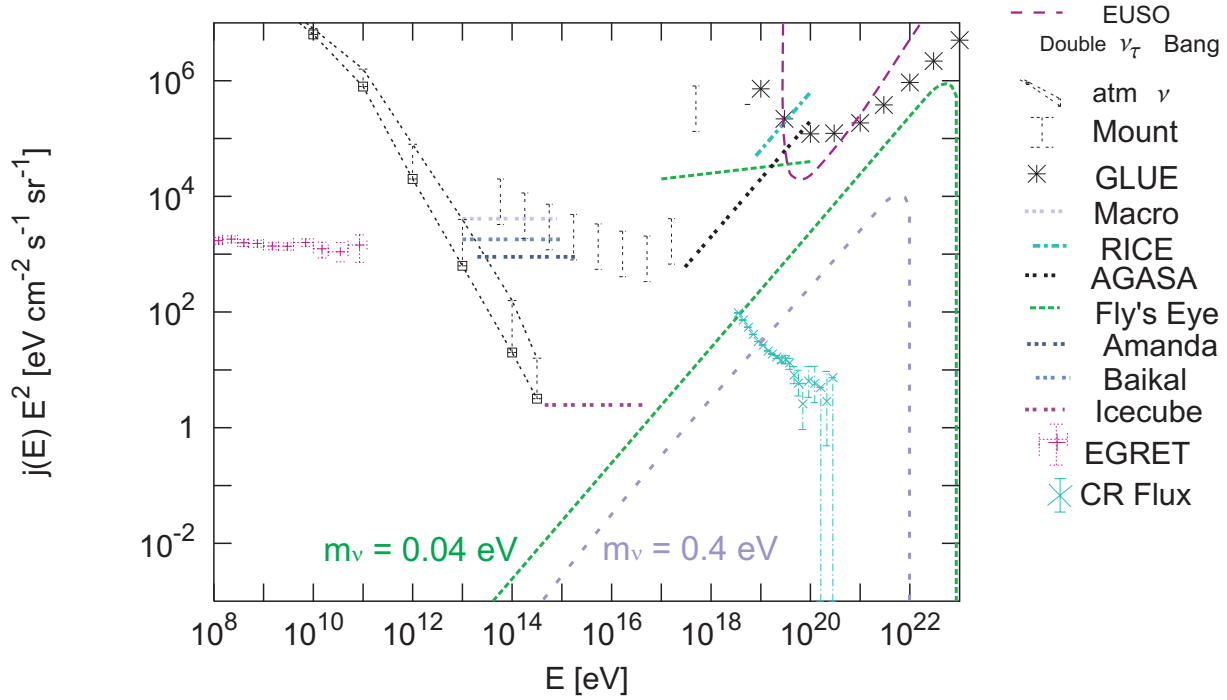


**Figure 29.** EUSO threshold for Double bang  $\tau$  Neutrino over other  $\gamma$ ,  $\nu$  and Cosmic Rays (C.R.) Fluence and bounds in different energy windows. The Fluence threshold for EUSO has been estimated for a three year experiments lifetime. Competitive experiment are also shown as well as the Z-Shower expected spectra in most probable light neutrino mass values ( $m_\nu = 0.04, 0.4$  eV). [30],[26],[46], [28],[33].

the present Single Bang Shower. The relevant UHE neutrino signals, HORTAUs, as discussed below, are originated within the (much denser) Earth Crust.

### 7.7. HORTAUs in EUSO

As already mentioned the UHE  $\nu$  astronomy may be greatly strengthened by  $\nu_\tau$  appearance via flavor mixing and oscillations. The consequent scattering of  $\nu_\tau$  on Mountains or into the Earth Crust may lead to Horizontal Tau air-showers: HORTAUs (or so called Earth Skimming Showers [26],[27],[30][36] [34]). Indeed UHE  $\nu_\tau$  may skip below the Earth and escape as  $\tau$  and finally decay in flight, within the air atmosphere, as well as inside the Area of view of EUSO, as shown in Fig.26. Any UHE-GZK Tau Air Shower induced event is approximately born within a wide ring (whose radiuses extend between  $R \geq 300$  km and  $R \leq 800$  km from the EUSO Area center). Because of the wide area and deep  $\tau$  penetration [30],[31],[33] the amount of interacting matter where UHE  $\nu$  may lead to  $\tau$  is huge ( $\geq 2 \cdot 10^5 km^3$ ); however only a tiny fraction of these HORTAUs will beam and Shower within the EUSO Area within EUSO. After carefully estimate (using also results in [30],[31], [32],[33]) I probed a lower bound (in sea matter) for these effective Volumes respectively at  $(1.1 \cdot 10^{19} eV)$  and at  $(3 \cdot 10^{19} eV)$  energy:

$$V_{eff} \simeq 5.13 \cdot 10^3 km^3$$

$$V_{eff} \simeq 6.25 \cdot 10^3 km^3$$

Therefore at GZK energies  $(1.1 \cdot 10^{19} eV)$  the horizontal  $\tau$ s by HORTAUs are more than 50 times abundant than any corresponding Horizontal Air Induced neutrino Showers as shown in Fig.31.

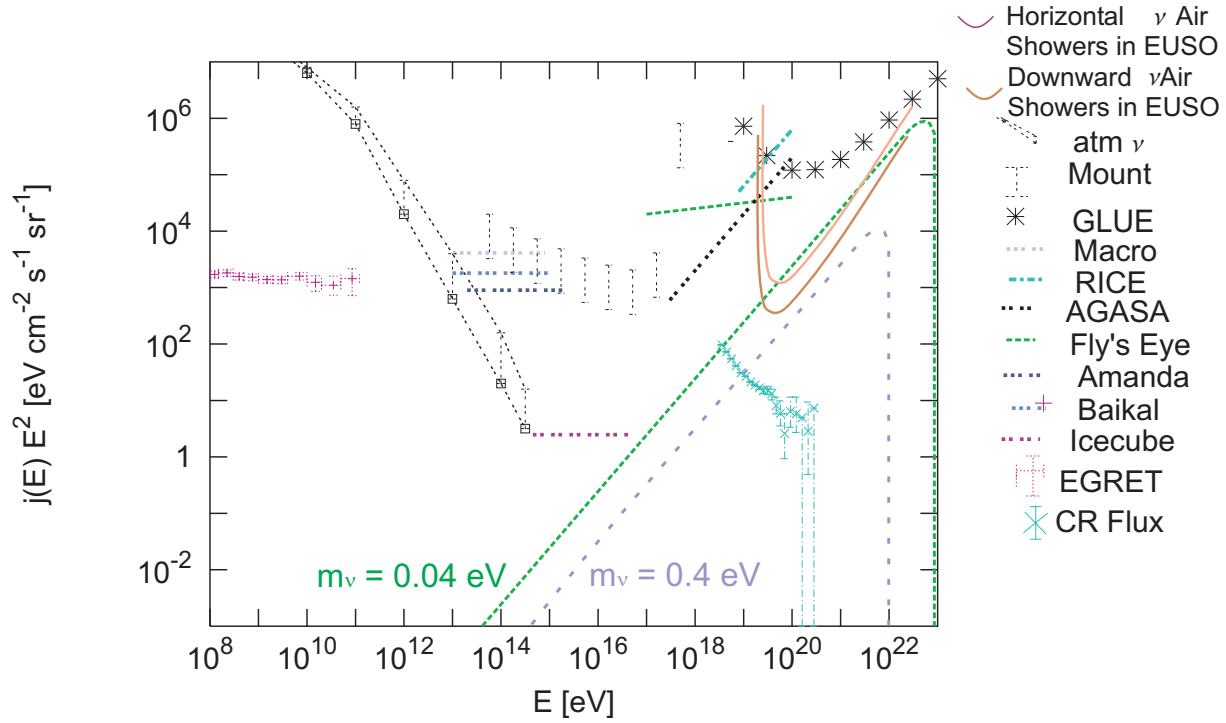


**Figure 30.** EUSO thresholds for Horizontal and Vertical Downward Neutrino Air induced shower over other  $\gamma$ ,  $\nu$  and Cosmic Rays (C.R.) Fluence and bounds. The Fluence threshold for EUSO has been estimated for a three year experiment lifetime. Competitive experiments are also shown as well as the Z-Shower expected spectra in light neutrino mass values ( $m_\nu = 0.04, 0.4$  eV). [30], [26],[46], [28],[33].

However the air-shower induced neutrino may reflect all three light neutrino flavors, while HORTAUs are made only by  $\nu_\tau, \bar{\nu}_\tau$  flavor. Nevertheless the dominant role of HORTAUs overcomes (by a factor  $\geq 15$ ) all other Horizontal EUSO neutrino events: their expected event rates are, at  $\Phi_\nu \geq 3 \cdot 10^3$  eV  $cm^{-2}s^{-1}$  neutrino fluence (as in Z-Shower model in Fig.27-31), a few hundred events a year and they may already be comparable or even may exceed the expected Horizontal CR rate. Dash curves for both HORTAUs and Horizontal Cosmic Rays are drawn assuming the EUSO threshold at  $10^{19}$ eV. Because of the relativistic  $\tau$  flight distance growth and because of the finiteness of the terrestrial atmosphere, the main signal is better observable at  $1.1 \cdot 10^{19}$ eV than at higher energies (as emphasized in Fig.30,31,32 at different threshold curves).

### 7.8. Visibility and Signatures of UHE neutrino in EUSO

Highest Energy Neutrino signals may be well observable by next generation satellite as EUSO: the main sources of such neutrino traces are UPTAUs (Upward Tau blazing the telescope born in Earth Crust) and mainly HORTAUs (Horizontal Tau air-showers originated by Earth-Skimming UHE  $\nu_\tau$ ). These showers will be opened in a characteristic twin fan-jet ovals looking like the 8-shape horizontal cosmic rays showers observed on Earth. The UPTAUs will arise mainly at PeV energies (because the Earth neutrino opacity at higher energies and because the shorter  $\tau$  boosted length, at lower energies)[30]; UPTAUs will be detected as a thin stretched multi-pixel event by EUSO, whose orientation is polarized orthogonal to the local geo-magnetic field. The EUSO sensibility (effective volume ( $V_{eff} \sim 0.1 km^3$ ) for 3 years of detection) will be an order of

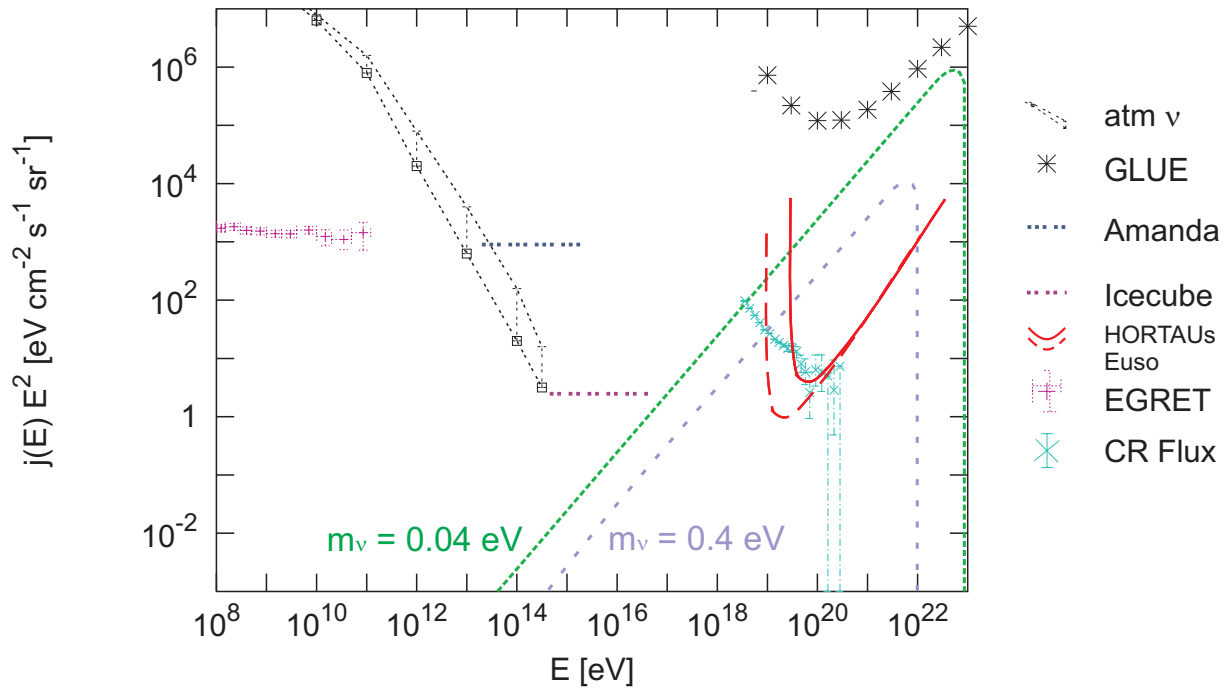


**Figure 31.** EUSO thresholds for Horizontal Tau air-shower HORTAUs over other  $\gamma$ ,  $\nu$  and Cosmic Rays (C.R.) fluence and bounds. Dash curves for HORTAUs are drawn assuming an EUSO threshold at  $10^{19}$  eV. Because the bounded  $\tau$  flight distance (due to the contained terrestrial atmosphere height) the main signal is better observable at  $1.1 \cdot 10^{19}$  eV than higher energies. The Fluence threshold for EUSO has been estimated for a three year experiment lifetime. Z-Shower or Z-Burst expected spectra in light neutrino mass values ( $m_\nu = 0.04, 0.4$  eV) are shown. [30], [26],[46], [28],[33].

magnitude below present AMANDA-Baikal bounds. Horizontal Tau air-showers at GZK energies will be better searched and revealed. They are originated along huge Volumes around the EUSO Area. Their horizontal skimming secondary  $\tau$  decays occur far away  $\geq 500$  km, at high altitude ( $\geq 20 - 40$  km) and it will give clear signals distinguished from downward horizontal UHECR. HORTAUs are grown by UHE neutrino interactions inside huge volumes ( $V_{eff} \geq 5130 - 6250 km^3$ ); see for more details [31],[32],[33]. As summarized in last Fig.32 the expected UHE fluence

$$\Phi_\nu \simeq 10^3 eV cm^{-2} s^{-1}$$

needed in most Z-Shower models (as well as in most topological relic scenarios) to solve GZK puzzle, will lead to a hundred of horizontal events comparable to UHECR ones. Even in the most conservative scenario where a minimal GZK- $\nu$  fluence must take place at least at

$$\Phi_\nu \simeq 10 eV cm^{-2} s^{-1}$$

(just comparable to well observed Cosmic Ray fluence), a few or a ten of such UHE astrophysical neutrinos must be observed (respectively at  $3 \cdot 10^{19}$  eV and  $10^{19}$  eV energy windows). To improve their visibility EUSO, on our opinion, may:

- a) Improve the fast pattern recognition of Horizontal Shower Tracks with their forking signature.
- b) Enlarge the Telescope Radius to embrace also lower  $10^{19}$  eV showers.
- c) Consider a detection threshold at angular  $\Delta\theta$  and at height  $\Delta h$  level within an accuracy  $\Delta\theta \leq 0.2^\circ, \Delta h \leq 2$  km.

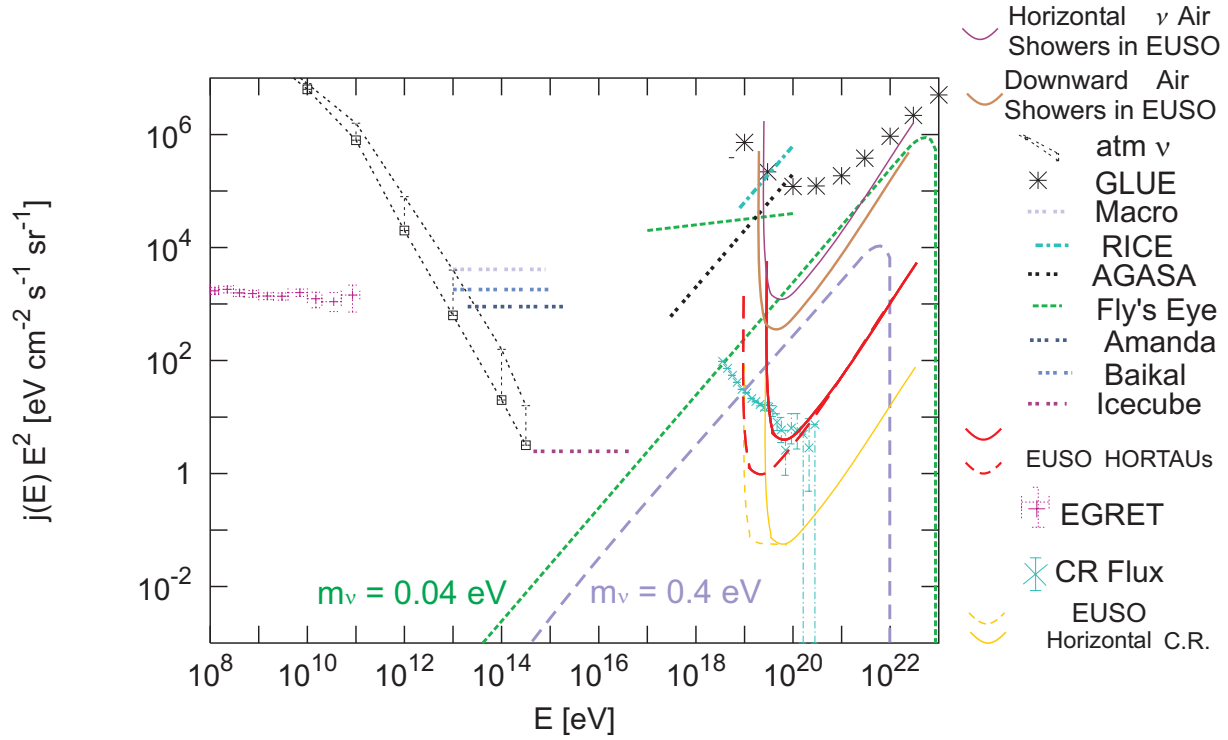


**Figure 32.** EUSO thresholds for Horizontal Tau air-shower shower, HORTAUs (or Earth Skimming Showers) over all other  $\gamma$ ,  $\nu$  and Cosmic Rays (C.R.) fluence and bounds. The fluence threshold for EUSO has been estimated for a three year experiments lifetime. Competitive experiment are also shown as well as the Z-Shower expected spectra in two different light neutrino mass values ( $m_\nu = 0.04, 0.4$  eV). As above dash curves for both HORTAUs and Horizontal Cosmic Rays are drawn assuming an EUSO threshold at  $10^{19}$  eV. [30], [26],[46], [28],[33].

Even the above results have been derived carefully in minimal realistic scenarios they may be used within 10% approximated value due to present uncertainties in EUSO detection capabilities.

## 8. Conclusions

In the present article we have considered the connection between Ultra High Energy Cosmic Ray Astronomy, relic neutrino masses and UHE neutrino scattering or relic ones (the Z-Shower solution) to solve the GZK puzzles: indeed because of the UHECR rigidity we do expect the rise of a new UHE particle astronomy. But because UHECR interactions on relic cosmic photons this UHECR astronomy must be very local, within our nearby Universe. The absence of any defined known structure (as our galactic plane and super-galactic group) is puzzling. The absence of the GZK cut-off is also puzzling. Because of photopion production along the UHECR path we must expect also a secondary neutrino astronomy at GZK energies. In Z-Showering model, on the contrary, larger UHE neutrino fluxes are the primary of UHECR. These UHE neutrino may hit relic ones whose lightest masses are reflecting into highest Z-boosted resonance peaks and are modulating highest un-explored UHECR tails. UHE neutrino at ZeV energies may be needed. We have investigated the interplay between neutrino masses and UHECR spectra. We also studied the possibility to test part of this UHE neutrino astronomy by Tau Air-Showers. In particular we have shown the virtue of such tau astronomy at

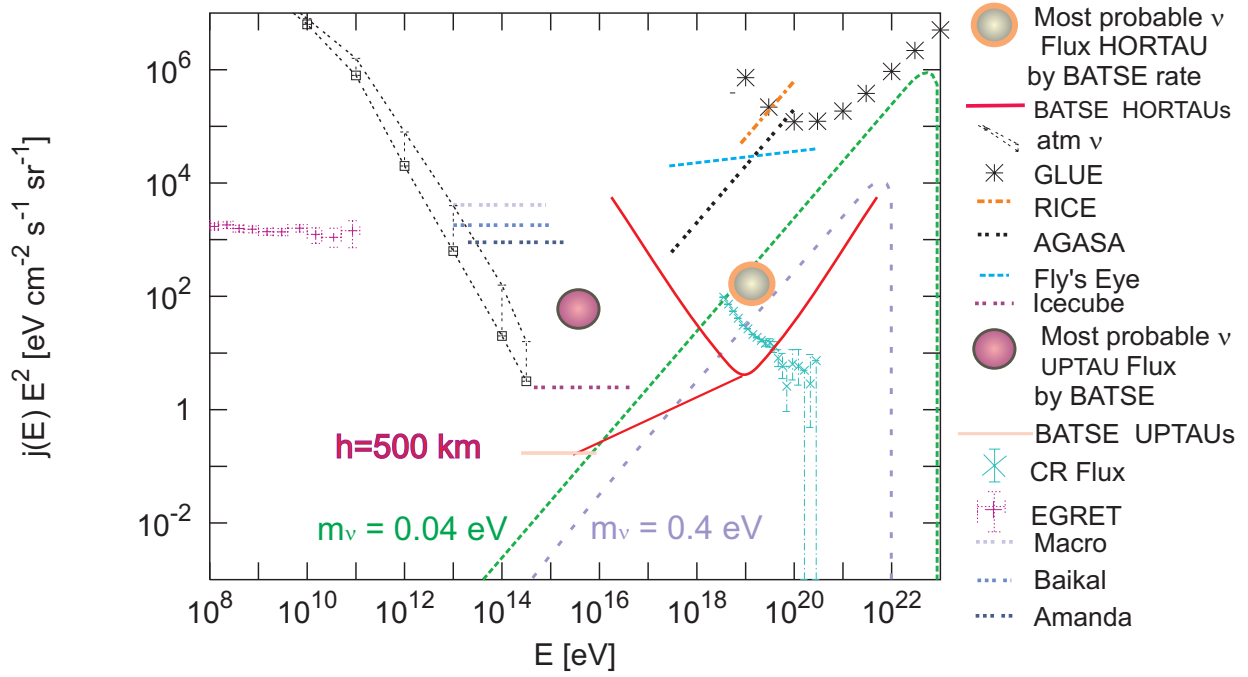


**Figure 33.** Neutrino Flux derived by BATSE Terrestrial Gamma Flashes assuming them as  $\gamma$  secondaries of upward Tau Air-showers. These fluxes are estimated using the Tab.5 normalized during their most active trigger and TGF activities (3 + 4) as labeled in last column. The UPTAUs and HORTAUs rate are normalized assuming that the events at geo-center angle above  $50^\circ$  might be of HORTAU nature.

PeVs and at EeVs energy window as Upward and Horizontal Tau air-showers (UPTAUs-HORTAUs). Tau showering are able to leave a strong imprint in detectors located either beyond a mountain chain or, better, above mountain peak or an plane, balloons and satellites. In particular we estimated the detectable mass via Tau air-shower observing by any quota. We had estimated the terrestrial crust mass and the consequent event rate for given neutrino flux. We also discussed the possibility to observe the same horizontal tau air-showers within the next generation telescope (EUSO like). We also discussed the possibility that the same upward and horizontal air-showers will cross upward the terrestrial atmosphere leading to UPTAUs or HORTAUs. These events may be already recorded on best gamma satellites as very sharp (millisecond) gamma bursts. Indeed the last Gamma Ray Observatory did recorded , in BATSE experiment, rare upward gamma flashes, the Terrestrial Gamma Flashes. Their fluence and duration are well in agreement with expected UPTAUs and HORTAUs power and shower dispersion at high altitude. We reconsidered their maps in celestial coordinates in correlation with known EGRET and AGASA anisotropies and sources. We also correlated the observed TGF rate with the expected neutrino flux threshold finding a first estimate of the UPTAUs and HORTAUs fluxes. Both their fluence  $\Phi_\nu \simeq 100 eV cm^{-2} s^{-1} sr^{-1}$  are nearly one order of magnitude below present bounds and might be confirmed in a very near future by EUSO and other experiments.

## 9. Appendix A: Influence of Atmosphere depth in HORTAUs

As soon as the altitude  $h_1$  and the corresponding energy  $E_{\tau_{h_1}}$  increases the corresponding air density decreases. At a too high quota there is no more  $X$  slant depth for any air-

showering to develop. Indeed its value is :

$$\begin{aligned}
X &= \int_{\frac{d_u}{2} + c\tau\gamma_t}^{d_1 + \frac{d_u}{2}} n_0 e^{-\frac{R_\oplus}{h_0} \left[ \sqrt{\left(1 - \frac{h_2}{R_\oplus}\right)^2 + \left(\frac{x}{R_\oplus}\right)^2} - 1 \right]} dx \\
&\simeq \int_{\frac{d_u}{2} + c\tau\gamma_t}^{d_1 + \frac{d_u}{2}} n_0 e^{-\frac{x^2}{2R_\oplus h_0}} dx \leq n_0 h_0
\end{aligned} \tag{38}$$

In order to find this critical height  $h_1$  where the maximal energy HORTAU terminates we remind our recent approximation. The transcendental equation that defines the Tau distance  $c\tau$  has been more simplified in:

$$\int_0^{+\infty} n_0 e^{-\frac{\sqrt{(c\tau+x)^2 + R_\oplus^2} - R_\oplus}{h_0}} dx \cong n_0 h_0 A \tag{39}$$

$$\int_0^{+\infty} n_0 e^{-\frac{(c\tau+x)^2}{2h_0 R_\oplus}} dx \cong n_0 h_0 A \tag{40}$$

$$c\tau = \sqrt{2R_\oplus h_0} \sqrt{\ln\left(\frac{R_\oplus}{c\tau}\right) - \ln A} \tag{41}$$

Here  $A = A_{Had.}$  or  $A = A_\gamma$  are slow logarithmic functions of values near unity; applying known empirical laws to estimate this logarithmic growth (as a function of the X slant depth) we derived respectively for hadronic and gamma UHECR showers [30], [26]:

$$A_{Had.} = 0.792 \left[ 1 + 0.02523 \ln\left(\frac{E}{10^{19} eV}\right) \right] \tag{42}$$

$$A_\gamma = \left[ 1 + 0.04343 \ln\left(\frac{E}{10^{19} eV}\right) \right] \tag{43}$$

The solution of the above transcendental equation leads to a characteristic maximal UHE  $c\tau_\tau = 546 \text{ km}$  flight distance, corresponding to  $E \leq 1.1 \cdot 10^{19} eV$  energy whose decay occurs at height  $H_o = 23 \text{ km}$ ; nearly 600 Km far from the horizon it was originated from there on the HORTAUs begins to shower. At higher quotas the absence of sufficient air density lead to a suppressed development or to a poor particle shower, hard to be detected. At much lower quota the same air opacity filter most of the electromagnetic shower allowing only to muon bundles and Cherenkov lights to survive at low a somehow ( $\leq 10^{-3}$ ) level.

## 10. Appendix B: The UPTAUs area

The Upward Tau air-showers, mostly at PeV energies, might travel a minimal air depth before reaching the observer in order to amplify its signal. The UPTAUS Disk Area  $A_U$  underneath an observer at height  $h_1$  within a opening angle  $\tilde{\theta}_2$  from the Earth Center is:

$$A_U = 2\pi R_\oplus^2 (1 - \cos \tilde{\theta}_2) \tag{44}$$

Where the  $\sin \tilde{\theta}_2 = (x_2/R_\oplus)$  and  $x_2$  behaves like  $x_1$  defined above for HORTAUs. In general the UPTAUs area are constrained in a narrow Ring (because the mountain presence itself or because the too near observer distances from Earth are encountering a too short air slant depth for showering or a too far and opaque atmosphere for the horizontal UPTAUs)[31],[32]:

$$A_U = 2\pi R_\oplus^2 (\cos \tilde{\theta}_3 - \cos \tilde{\theta}_2) \tag{45}$$

An useful Euclidean approximation is:

$$A_U = \pi h_1^2 (\cot \theta_2^2 - \cot \theta_3^2) \quad (46)$$

Where  $\theta_2, \theta_3$  are the outgoing  $\tau$  angles on the Earth surface [30].

For UPTAUs (around  $3 \cdot 10^{15} eV$  energies) these volumes have been estimated in [30], assuming an arrival values angle  $\simeq 45^\circ - 60^\circ$  below the horizons. For two characteristic densities one finds respectively:

$$\Delta M_{eff.}(h_1 = 500km)(\rho_{Water}) = 5.9 km^3;$$

$$\Delta M_{eff.}(h_1 = 500km)(\rho_{Rock}) = 15.6 km^3$$

Their detection efficiency is displayed in last figure (Fig.27), and it exceed by more than an order of magnitude, the future ICE-CUBE threshold.

### Acknowledgment

The authors wish to thank Prof. Livio Scarsi, M. Teshima for inspiring discussions and C. Leto, Massimo De Santis for technical support in the figure preparation. The work of one of us (M. Khlopov) was partially performed in the framework of Russian State Contract 40.022.1.1.1106 and supported in part by RFBR grant 02-02-17490 and grant UR.02.01.026.

### References

- [1] Atkins R. et.al, astro-ph/0001111, 2000
- [2] Aoki T. et al. ICRC 2001, p.915-918.2001
- [3] Becattini F. and Bottai S 2001 Astropart. Phys. 15 323
- [4] Bellido J. A., Clay R. W., Dawson B. R., Johnston-H.M. 2001 Astropart. Phys. 15 167-175
- [5] Barger V. and Marfatia D., hep-ph/0212126
- [6] Berezhinsky V. S. et al. 1990 Astrophysics of Cosmic Rays (North Holland ed.)
- [7] Berezhinsky V. S., Gazizov A. Z. and Grigorieva S. I. 2002 hep-ph/0204357
- [8] Bertou X., Billoir P., Deligny O., Lachaud C., Letessier-S.A. 2002 Astropart. Phys. 17 183-193
- [9] Bhattacharjee P., Sigl G., Phys.Rept.327,109-247,2000
- [10] Blasi P., Sheth R., Phys.Lett.B486,233-238,2000
- [11] Belotsky K.M., Damour T., Khlopov M.Yu. Phys.Lett. B 529, 10-18, 2002
- [12] Dolgov A. 2002 Phys.Rept. 370 , 333-535; 2002 hep-ph/0202122
- [13] . Doroshkevich, A.G., Zeldovich, Ya.B., Sunyaev, R.A., and Khlopov, M.Yu, Sov. Astron. Lett. 6, 252, 1981.
- [14] Dutta Iyer S., Reno M. H., Sarcevic I. and Seckel D. 2001 Phys. Rev. D63 094020
- [15] Elbert J.W., Sommers, P., Apj, 441, 151, 1995
- [16] Enqvist K., Kainulainen K., Maalampi J., Nucl.Phys.B317, 647.1989
- [17] Fargion D., Nuovo Cimento, 77B, 111, 1983
- [18] Fargion D. and Salis A. 1997 Proc.25th ICRC HE-4-6 153
- [19] Fargion D., Golubkov Yu.A., Khlopov M.Yu.,  
Konoplich R.V., Mignani R., JETP Lett. 69,434,1999
- [20] Fargion D., Mele B. and Salis A. 1999 Ap. J. 517, 725; astro-ph/9710029
- [21] Fargion D., Khlopov M., Konoplich R., Mignani R., Phys. Jetp Lett. 68, 685-690 (1998)
- [22] Fargion D., Aiello A., Conversano R., 26th ICRC HE6.1.10 396-398, 1999; astro-ph/9906450

- [23] Fargion D., Konoplich R., Grossi M., Khlopov M., *Astroparticle Physics* 12,307-314, 2000
- [24] Fargion D. and Grossi M., De Sanctis Lucentini P. G., Di Troia C. and Konoplich R. V.; *Dark2000*, Heidelberg 10-14,July, Ed. Klapdor-Kleingrothaus H V Springer 2001 p. 455-468
- [25] Fargion D. et all. astro-ph/0102426, Heidelberg, DARK 2001
- [26] Fargion D. 2001 27th ICRC 2001 HE2.5 1297-1300 2001 astro-ph/0106239
- [27] Fargion D. 2001 27th ICRC 2001 HE1.8 Germany 903-906 2001 astro-ph/0107094
- [28] Fargion D., Grossi M., De Sanctis Lucentini P. G. and Troia C J 2001 *Phys. Soc. Jpn.* 70 46-57
- [29] Fargion D., Grossi M., De Sanctis Lucentini P G , ICRC2001, HE3.05,1578-1581,2001
- [30] Fargion D. 2002 *Ap. J.* 570 (2002) 909-925, astro-ph/0002453; astro-ph/9704205
- [31] Fargion D. 2002 hep-ph/0206010.
- [32] Fargion D. 2002 SPIE Conference 4858-01 2002 hep-ph/0208093
- [33] Fargion D. 2002 Oulu, Beyond the Standard Model Conference 2002 hep-ph/0211153
- [34] Fargion D. 2002 astro-ph/0212342
- [35] Farrar et all., *Phys.Rev.Lett.* 84, 3527, 2000
- [36] Feng J. L., Fisher P., Wilczek F. and Terri M. Yu. hep-ph/0105067
- [37] Fodor Z., Katz S.D, Ringwald A. hep-ph/0105336,2001
- [38] Fodor Z., Katz S. D. and Ringwald A. 2002 hep-ph/0210123
- [39] Fukuda Y. *et al.* [Super-Kamiokande Collaboration] 1998 *Phys. Rev. Lett.* 81 1562
- [40] Gallex Collaboration, 1992, *Phys.Letter.B* 285 (1992) 376.
- [41] Gorbunov D. S., Tinyakov P. G. ,Tkachev I. and Troitsky S. V. 2002 astro-ph/0204360 and 2002 *Astrophys.J.* 577 L93
- [42] Greisen K. 1966 *Phys. Rev. Lett.* 16 748
- [43] Hayashida N. et al. AGASA collaboration 1999 *Astropart. Phys.* 10 303-311
- [44] Horns D., Schmele D. ICRC26th,astro-ph/9909125,1999
- [45] Kalashev O.E., Kuzmin V.A., Semikoz D.V., astro-ph/0006349, 2000
- [46] Kalashev O. E., Kuzmin V. A., Semikoz D.V. and Sigl G. 2002 *Phys. Rev. D* 66 063004
- [47] KamLand Collaboration, 2002, hep-ex/0212021.
- [48] Kifune T.,*Astrophys.J.Lett.* 518, L21.1999
- [49] Klapdor-Kleingrothaus H. V., Dietz A., Harney H. L. and Krivosheina I. V. 2001 *Mod. Phys. Lett. A* 16 2409;
- [50] Golubkov Yu. A., Konoplich R.V.,*Phys.Atom.Nucl.* 61,602,1998
- [51] Halzen F. and Saltzberg D. 1998 *Phys. Rev. Lett.* 81 4305-4308
- [52] Hill C.T., *Nucl.Phys.B*224, 469.1983
- [53] Hou G. W. S. and Huang M. A. 2002 astro-ph/0204145
- [54] Gandhi R., Quigg C., Reno M. H. and Sarcevic I. 1998 *Phys. Rev. D* 58 093009
- [55] Glushkov A.V.,SleptovI.Ye.ICRC2001,414-416,2001
- [56] Learned J. G. and Pakvasa S. 1995 *Astropart. Phys.* 3 267
- [57] Particle Data Group, *Phys.Rev.D.*1996
- [58] Protheroe R.J., Biermann P.L.,*Astpart.Phys* 7,181,1997
- [59] Protheroe R.J., Meyer H., astro-ph/0005349, 2000
- [60] Singh S., Ma C. P., astro-ph/0208419.
- [61] SNO Collaboration, 2002, *Phys.Rev.Lett.* 89 (2002) 011302
- [62] Takeda M. and AGASA Collab. 2001 *J Phys. Soc. Jpn.* 70 15-21
- [63] Takeda M., AGASA collaboration.EHE Workshop,2001
- [64] Takeda M. et all.ICRC 2001,p.341-344.2001
- [65] Tinyakov P. and Tkachev I. 2001 *J. Phys. Soc. Jpn.* 70 58-63

- [66] Tinyakov P. and Tkachev I. 2001, astro-ph/0102101
- [67] Tinyakov P.G, Tkachev I.I,EHE Kashiwa Workshop,2001
- [68] Yoshida S, Sigl G and Lee S 1998 Phys. Rev. Lett. 81 5505
- [69] Yoshida S. et al., ICRC 2001,1142,2001
- [70] Uchihori Y. et al.,Astropart.Phys. 13, 151-160.2000
- [71] Weiler T. 1999 Astropart. Phys. 11 303
- [72] Zatsepin G.T. and Kuzmin V.A. 1966 JETP Lett. 4 78